

Aus dem Theodor–Boveri–Institut für Biowissenschaften
der Universität Würzburg

Lehrstuhl für Physiologische Chemie II

Vorstand: **Prof. Dr. W. Sebald**

Structural and Functional Analysis of Chordin-like 2 / BMP-2 Interaction

Inaugural Dissertation

zur Erlangung der Doktorwürde

der Medizinischen Fakultät

der Bayerischen Julius-Maximilians-Universität Würzburg

vorgelegt von

Yi Huang

aus ChongQing, CHINA



Würzburg, im April 2008

Referentin: Prof. Dr. W. Sebald

Korreferent: Prof. Dr. med. F. Jakob

Dekan: Prof. Dr. med. M. Frosch

Tag der mündlichen Prüfung: 09. 09. 2008

Der Promovend ist Arzt

CONTENTS

1. INTRODUCTION	1
1.1 BMPs and TGF- β superfamily proteins.....	1
1.2 Structure of BMPs	2
1.3 Receptors of BMPs	4
1.4 Signal transduction pathways of BMPs.....	6
1.5 Modulation of BMP signaling	9
1.5.1 Intracellular modulation.....	10
1.5.2 Membrane receptor modulation	11
1.5.3 Extracellular modulation.....	12
1.5.4 Chordin family	15
1.6 Chordin-like 2 (CHL2)	21
1.6.1 Structure of CHL2 protein.....	21
1.6.2 Structure of CHL2 gene	22
1.6.3 Normal expression of CHL2	23
1.6.4 CHL2 mRNA expression in diseased cartilage.....	24
1.6.5 Interaction of CHL2 and BMPs	25
1.7 Aims of the thesis work	25
2. MATERIALS AND METHODS	26
2.1 Abbreviations.....	26
2.2 Chemicals.....	27
2.3 Enzymes.....	27
2.4 Kits.....	28
2.5 Vectors and oligonucleotides.....	28
2.5.1 Expression vector QKA for <i>E.coil</i>	28

2.5.2	Baculovirus transfer vector pAcGP67-B/Th.....	28
2.5.3	Oligonucleotides	28
2.6	Bacterial strain	30
2.7	Cell line.....	30
2.8	BMP-2.....	31
2.9	Antibodies.....	31
2.10	Microbiological methods	31
2.10.1	Sterilization.....	31
2.10.2	Culture media.....	31
2.10.3	Culturing of bacteria	32
2.10.4	Storage of bacterial culture	32
2.10.5	Preparation of competent <i>E. coli</i> cells	32
2.11	Molecular biological methods	33
2.11.1	Site directed mutagenesis by PCR.....	33
2.11.2	Determination of the concentration of nucleic acids	35
2.11.3	Purification of DNA.....	35
2.11.3.1	Phenol/Chloroform extraction of DNA	35
2.11.3.2	Ethanol precipitation of DNA.....	35
2.11.3.3	Gel extraction kit	36
2.11.4	Digestion of DNA.....	36
2.11.5	Ligation of DNA to the vector.....	36
2.11.6	Transformation of recombinant plasmid DNA to competent <i>E. coli</i>	37
2.11.7	Recombinant plasmid DNA mini-preparation.....	37
2.11.8	Recombinant plasmid DNA maxi-preparation	38
2.11.9	DNA sequencing.....	39
2.12	Protein chemical methods.....	39
2.12.1	Determination of the protein concentration	39
2.12.2	Lyophilization of proteins.....	40

2.12.3	SDS - polyacrylamide gel electrophoresis.....	40
2.12.4	Concentration of protein samples by TCA	41
2.12.5	Protein mass spectrometry	42
2.13	Western-Blot.....	42
2.14	Expression of recombinant protein in <i>E.coli</i>	44
2.14.1	Analytical protein expression	44
2.14.2	Preparative protein expression.....	45
2.14.3	Preparation of inclusion bodies.....	45
2.14.4	Denaturation and refolding of protein	46
2.15	Expression of protein in SF9 cells	47
2.15.1	Co-transfection of BaculoGold DNA and a transfer vector into SF9 cells	47
2.15.2	Plaque-assay for getting single virus clone.....	48
2.15.3	First virus amplification (A1)	49
2.15.4	Second virus amplification (A2).....	50
2.15.5	Western-Blot for positive clone.....	50
2.15.6	Third virus amplification (A3).....	50
2.15.7	Forth virus amplification (A4).....	51
2.15.8	Expression.....	51
2.16	Purification of proteins by chromatography	52
2.16.1	Ni-NTA chelating chromatography	52
2.16.2	Cation-exchange chromatography on SP sepharose	52
2.16.3	BMP-2 affinity chromatography.....	53
2.16.4	Size exclusion chromatography on Superdex TM 200	54
2.16.5	Reversal phase HPLC	55
2.17	Analysis of Protein-Protein interaction by BIAcore technology	56
2.17.1	Immobilizing of proteins through biotin-streptavidin coupling	57
2.17.2	Measurement of binding of analytes.....	58
2.18	Biological activity in cell line	59

2.19	Crystallization of proteins.....	60
2.19.1	Preparation of protein samples for crystallization	60
2.19.2	Crystallization of proteins by vapour diffusion method	60
3.	RESULTS.....	63
3.1	Preparation of mCHL2 and its mutants in SF9 cells	63
3.1.1	Modification of pAcGP67-B/Th vector	63
3.1.2	Cloning of mCHL2 and its mutants into pAcGP67-B/Th/m.....	64
3.1.3	Co-transfection of BaculoGold DNA and the transfer vectors into SF9 insect cells and amplification of the recombinant virus	67
3.1.4	Expression and purification of mCHL2 and its mutants.....	70
3.1.4.1	Purification of proteins by Ni-NTA chelating chromatography	70
3.1.4.2	Purification of proteins by cation-exchange chromatography.....	71
3.1.4.3	Purification of proteins by BMP-2 affinity chromatography.....	73
3.1.4.4	Purification of proteins by size exclusion chromatography.....	74
3.2	Preparation of mCHL2-VWC1 in <i>E.coli</i>	75
3.2.1	Cloning of mCHL2-VWC1 into QKA vector	75
3.2.2	Expression and purification of mCHL2-VWC1.....	76
3.3	Preparation of mCHL2-VWC2 in SF9 cells.....	79
3.3.1	Cloning of mCHL2-VWC2 into pAcGP67-B/Th/m.....	79
3.3.2	Co-transfection of BaculoGold DNA and the transfer vector into SF9 insect cells and amplification of the recombinant virus.....	79
3.3.3	Expression and purification of mCHL2-VWC2.....	80
3.4	Preparation of mCHL2-VWC3 and its mutants.....	81
3.4.1	Preparation of mCHL2-VWC3 in SF9 cells	81
3.4.2	Preparation of mCHL2-VWC3 and its mutants in <i>E.coli</i>	82
3.4.2.1	Cloning of mCHL2-VWC3 and its mutants into QKA vector	82
3.4.2.2	Expression and purification of mCHL2-VWC3 and its mutants.....	84

	a) Expression of proteins in <i>E.coli</i>	
	b) Preparation of inclusion body of proteins	
	c) Denaturation and refolding of proteins	
	d) Purification of proteins by cation-exchange chromatography	
	e) Purification of mCHL2-VWC3 by BMP2 affinity chromatography	
	f) Purification of proteins by size exclusion chromatography	
	g) Purification of proteins by HPLC	
3.5	Functional analysis of mCHL2 and its VWC domains.....	90
3.5.1	Binding of mCHL2 and its VWC domains to BMPs.....	90
3.5.2	Binding epitopes of BMP-2 for mCHL2.....	92
3.5.3	Binding mode of mCHL2 and BMP-2.....	94
3.5.4	Competition of mCHL2/VWCs with receptors for BMP-2 binding.....	98
3.5.5	Biological activity in cell lines.....	99
3.5.6	Analysis of mCHL2-VWC3 mutants and BMP-2 interaction.....	101
3.5.7	Binding of mCHL2/VWCs to Tsg.....	102
3.6	Protein complex formation and crystallization of the complex.....	105
3.6.1	Crystallization of mCHL2/ BMP-2 complex.....	105
3.6.2	Crystallization of mCHL2-VWC3/ BMP-2 complex.....	106
4.	DISCUSSION.....	111
5.	SUMMARY.....	120
6.	REFERENCES.....	122
	ACKNOWLEDGEMENTS.....	133
	CURRICULUM VITAE.....	134

1 Introduction

The communication between different cells through defined signaling networks is crucial for the development from a single cell in the early embryo to the fully developed human being. The communication is either mediated through direct cell-cell interaction or by direct binding of secreted soluble factors to specific receptors at the plasma membrane. Among these factors are cytokines, hormones, neurotransmitters as well as growth factors. A variety of signal transduction pathways induced by many factors create a complex network. Perturbation of the network can cause pathological conditions, resulting in defective development of an organism, and following premature death or physiological disability and disease.

Bone morphogenetic proteins (BMPs) are multifunctional growth factors which belong to the transformation growth factor β (TGF- β) superfamily. The aim of this thesis was to investigate the interaction of BMPs and its novel inhibitor - Chordin-like 2 (CHL2). Therefore, the function, signal transduction and regulation of BMPs will be described in the followings.

1.1 BMPs and TGF- β superfamily proteins

BMPs and other members of the TGF- β superfamily exist in vertebrate and invertebrate animals. BMPs were originally isolated by their ability to induce ectopic bone and cartilage formation in vivo (Urist, 1965), but it became rapidly evident that BMPs also act as multifunctional regulators in morphogenesis during development in animals (Graff, 1997; Wozney, 1998). So far, at least 30 TGF- β like proteins have already been described (Hogan, 1996; Schmierer and Hill, 2007), including BMPs, TGF- β s, Growth and differentiation factors (GDFs), Activin β -chains, Nodal, and Anti-Mullerian hormone (AMH, also termed Mullerian inhibiting substance, MIS).

Members of this family regulate a large variety of biologic responses in many different cells and tissues during early embryogenesis (De Robertis and Kuroda, 2004), and later in organogenesis (Hogan, 1996; Kingsley, 1994). During the postnatal life, BMPs and their

analogues are also essential for tissue repair and homeostasis (Reddi, 1998; Rosen and Thies, 1992) as well as for growth control (Massague et al., 2000).

Furthermore, BMPs and other TGF- β like proteins play important roles after birth in pathophysiology of several diseases including osteoporosis (Medici et al., 2006; Turgeman et al., 2002; Wu et al., 2003), osteoarthritis (Blaney Davidson et al., 2007; Chen et al., 2004; Drissi et al., 2005), kidney diseases (Bottinger, 2007; Gagliardini and Benigni, 2007; Zhu et al., 2007), cerebrovascular diseases (Chang et al., 2003; Dabek et al., 2006; Florio et al., 2007) and cancer (Buck and Knabbe, 2006; Hahn and Akporiaye, 2006; Sekimoto et al., 2007).

1.2 Structure of BMPs

The TGF- β superfamily proteins can be organised into subfamilies according to the similarities of their amino acid sequences (Figure 1.1) (Schmierer and Hill, 2007; Sebald et al., 2004). On a molecular level, the proteins of the TGF- β superfamily are very similar. The overall fold of the protein backbones is almost identical even though the similarity in amino acid sequences of TGF- β superfamily members is very low. A typical feature of all proteins is a small cystine-knot motif, which is formed by seven well-conserved cysteine residues in the carboxy-terminal domain of the proteins (McDonald and Hendrickson, 1993). One of these cysteine residues is used for covalent interchain disulfide bridging, and the others are involved in an intramolecular ring formation, known as the cystine knot configuration. The cystine knot is a folding motif that forces exposure of hydrophobic residues to the aqueous surrounding, and prevents the molecule from assuming a globular protein structure. Instead, it drives the molecules to undergo dimerization, resulting in highly stable dimeric proteins with a butterfly-shape structure (Figure 1.2) (Scheufler et al., 1999; Sebald et al., 2004).

The precursor dimers are secreted as propeptides, which are activated by protease cleavage, such as the furin-type serine endoprotease at an Arg-x-x-Arg recognition sequence. The monomer could be described as a left hand: the N-terminal end as the thumb; the two β -sheets (each two-stranded) as the two fingers; and the central α -helix as

the wrist (Figure 1.2, B). In the dimer, the wrist of one monomer fits into the concave side of the fingers of the other monomer. The topology of the dimer (shown in Figure 1.2, A for BMP-2) is highly conserved in the TGF- β superfamily. BMP-2 exhibits two different types of surface-epitopes to interact with the respective receptors, the wrist and the knuckle epitopes (Figure 1.2, A).

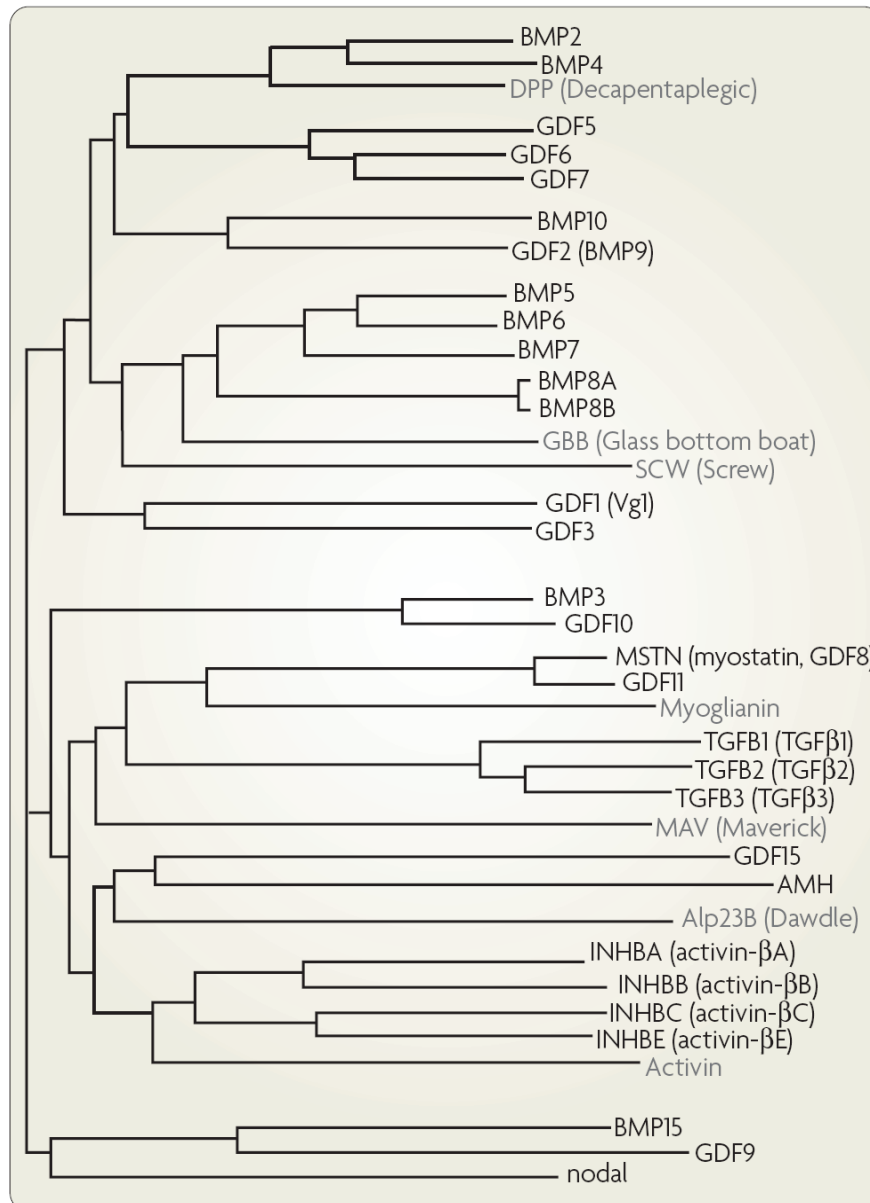


Figure 1.1: Phylogenetic trees derived from protein alignments of ligands in the TGF- β superfamily in human and *Drosophila melanogaster*. Human proteins are shown in black and *Drosophila melanogaster* proteins are in grey (Schmierer and Hill, 2007).

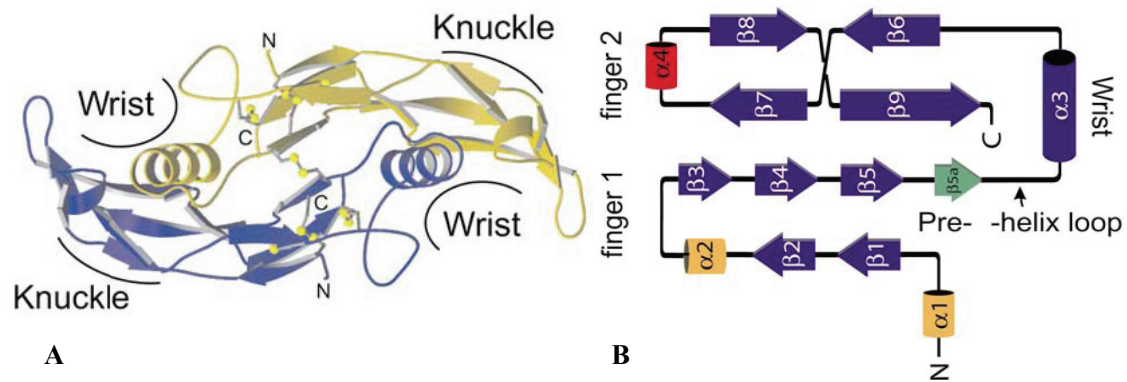


Figure 1.2: Crystal structure (A) and secondary structure elements (B) of BMP-2. The wrist epitopes for type I and knuckle epitopes for type II receptor binding as well as the finger- and wrist-like parts of the hand-like monomer are labelled (Sebald et al. 2004).

1.3 Receptors of BMPs

Members in the TGF- β superfamily signal into a cell by assembling type I and type II serine-threonine kinase receptors in the cell membrane. The activated type I receptors then phosphorylate the the cytoplasmic Smads proteins (Derynck et al., 1998; Liu et al., 1995). Up to now seven type I and five type II receptor chains have been identified in mammals (Figure 1.3) (Newfeld et al., 1999).

The structures of type I and type II receptors are similar. They have a short extracellular ligand-binding domain with some conserved cysteine residues, a single transmembrane domain, and an intracellular domain containing a serine–threonine kinase motif. The type I receptors, but not type II receptors, contain upstream of the kinase domain a GS-box with a characteristic repetition of serines and glycines (SGSGSG). Upon ligand dimer binding, two type II receptors form a heterohexameric complex with two type I receptors. Subsequently the constitutive kinases of the type II receptors activate the type I receptors and initiates the signal transduction cascade by phosphorylating downstream nuclear factors, which then translocate to the nucleus to activate or inhibit transcription. Thus signal transduction for BMPs requires both type I and type II receptors. Type I receptors are activated by type II receptors, and signals are mediated through type I receptors (Ebara and Nakayama, 2002).

According to the crystal structure of the BMP2/BMPR-IA_{EC} complex, one BMP binds two receptor ectodomains at the ‘wrist’ epitope of the BMP (Keller et al., 2004; Kirsch et al., 2000) (Figure 1.4, A). In the BMP-7/ActR-II_{EC} complex (Greenwald et al., 2003) and in the ActA/ActR-IIB_{EC} complex (Thompson et al., 2003), the type II receptor binds to the ‘knuckle’ epitope formed by the backside of the finger regions of the ligand monomer (Figure 1.4, B, C). The crystal structure of the ternary complexes of BMP-2/BMPR-IA_{ECD}/ActR-II_{ECD} and BMP-2/BMPR-IA_{ECD}/ActR-IIB_{ECD} reveals that the fold and assembly of BMP-2 or BMP-7 in binary and ternary complexes with type I and type II receptors are very similar, the receptor ectodomains bind independently and have no direct contacts. The BMPs function as rigid scaffolds which hold the receptor ectodomains together for transactivation (Figure 1.4, D) (Allendorph et al., 2006; Weber et al., 2007).

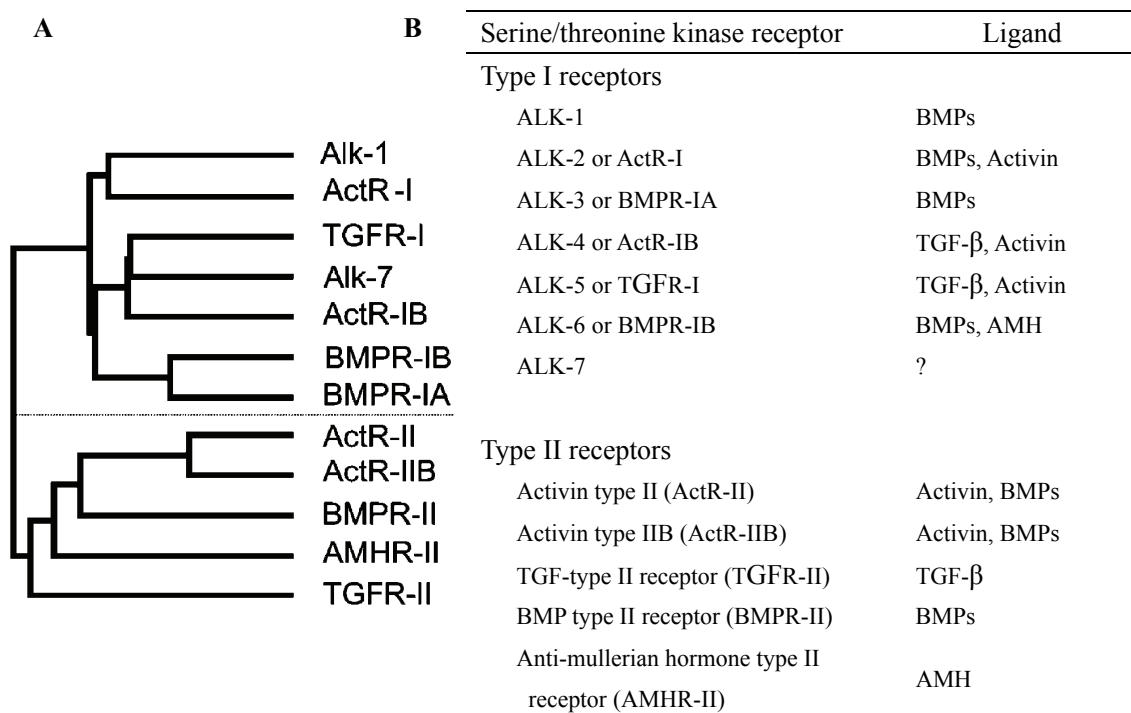


Figure 1.3: **A**, Sequence similarities of receptor ectodomains in the TGF- β superfamily (Sebald et al. 2004). **B**, Type I and Type II Serine/Threonine Kinase Receptors involved in the signaling pathway of TGF- β superfamily members and their ligands (Balemans and Van Hul, 2002).

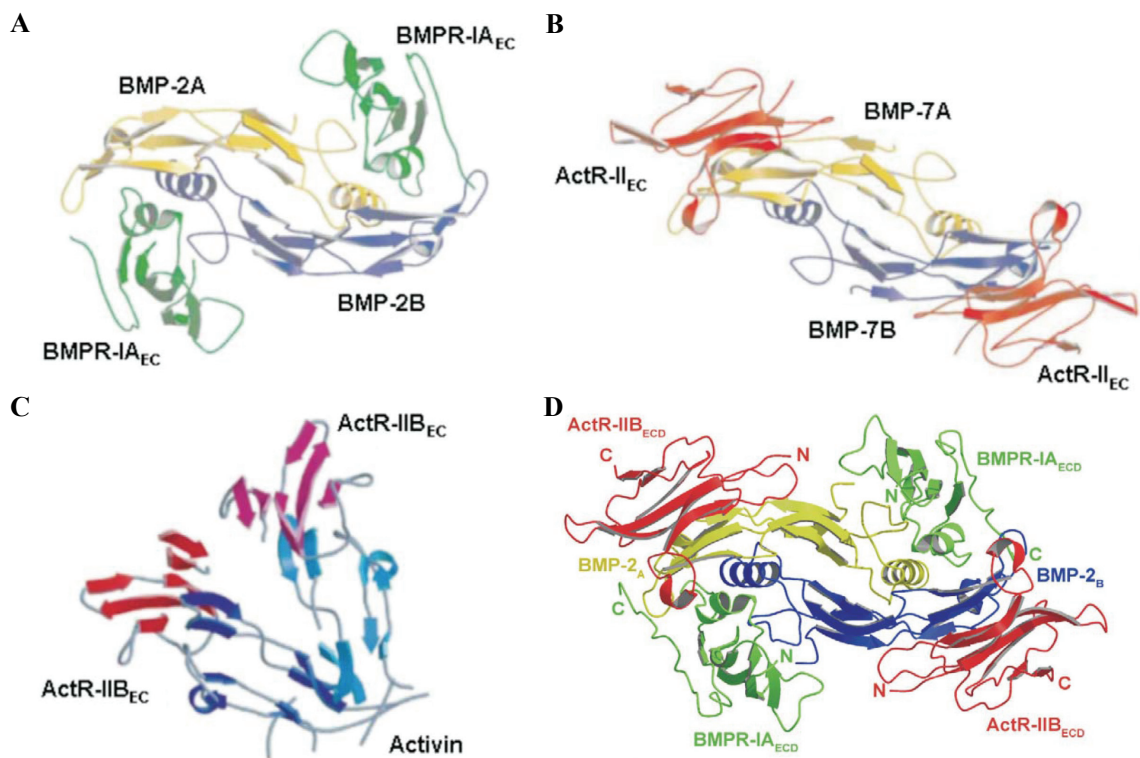


Figure 1.4: Crystal structure of BMPs or activin complexed with receptor ectodomains. **A**, BMP-2 and the BMPR-IA ectodomain (Kirsch et al., 2000a and Keller et al., 2004). **B**, BMP-7 and the ActR-II ectodomain (Greenwald et al., 2003). **C**, Activin and the ActR-IIB ectodomain (Thompson et al., 2003). **D**, Ternary complex of BMP-2/BMP-IA/ActR-IIB ectodomain (Weber et al., 2007).

1.4 Signal transduction pathways of BMPs

BMP signals by at least two different intracellular pathways (Figure 1.5). The so called Smad-dependent pathway employs Smad proteins; one so called Smad-independent pathways include p38-MAPK and ERK pathway.

Smad-dependent pathway

At least eight Smads have been identified in mammals and two additional Smads, Smads 9 and 10, in lower species. There are three classes of Smads: 1) receptor regulated Smads (R-Smads) that can be activated by the type I receptors, such as BMP activated Smad 1/5/8, or TGF- β and Activin activated, Smad 2/3; 2) common TGF- β and BMP mediator Smads (Co-Smad), Smad 4, which oligomerizes with activated R-Smads; and 3)

inhibitory Smads (I-Smads), Smad 6 and 7, which get activated upon ligand stimulation. Smad6/7 exert a negative feedback effect by marking the receptors for degradation and by competing with R-Smads for receptor interaction (Canalis et al., 2003).

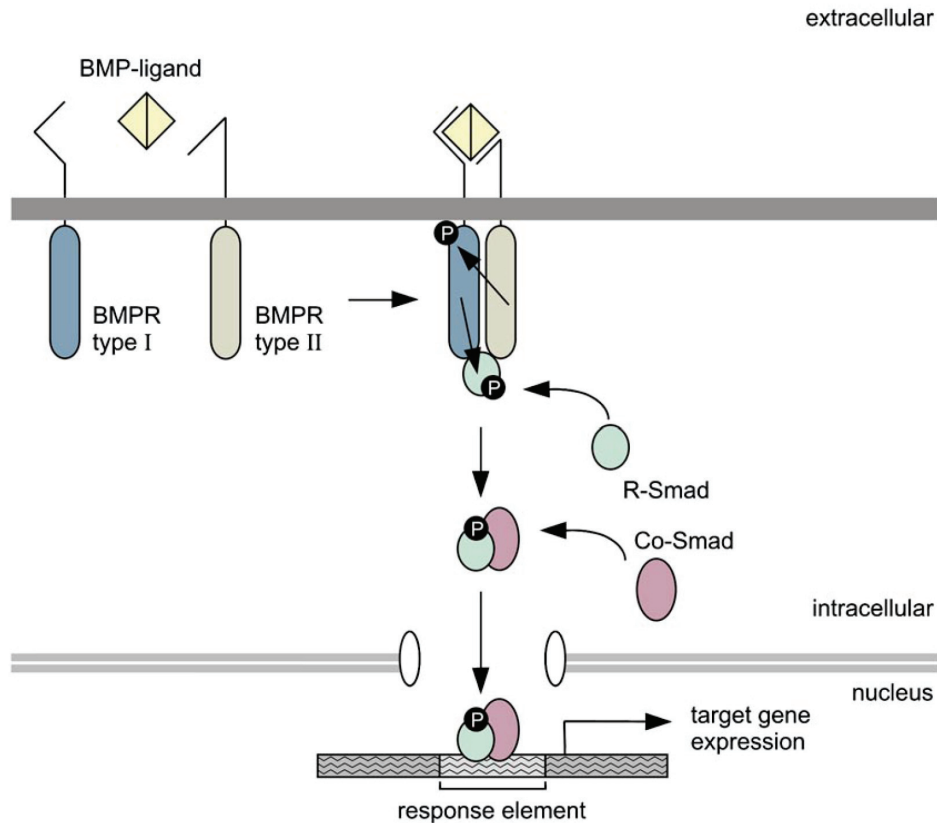


Figure 1.5: Cascade of BMP Smad signaling pathway. BMP dimers bind to serine/threonine kinase receptors type I and II. Upon ligand binding, type II receptors transphosphorylate type I receptors. The latter phosphorylate members of the Smad family of transcription factors. These Smads are subsequently translocated to the nucleus, where they activate transcription of target genes (Balemans and Van Hul, 2002).

Smad proteins have conserved N- and C-terminal regions, named the MH1 and MH2 (MAD homology) domains, respectively. Both domains are bridged by a proline-rich linker region. The MH1 domain of R- and Co-Smads binds to DNA sequences and regulates nuclear import, and the MH2 domain binds to proteins, creating protein-protein interactions in gene transactivation. After ligand binding, the activated type I receptors phosphorylate intracellular Smad1/5/8 (BMPs as ligand) or Smad2/3 (TGF- β and Activin as ligand) on two serine residues near the c-terminal. Upon phosphorylation, the Smads interact with the Co-Smad, Smad4, and form Smad1/5/8-Smad4 or Smad2/3-Smad4 complex, which is translocated into the nucleus to regulate transcription (Liu et al., 1996;

Macias-Silva et al., 1996).

In the nucleus, Smads regulate transcription of target genes by binding to specific DNA sequences, or by interacting with some DNA-binding proteins. 1) Smad-binding DNA sequences. Smad3 and Smad4 directly bind to Smad-binding elements (SBEs; AGAC or GTCT sequence). Smad2 forms a complex with Smad3 and Smad4, and indirectly binds to SBEs. In contrast, Smad1/5/8 bind to the AGAC/GTCT sequence only weakly, and instead bind to the GCCGnCGC sequence of some target genes (Kim et al., 1997; Kusanagi et al., 2000). 2) Smad-interacting proteins. Some proteins, including transcription factors and transcriptional co-activators/co-repressors, interacting with R-Smads in the nucleus also play critical roles in mediating BMP-specific signals by regulating the transcription of target genes. Runx2, a member of transcription factors, can physically interact with R-Smads upon activation of BMP signaling, and co-operatively regulate the transcription of target genes, leading to osteoblast differentiation of mesenchymal progenitor cells (Ito and Miyazono, 2003; Miyazono et al., 2004; Zhang et al., 2000). Menin, another transcription factor, can physically interact with R-Smads and Runx2 in mesenchymal stem cells, and facilitates transcriptional activity induced by BR-Smads and Runx2 in the earlier stage (commitment phase) of osteoblast differentiation (Sowa et al., 2004). Furthermore some transcriptional co-activators (p300, CBP, GCN5 and P/CAF) and co-repressors (c-Ski and SnoN) physically interact with R-Smads upon ligand stimulation and regulate Smad-dependent transcription of target genes (Miyazono et al., 2005). 3) A number of direct BMP target genes have been identified, such as Xvent2 and Xvent2B, msx1, msx2, Id1, Id2, Id3, GATA2, Dlx5, Tob, and FGFR2 (Friedle and Knochel, 2002; Hollnagel et al., 1999; Hussein et al., 2003; Korchynskiy and ten Dijke, 2002; Ladher et al., 1996; Miyama et al., 1999; Peiffer et al., 2005; Rastegar et al., 1999; von Bubnoff et al., 2005; Yoshida et al., 2000).

Smad-independent pathway

In addition to Smad activation, BMPs and TGF- β can activate Smad-independent pathways. The small GTPase and the mitogen-activated protein kinases (MAPKs) ERKs, p38 and c-Jun N-terminal kinases (JNKs) are the main signaling proteins in

Smad-independent pathways (Moustakas and Heldin, 2005). The p38 is essential in BMP-2 induced up-regulation of type I collagen, osteocalcin, and alkaline phosphatase activity; p38 and ERK mediate BMP2 stimulation of fibronectin and osteopontin (Attisano and Wrana, 2002; Lai and Cheng, 2002).

1.5 Modulation of BMP signaling

BMP signaling is delicately regulated at multiple levels: intracellularly, at the cell membrane site, and extracellularly (Figure 1.6).

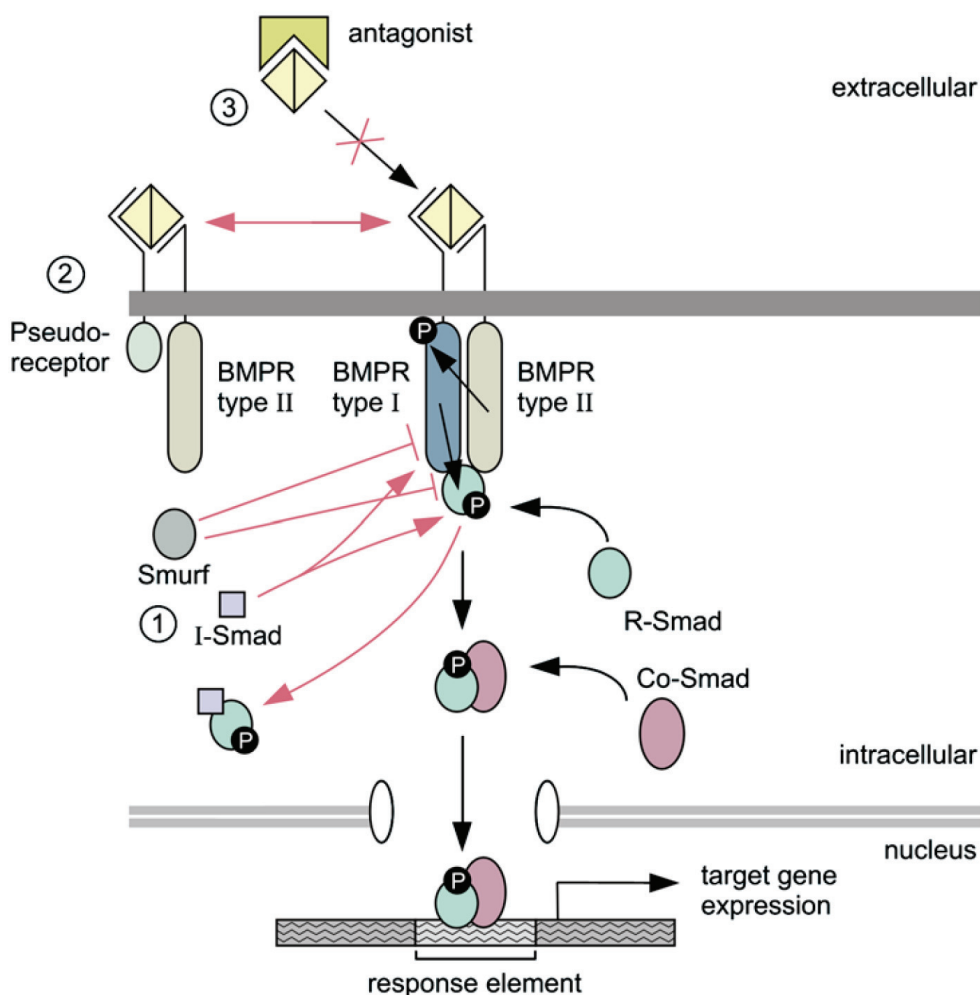


Figure 1.6: Three levels of modulation of BMP signaling. (1) I-Smads and Smurfs regulate intracellular signaling by preventing further Smad signaling and consequent activation of gene transcription, (2) Pseudoreceptor BAMBI/Nma modulates BMP signaling at the membrane site by binding to BMP type II receptors, and (3) Extracellular antagonists modulate binding of BMP dimers to the BMP type I and type II receptors (Balemans and Van Hul, 2002).

1.5.1 Intracellular modulation

The first level of regulation resides within the cell cytoplasm, where inhibitory Smads, Smurfs and some other intracellular proteins act as modulators.

Inhibitory Smads

Smads have conserved N- and C-terminal domains, termed MH1 and MH2 domains respectively. Inhibitory Smads (I-Smads), Smad6 and Smad7, have MH2 domains, but their N-terminal sequences are highly divergent from the MH1 domains of other Smads (Miyazono, 2000). Smad6 preferentially inhibits BMP signaling, whereas Smad7 inhibits both TGF- β /Activin and BMP signaling. I-Smads antagonize the TGF- β signaling pathway either by interacting with phosphorylated type I receptors and thereby preventing the activation of R-Smads, or through competition with Co-Smads for the formation of the R-Smad/Co-Smad complexes (Itoh et al., 2001). The expression of I-Smads also can be regulated by multiple stimuli, including epidermal growth factor (EGF) and various TGF- β family members, such as TGF- β 1, Activin, and BMP-7 (Miyazono et al., 2005).

Smurfs

Smads can be regulated at the level of degradation which is controlled by the ubiquitin-proteasome system. Ubiquitin is a highly conserved protein that covalently binds and recruits target proteins for their degradation by the proteasome. It regulates in particular the level of nuclear factors and thereby modifies transcription (Conaway et al., 2002). Two closely related Smurfs (Smad ubiquitination regulatory factors), Smurf1 and Smurf2, have been identified in vertebrates and are mediators of the final step in ubiquitination of target proteins (Zhu et al., 1999). Smurfs, containing HECT catalytic domains characteristic of E3-ubiquitin ligases, induce export of I-Smads from the nucleus to the cytoplasm and interact with activated type I receptors through I-Smads. In fact, interaction of I-Smads with type I receptors is enhanced by Smurfs, resulting in suppression of TGF- β signaling (Ebisawa et al., 2001; Kavsak et al., 2000). Moreover, Smurfs induce ubiquitin-dependent degradation of the type I receptors and R-Smad, leading to down-regulation of the number of receptors and R-Smad (Lin et al., 2000;

Miyazono et al., 2005; Zhang et al., 2001).

Ski* and *SnoN

Ski is a nuclear oncoprotein homologous to the transforming protein (v-Ski) of the avian Sloan-Kettering retrovirus, which is an important TGF- β negative regulator. SnoN is structurally closely related to Ski. Ski interacts with the Smad 2/3 and Smad 4, interfering with the formation of functional Smad complex (Luo, 2003). Ski inhibits TGF- β and BMP signaling through several mechanisms: 1) stabilization of pre-formed Smad complexes on DNA preventing the access of newly activated Smads to the Smad binding element; 2) interference of Smad binding to transcriptional activators; and 3) recruitment of nuclear co-repressors and the histone deacetylase complex (HDAC) (Suzuki et al., 2004).

Tob

The transducer of ErbB-2 (*tob*) gene is a member of the PC3/BTG/*Tob* family of genes, which are involved in cell replication and differentiation. *Tob* decreases BMP signaling by binding Smad 1/5/8 and by interacting with BMP type I receptors associated with I-Smads. The *tob* gene is expressed in osteoblastic cells and its transcript levels are up-regulated by BMP-2 (Gazzerro and Canalis, 2006; Yoshida et al., 2003).

1.5.2 Membrane Receptor Modulation

The transmembrane protein BAMBI (BMPs and Activin membrane bound inhibitor), playing a role in attenuating BMP signaling, was identified in *Xenopus*. BAMBI encodes a TGF- β pseudoreceptor, which is a putative transmembrane protein with an extracellular domain similar to that of type I TGF- β and BMP receptors, but lacks intracellular serine/threonine kinase domain. BAMBI interferes with BMPs, Activin, and TGF- β signaling by stably associating with type IA and IB BMP receptors, thus preventing the formation of active receptor complexes. BAMBI is co-expressed with BMP-4 during embryogenesis and plays a critical role in defining BMPs action in embryo dorsalization

(Onichtchouk et al., 1999). BAMBI is expressed in terminally differentiated osteoblasts and its transcripts are up-regulated by BMPs, TGF- β and Wnt (Kalajzic et al., 2005).

1.5.3 Extracellular Modulation

In the extracellular space, there is another control system to modulate BMPs action through a group of secreted polypeptides. These extracellular BMP antagonists prevent BMP signaling by binding BMPs, therefore precluding their binding to specific cell surface receptors. Extracellular BMP antagonists include noggin, Dan family members, twisted gastrulation, follistatin and Chordin family members.

Noggin

Noggin is secreted as a homodimeric glycosylated protein. The primary structure of noggin consists of an acidic aminoterminal region and a cysteine-rich carboxyterminal region containing a cystine knot. Noggin binds to BMP-2/4/5/6/7, GDF-5/6 with various degrees of affinity, but not to other members of the TGF- β family (Gazzerro and Canalis, 2006). The crystal structure of the antagonist Noggin binding to BMP-7 show that Noggin inhibits BMP signalling by blocking the binding epitopes for both type I and type II receptors (Groppe et al., 2003).

Noggin was first isolated from *X. laevis* based upon its ability to rescue dorsal development in embryos ventralized by UV treatment (Smith and Harland, 1992) and is expressed during early stages of gastrulation in the Spemann organizer (McMahon et al., 1998). In the zebrafish embryo, three noggin orthologues have been isolated, *noggin1*, *noggin2*, and *noggin3*. *Noggin1* is expressed in the organizing center of the zebrafish, and *noggin2* transcripts first appear at the end of gastrulation. Both genes are expressed during somitogenesis and during formation of the nervous system. *Noggin1* and *noggin2* overexpression strongly dorsalizes the embryo, and play a role in dorsoventral patterning of the zebrafish (Bauer et al., 1998). During the early stages of mouse embryonic development, *noggin* is expressed in the node. Later on in mouse embryonic development, *noggin* expression is seen in the notochord, the roof of the neural tube, the dorsal aspect

of the somites, and the limbs. Expression of noggin in these later sites has profound effects on development (Bachiller et al., 2000). Noggin's function is essential in skeletal and joint development in mice: homozygous mice for noggin-null mutant had excess cartilage and failed to initiate joint formation (Brunet et al., 1998). The importance of the noggin gene was confirmed by human studies, which demonstrated that different heterozygous missense mutations of noggin coding sequence lead to proximal symphalangism and multiple synostosis syndromes (Gong et al., 1999; Marcelino et al., 2001). The gene substitutions identified in these patients seem to affect noggin protein folding and stability rather than BMP binding affinity (Groppe et al., 2003).

Dan Family

Differential screening-selected gene aberrative in Neuroblastoma (Dan) is a member of Dan family of secreted glycoproteins capable of binding BMPs. At least nine members of the Dan family have been described: Gremlin, Dan, uterine sensitization associated gene (USAG-1), Cerberus, Caronte, Coco, protein related to Dan, Cerberus (PRDC) and Dante. Protein sequence alignments reveal that these proteins share a common carboxyterminal cysteine-rich domain consisting of nine cysteines. Outside the cysteine-rich domain, they have limited homology. Most of the Dan family members can bind to BMP-2/4/5/6/7 with various degrees of affinity and have the capability of inhibiting BMP signaling. Most of the members of the Dan family are expressed primarily during embryonic development and play a minor role in skeletogenesis. Gremlin, however is an important regulator of BMP activity in the adult skeleton (Gazzerro and Canalis, 2006).

Twisted gastrulation

Twisted gastrulation (Tsg) is a secreted glycoprotein which was originally identified in *Drosophila* and is required for the proper establishment of the dorso-ventral axis (Mason et al., 1994). Tsg is expressed during embryonic development and in a wide variety of adult tissues (Oelgeschlager et al., 2003).

Tsg has two evolutionary conserved cysteine-rich domains. The amino-terminal cysteine-rich domain has some analogies with the cysteine-rich domains of Chordin and

is responsible for a direct interaction between Tsg and BMP-2/-4. The carboxy-terminal region does not have significant homology to known protein motifs, and interacts with Chordin. Tsg display both BMP antagonist and agonist functions. As a BMP antagonist, Tsg binds directly with BMP-2/4 or generates a trimolecular complex with a BMP-Chordin preformed complex, which is more efficient than its individual components in inhibiting BMP signaling (Chang et al., 2001; Ross et al., 2001; Scott et al., 2001; Wills et al., 2006). As a BMP agonist, Tsg can enhance Chordin cleavage by tolloid/xolloid, and prevent the residual anti-BMP activity of Chordin proteolytic products (Larrain et al., 2001; Oelgeschlager et al., 2000). The relative levels of Tsg, Chordin, and tolloid/xolloid appear to dictate whether Tsg inhibits or enhances BMP actions in a specific cell environment.

Follistatin

The follistatin protein has been isolated on the basis of its involvement during the reproductive cycle and is expressed in a wide range of embryonic and adult tissues, including brain, testis, ovary, bone marrow, placenta, and the anterior pituitary (Patel, 1998). Follistatin was initially identified as an Activin-binding protein that prevents Activin from binding to its receptor (Hemmati-Brivanlou et al., 1994), but it also can bind BMP-2, -4 and -7 (Iemura et al., 1998; Yamashita et al., 1995).

The three dimensional structure of follistatin-Activin complex is known. In follistatin-Activin complex, two follistatin monomers surround the dimeric ligand and bury the binding sites for type I and type II receptors (Harrington et al., 2006; Thompson et al., 2005). Mutational analysis revealed that only residues at the type II receptor-binding surface of Activin are critical for high-affinity follistatin binding and the interaction surface of Activin for type II receptors and follistatin are overlapping but not identical (Harrison et al., 2006).

Chordin Family

This thesis focuses on the Chordin family member Chordin-like 2. Therefore the introductions of Chordin family and Chordin-like 2 are listed under separate subtitles

below (see 1.5.4 and 1.6).

1.5.4 Chordin family

VWC-containing proteins

As described above, the activity of BMPs is modulated by a large number of extracellular regulator proteins. These proteins include Chordin-like proteins which contain Von Willebrandt factor type C (VWC) domains. VWC domain, also called cysteine-rich domain (CR), typically contains less than 100 residues and have in common a conserved CXXCXC motif in the middle and CCXXC motif in the carboxyterminus. Otherwise, the sequences of the VWC domain are highly diverse. The VWC exists in about 500 extracellular proteins from drosophila to human (82 proteins in h. sapiens and 85 proteins in m. musculus, available at www.sanger.ac.uk/cgi-bin/Pfam/getacc?PF00093). The cellular role of most VWCs is as yet unknown. For some VWCs existing in proteins of the Chordin family, however, it has been established that they bind BMPs and thereby modulate their activity during development. These proteins play important roles in development and diseases. The VWC-containing proteins, no matter if they inhibit or promote BMP activity, all bind BMPs via their VWC domains. These proteins include Chordin, Kielin, Crossveinless-2, members of CCN family, Chordin-like 1, Chordin-like 2 and others (Garcia Abreu et al., 2002).

Chordin is a typical VWC-containing protein and its VWC domains are shown in Figure 1.7 (Garcia Abreu et al., 2002; Zhang et al., 2007) and Figure 1.8. Chordin has four VWC domains of about 70 amino acids each. These domains, particularly VWC1 and VWC3, determine the function of Chordin and its ability to bind BMPs. Chordin binds specifically BMP-2/4/7 and prevents their interaction with BMP receptors (Larrain et al., 2000; Piccolo et al., 1996).

Chordin was initially identified in the *Xenopus* Spemann Organizer for its ability to antagonize BMP action and is the homolog of Short Gastrulation (Sog) in *Drosophila*. Chordin is highly expressed in undifferentiated chondrocytes where it acts as an inhibitor of cell differentiation. The levels of Chordin decline in mature cartilage tissue (Gazzerro and Canalis, 2006). Chordin deficient mice demonstrate early lethality and a ventralized

gastrulation phenotype (Bachiller et al., 2000). Surviving mutant embryos die perinatally, and they display an extensive array of malformations in pharyngeal and cardiovascular organization that encompass most features of *DiGeorge* and *Velo-Cardio-Facial* syndromes in humans (Bachiller et al., 2003).

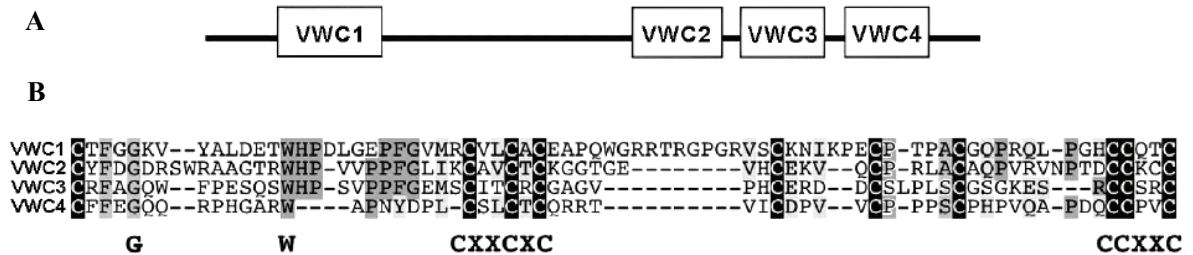


Figure 1.7: Diagram showing the position of the four VWCs (VWC1–4) of Chordin (A) and sequence alignment showing amino acid similarities between VWC-1, VWC-2, VWC-3 and VWC-4 of human Chordin (B). Ten cysteines highlighted in black are conserved and present in a typical spacing found in all vertebrate Chordins, in *Drosophila* Sog and in many VWC-containing proteins. A glycine (G), tryptophan (W) and the CXXCXC and CCXXC motifs are highly conserved among VWCs. (Garcia Abreu et al., 2002)

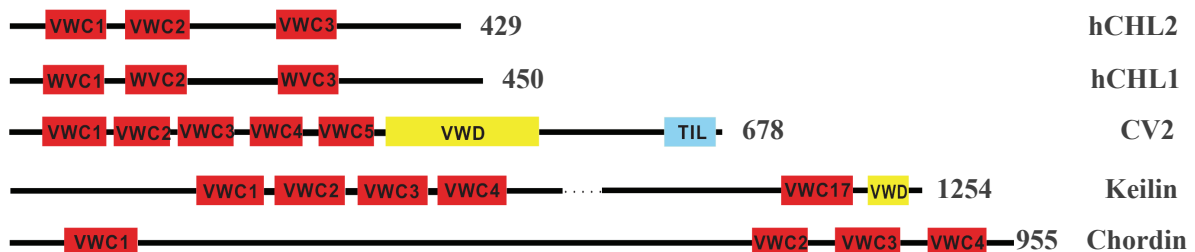


Figure 1.8: Domain composition of VWC containing proteins. hCHL2, human Chordin-like 2; hCHL1, human Chordin-like 1; CV2, crossveinless-2 (Chicken); Keilin (mouse); Chordin (human). VWC, Von Willebrandt factor type C domain; VWD, Von Willebrandt factor type D domain; TIL, trypsin Inhibitor-like cysteine-rich domain.

Chordin is regulated by interactions with other secreted proteins of the extracellular matrix, such as the zinc metalloprotease Tolloid/Xolloid, which cleaves Chordin to inactivate its biological activity and to release free BMPs to the extracellular space (Piccolo et al., 1997). Tolloid/Xolloid is expressed in articular and growth plate chondrocytes and in osteoblastic cells (Reynolds et al., 2000). The proteolytic activity of Tolloid/Xolloid is specific for Chordin and does not modify the action of other BMP

antagonists. Tolloid/Xolloid action can be inhibited by secreted Frizzled-related protein (sFRP) -Sizzled. The Xolloid-related proteinase has similar affinities for its endogenous substrate Chordin and for its competitive inhibitor Sizzled. Therefore Sizzled can competitively inhibit Chordin binding to the active site of the Xolloid-related metalloprotease, and thus stabilize Chordin levels and regulate BMP signaling in the embryo (Lee et al., 2006).

Chordin cleavage by Xolloid is modulated by Tsg. Tsg has two distinct and sequential activities on BMP signaling. First, Tsg makes Chordin a better BMP antagonist by forming a ternary complex that prevents binding of BMP to its cognate receptor. Second, after full-length Chordin is cleaved by Xolloid, Tsg competes the residual anti-BMP activity of Chordin fragments and facilitates their degradation, providing a permissive

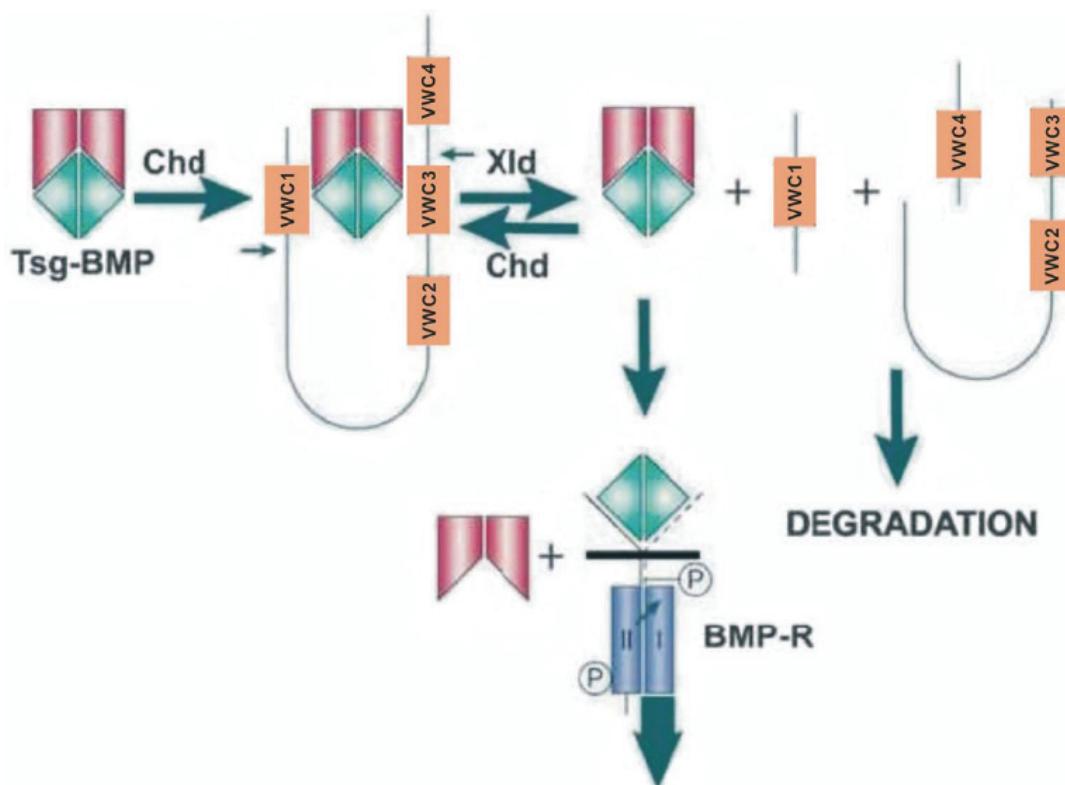


Figure 1.9: Model for a biochemical pathway that regulates BMP signaling in the extracellular space. This model explains why Tsg has the dual ability to increase BMP antagonism by full-length Chordin and to promote BMP signaling after Xolloid cleavage. Tsg-BMP complexes can be bound by full-length Chordin to form a ternary complex that is a potent BMP antagonist. Xolloid cleaves Chordin releasing Tsg-BMP binary complexes and Chordin fragments. In the presence of full-length Chordin, the binary complex will re-bind to Chordin, reforming the ternary complex. After full-length Chordin is cleaved by Xolloid, however, Tsg is able to dislodge BMP from Chordin and to destabilize the Chordin proteolytic products, displacing the equilibrium. (Modification from Larrain J et al. 2001).

signal that promotes BMP binding to its cognate receptor. Therefore Tsg has the dual ability to increase BMP antagonism by full-length Chordin and to promote BMP signaling after Xolloid cleavage (Figure 1.9)(Larrain et al., 2001).

In addition, another model for Chordin (Sog) regulating mechanism in which Chordin/Tsg functions as BMP transporter has been described in *drosophila* (Shimmi et al., 2005). Decapentaplegic (Dpp) and Screw (Scw), the homologues of vertebrate BMP2/4 and BMP6/7, are required for patterning the dorsal surface of the *drosophila* blastoderm embryo. The ventral/dorsal sides of *drosophila* are reverse to those in vertebrate. In *drosophila*, Thick veins (Tkv) and Saxophone (Sax) are type I receptors that act synergistically to transduce the Dpp and Scw signals, respectively (Haerry et al., 1998; Neul and Ferguson, 1998; Nguyen et al., 1998). Signaling of Dpp/Scw is regulated at the extracellular level by the BMP binding proteins Sog and Tsg. Homodimers and heterodimers of Dpp and Scw are produced throughout the dorsal domain. Sog is expressed and secreted in the ventral lateral region and diffuses toward the dorsal side. Dpp and Scw homodimers do not bind to Sog and Tsg with high affinity and produce only low-level signals that can activate targets. In contrast, Dpp/Scw heterodimers bind with high affinity to Sog and Tsg. Net flux of the complex toward the dorsal midline leads to an increase in the heterodimer concentration at the midline. Tolloid processes Sog at the midline to release the ligand, which then binds to a receptor complex containing both Sax and Tkv. This complex produces a synergistic high signal that activates high-level response genes and leads to specification of the amnioserosa, a typical phenotype of BMP-enhancing (pro-BMP) activity of Sog/Tsg in *Drosophila*. So the heterodimer of Dpp and Scw, but not the Dpp homodimer, is the primary transported ligand and the heterodimer signals synergistically through the two type I BMP receptors Tkv and Sax. The Dpp/Scw heterodimer is a preferred binding partner for Sog/Tsg and preferentially stimulates Sog cleavage by Tolloid (Figure 1.10).

Kielin is a kind of Chordin-like secreted protein of *Drosophila* which contains 27 VWC domains. Kielin also contains an aminoterminal TSP domain and a carboxylterminal Von Willebrandt factor type D (VWD) domain (Matsui et al., 2000). Mouse

Kielin/Chordin-like protein (KCP), the homology of *Drosophila* Kielin which contains 17 VWC domains, could attenuate the pathology of renal fibrotic disease by enhancing BMP signaling while suppressing TGF- β activation (Lin et al., 2005; Lin et al., 2006). It binds BMP7 and enhances the BMP7 binding to type I receptor. However, which domain of Kielin is involved in BMP binding is unknown.

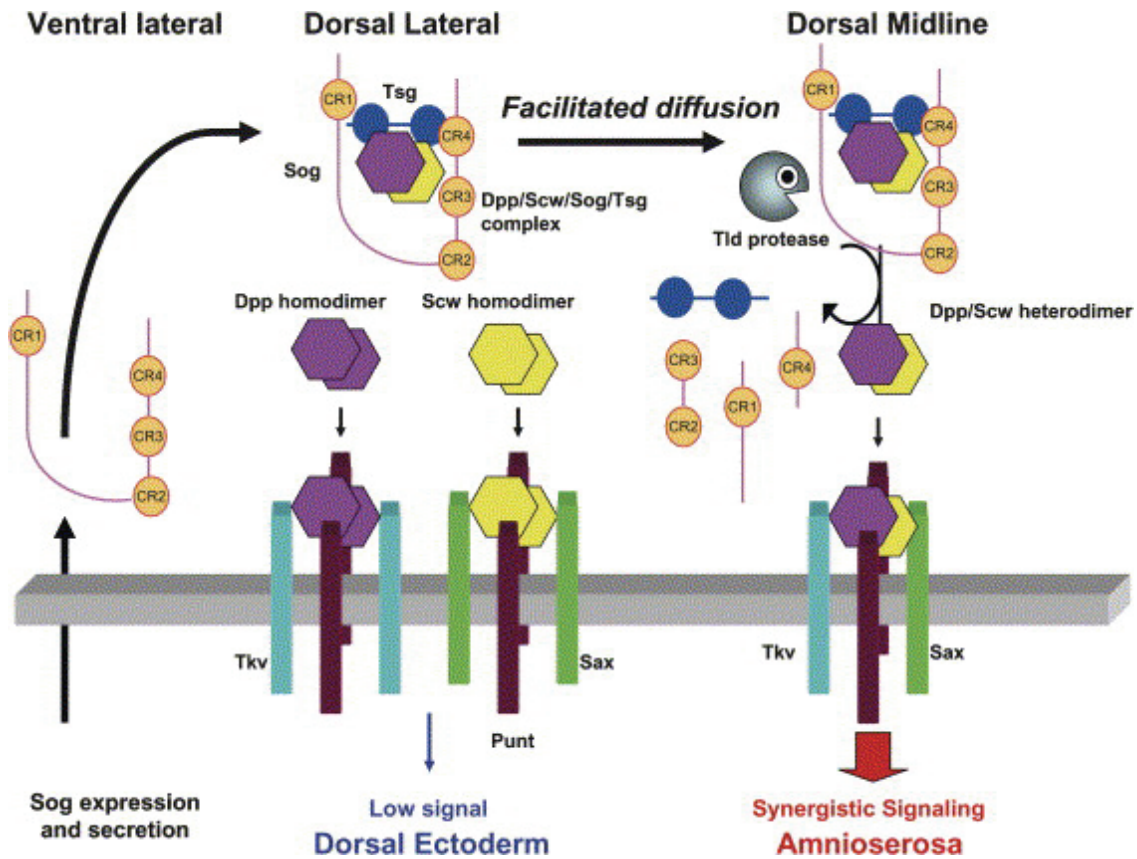


Figure 1.10: Model for patterning dorsal tissues in the *Drosophila* embryo. Homodimers and heterodimers of Dpp and Scw are produced throughout the dorsal domain. Sog is expressed and secreted in the ventral lateral region and diffuses toward the dorsal side. Dpp and Scw homodimers do not bind to Sog and Tsg with high affinity. As a result, they are free to bind with receptors, but they produce only low-level signals that can activate targets. In contrast, Dpp/Scw heterodimers bind with high affinity to Sog and Tsg. Net flux of the complex toward the dorsal midline leads to an increase in the heterodimer concentration at the midline. Tolloid (Tld) processes Sog at the midline to release the ligand, which then binds to a receptor complex containing both Sax and Tkv. This complex produces a synergistic high signal that activates high-level response genes and leads to specification of the amnioserosa (Shimmi et al., 2005).

***Crossveinless-2* (CV2)** is a secreted protein that contains five VWC domains and a VWD domain at the carboxyterminus (Figure 1.8; Conley et al., 2000). CV2 plays essential pro-BMP roles in mouse organogenesis (Ikeya et al., 2006) and zebra fish gastrulation

(Rentsch et al., 2006). On the other hand, CV2 can also inhibit BMP signaling in certain context, especially in cell culture experiments (Binnerts et al., 2004). CV2 binds to BMP-2 via its VWC1 domain with high affinity and CV2-VWC1 domain governs all the binding affinity of CV2 to BMP (Zhang et al., 2007). Similar to full-length CV2, CV2-VWC1 could simultaneously block the binding of BMP-2 to both type I and type II receptors.

Chordin-like 1 (CHL1) contains three VWC domains (Nakayama et al., 2001). It is also called neuralin-1 (mouse) (Coffinier et al., 2001) or ventroptin (chick retina) (Sakuta et al., 2001). It antagonizes BMP-4,-5 and -6 and weakly interacts with TGF- β 1 and - β 2 in vitro (Nakayama et al., 2001; Sakuta et al., 2001). CHL1 interacts directly with BMPs in a competitive manner to prevent binding of BMPs to the type I BMP receptor ectodomain (Nakayama et al., 2001).

On mouse embryos CHL1 expression starts at neural plate stage and extends to the entire neural plate at late headfold stage. The latter neural expression becomes restricted to discrete regions of the forebrain and midbrain, as well as in the closing posterior neural folds. Starting at much later mouse embryos, CHL1 expression is observed in a population of neural crest cells that migrate from the hindbrain and colonize the branchial arches. In addition, the dorsal root ganglia and other neural crest derivatives are positive for CHL1 expression. During organogenesis, CHL1 expression in the nervous system is observed in dorsal root ganglia and in superficial layers of the CNS (Coffinier et al., 2001). In the adult brain, CHL1 (also called Neurogenesis-1) mRNA was intensely expressed in the hippocampus and moderately around the lateral ventricle. Immunohistochemistry revealed that astrocytes in the hippocampal dentate gyrus and the dentate granule cells adjacent to neural stem cells abundantly secreted CHL1. These results indicate that CHL1 also participates in adult hippocampal neurogenesis and induces neuronal differentiation in the adult brain (Ueki et al., 2003). Furthermore, high expression levels are seen in the developing skeletal structures, including limb bones, clavicles, calvaria, vertebra, and ribs. In the adult mouse, CHL1 is expressed in lung, kidney, and testis. Expression of CHL1 in nonskeletal mesenchymal cells has been demonstrated in many adult connective tissue cell types (Nakayama et al., 2001). CHL1

may function as a modulator of the BMP signaling in the neural plate and in bone formation, as well as in other processes.

1.6 Chordin-like 2

1.6.1 Structure of CHL2 protein

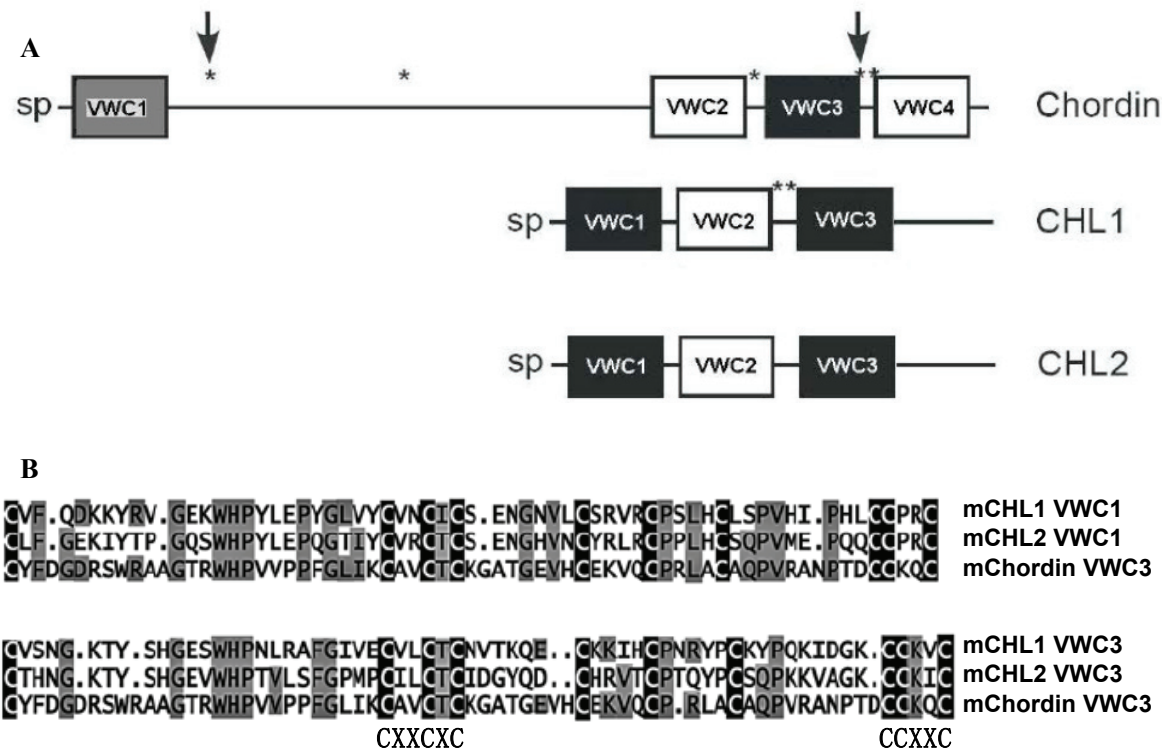


Figure 1.11: **A**, Schematic representation of chordin, CHL1 and CHL2. SP: signal peptide. The VWC1 and VWC3 regions in CHL1 and CHL2 (black boxes) are most homologous to VWC3 of chordin (in black). The chordin VWC1 (in gray) and VWC3 possess the BMP binding capability (Larrain et al., 2000). Putative BMP1/Tolloid cleavage sites are indicated with an asterisk, while actual Tolloid cleavage sites (Scott et al., 1999) are shown by vertical arrows. **B**, Amino acid sequence alignment showing sequence similarities between VWC1 or VWC3 of mouse CHL1 and CHL2, and VWC3 of mouse chordin. Ten conserved cysteines (highlighted in black) are found in the spacing typical of vertebrate chordin. Other conserved amino acids are highlighted in gray (Nakayama et al., 2004). The CXXXCX and CCXXC motifs are highly conserved among VWCs.

Chordin-like 2 (CHL2) is a novel Chordin-like protein, and structurally most homologous to CHL1 and Chordin. CHL2 contains a signal peptide and three VWC domains. Mouse CHL2 (mCHL2) and human CHL2 (hCHL2) contain 426 and 429 amino acids respectively. hCHL2 has 73% amino acids homology to mCHL2 (Nakayama et al., 2004). Figure 1.11 shows the sequence alignment of the mouse Chordin, CHL1 and CHL2 proteins and their VWC domains, indicating their high similarity. Between CHL1 and

CHL2, the similarity is further indicated in their length and amino acid sequence, the number and location of the VWC domains. The homology between CHL1 and CHL2 proteins is confined primarily to the VWC domains. A higher level of conservation is observed within each of the VWC domains, and highest is within VWC3 repeats (Nakayama et al., 2004).

1.6.2 Structure of CHL2 gene

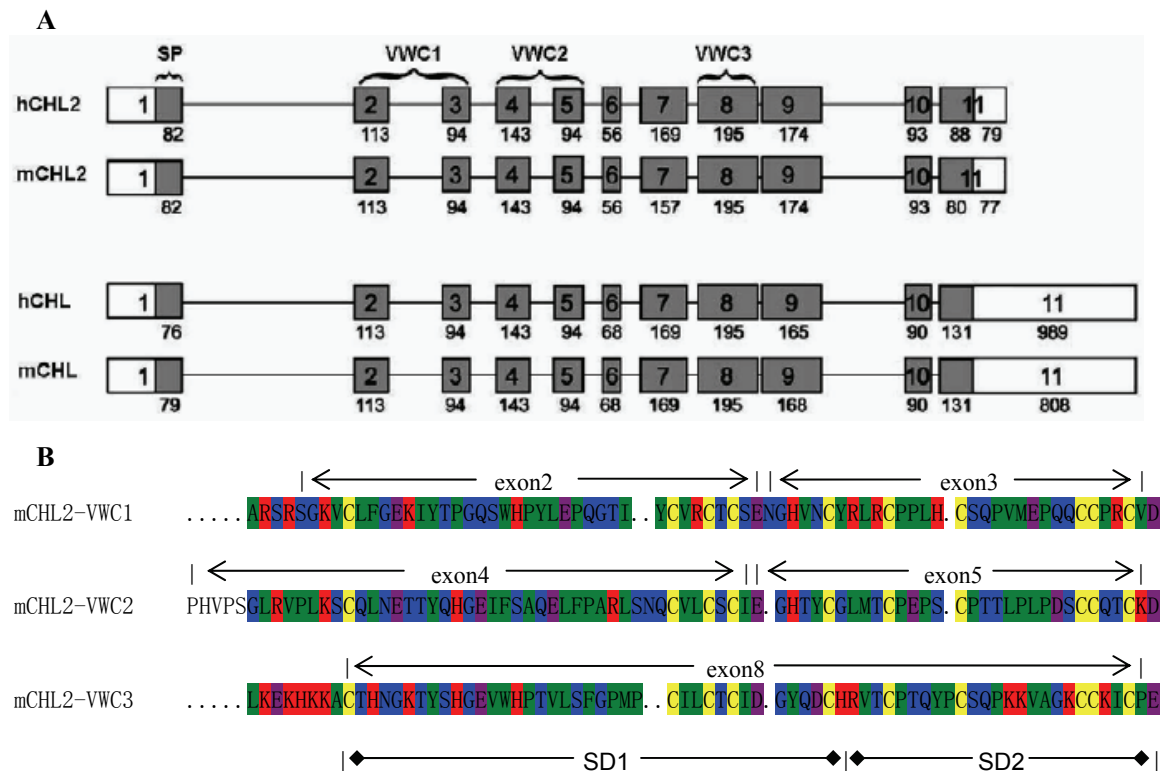


Figure 1.12: **A**, Schematic representation of the human and mouse CHL2 and CHL genes showing the intron– exon genomic organization of the genes. Exons are depicted as boxes, and their size is given in base pair. Introns, not drawn to scale, are shown as thin lines. Coding and untranslated sequences are depicted in gray and white, respectively. Sequences encoding for the signal peptide (SP) and the VWC domains are indicated on top. Note that VWC1 and VWC2 are each encoded by two exons, while VWC3 is encoded by a single exon (Oren et al., 2004). **B**, Sequence alignment of VWC domains of mouse CHL2 (Multalin) showing the encoding of sub-domains of VWCs by different exon. The exons are indicated on top of the sequence. Residues are coloured according to conservation (hydrophobic: green; cysteine: yellow; positive charged: red; negative charged: purple; uncharged hydrophilic: blue. SD1 and SD2, sub-domains 1 and 2 of mCHL2-VWCs.

The observable similarity between CHL1 and CHL2 also extends to the structure of their respective genes, in both the human and mouse genomes, including the size of their exons

and the peculiar spacing of the VWC domains. In the human and mouse genomes, CHL2 genes are composed of 11 exons that span a region of about 35 and 28 kb respectively. The structures of the human and mouse CHL2 genes (Figure 1.12, A) are very similar, in particular regarding the exon–intron boundaries, size of exons, and spacing of VWC domains within the exons. Two VWC domains are encoded each by two exons: exons 2 and 3 encode for VWC1; exons 4 and 5 encode for VWC2. VWC3 is encoded only by exon 8 (Oren et al., 2004). The NMR structure of the Col IIA VWC domain shows that each VWC domain contains two sub-domains (SD1 and SD2) (O'Leary et al., 2004). For the VWC1 of mCHL2, exon 2 encodes SD1 and exon 3 encodes SD2. Exons 4 and 5 encode SD1 and SD2 of mCHL2-VWC2 respectively. However, exon 8 encode two sub-domains of mCHL2-VWC3 (Figure 1.12, B).

1.6.3 Normal expression of CHL2

Skeletal Expression

Northern blot analysis revealed little mCHL2 mRNA in the mouse embryo, in contrast to the abundant expression of mouse Chordin and mouse CHL1. In mouse embryos, mCHL2 mRNA showed expression restricted to the surface chondrocytes of developing joint cartilage. In the adult mouse, mCHL2 was weakly expressed in cartilage of the femoral head, patella, articular facets of vertebrae and the annulus fibrosus of intervertebral discs. In general, mCHL2 expression in adult cartilage was weaker than that of embryonic cartilage. mCHL2 in normal cartilage was confined to articular chondrocytes, especially in the superficial zone. mCHL2 also showed low to moderate expression in sternal cartilage during embryogenesis and in joint cartilages of adult paws. But mCHL2 transcripts were never detected in growth plate cartilage or bone during development or adulthood. Thus, among skeletal compartments, mCHL2 seems to be expressed preferentially in the superficial zone chondrocytes of developing articular cartilage (Nakayama et al., 2004).

Non-Skeletal Expression

In mouse tissues, mCHL2 mRNA was shown to be expressed in the connective tissue of reproductive organs such as ligaments of the ovary and oviduct in females, and of testis, epididymis and certain male accessory sex glands in males. mCHL2 mRNA was also present in maternally derived placental tissues and uterine myometrium. Otherwise on the

mouse adult tissue blot, a faint mCHL2 transcript was detected in liver, kidney, skeletal muscle and testis extracts (Nakayama et al., 2004).

Northern blot analysis revealed hCHL2 transcript, which was highly expressed in uterus and was also detected in a variety of adult human tissues including colon, bladder, heart, stomach, prostate, ovary and testis (Nakayama et al., 2004; Oren et al., 2004). An analysis of fetal human tissues revealed expression of hCHL2 transcript in fetal liver. The immunohistochemical analysis of human tissues indicated expression of hCHL2 protein primarily in the secretory epithelial cells of uterine endometrium, fallopian tubes, endocervical glands, bladder, prostate, the transitional epithelium of the urinary bladder, as well as in bone osteoblasts (Oren et al., 2004).

1.6.4 CHL2 mRNA expression in diseased cartilage

In degenerating cartilage specimens from knees of adult humans, CHL2 mRNA was determined to be weakly expressed in human rheumatism (RA) patients, but expressed strongly in human osteoarthritis (OA) patients. Normally CHL2 is not relevant to normal pathways of chondrocyte proliferation and maturation. However, the upregulation of CHL2 transcripts specifically in middle zone cartilage of adult joints with OA revealed that CHL2 maybe has a role in cartilage repair by delaying and/or reducing the degree of chondrocyte hypertrophy, thereby amending cartilage degeneration. Thus CHL2 might negatively regulate cartilage formation/ regeneration in diseased joints (Nakayama et al., 2004). However, Aigner (Aigner, 2006) argued that an upregulation of CHL2 in osteoarthritic cartilage was not supported by two experimental evidences. First, he pointed out that upregulation of BMP-inhibitory activity in osteoarthritic cartilage did not agree with some of the published data, which have shown that an overall upregulation of anabolic activity occurs in osteoarthritic chondrocytes (Aigner et al., 1992; Lippiello et al., 1977), but not a downregulation. Second he argued that Nakayama (Nakayama et al., 2004) took osteophytic cartilage as osteoarthritic degenerated cartilage. Osteophyte tissues derive from mesenchymal precursor cells which become active matrix-producing chondrocytes after being in a chondroprogenitor cell state. Finally, some of the chondrocytes become hypertrophic. Osteophyte growth essentially re-capitulates chondroneogenesis in fetal development. Therefore, osteophytic chondrocytes resemble the fetal chondrocytes in many respects. Thus, in his opinion, Nakayama observed CHL2 being strongly expressed just in osteophytic chondrocytes, but not the chondrocytes of

osteoarthritic degenerated cartilage.

1.6.5 Interaction of CHL2 and BMPs

Nakayama et al. demonstrated that CHL2 bound directly to BMP-4 and prevented BMP-4 interacting with its BMPR-IB receptor. In cell-based assay CHL2 inhibited BMP-2/4/6/7 induced alkaline phosphatase (ALP) activity. The inhibitory potency is similar to noggin and stronger than that of Chordin (Nakayama et al., 2004).

1.7 Aims of the thesis work

The functions of VWC-containing proteins in development and diseases have been studied extensively. However, the structural basis of BMP/VWC-containing protein interaction is still poorly understood. VWC domains have been identified in more than 70 extracellular human proteins and seem to represent one of the most abundant protein modules. So far, only one structure of a VWC domain—the BMP-binding VWC domain of procollagen IIA, has been determined by NMR spectroscopy (O'Leary et al., 2004). But in that study, no possible binding epitopes were proposed and no binding activity for BMP was shown for the VWC domain used. VWC-containing proteins have different specificities and affinities for different BMPs. Therefore, different binding epitopes are likely to exist on the BMPs. To better understand the regulatory mechanisms of these proteins, it is necessary to know how these binding epitopes are constructed, how they overlap with the receptor-binding wrist and knuckle epitopes, and whether inhibitors could be generated for each type specifically.

In this article, the VWC domain-containing protein CHL2 was selected to study the structural basis of BMP-2/VWC protein interaction. The VWC domains in CHL2 that are involved in BMP binding are determined. The binding affinities, specificities and binding epitopes of BMP-2 for CHL2 and the interaction of CHL2/BMP-2 and Tsg, which is a novel partner of CHL2, were analyzed in detail. The isolation and crystallization of the complex of BMP-2 and CHL2 or its individual VWC domains hopefully will pave the way to solve the structures of these proteins.

2. Materials and Methods

The experiments described have been performed in the department of Physiological Chemistry II, University of Wuerzburg.

2.1 Abbreviations

ActR-IIB	Activin Type IIB Receptor
ALP	alkaline phosphatase
APS	ammonium persulfate
BMPR-IA	Bone Morphogenetic Protein Receptor Type IA
bp	base pair
cDNA	complementary deoxyribonucleic acid
CHL2	Chordin-like 2
Da	Dalton
DNA	deoxyribonucleic acid
dNTPs	deoxyribonucleoside triphosphates
dsDNA	double-stranded deoxyribonucleic acid
DTT	1,4-dithiothreitol
<i>E.coli</i>	Escherischia coli
EDTA	ethylene diamine tetraacetic acid
FCS	fetal calf serum
GDF	Growth and Differentiation Factor
HPLC	high pressure liquid chromatography
K_D	dissociation equilibrium constant
K_{off}	dissociation rate constant
K_{on}	association rate constant
LB	Luria Broth
mCHL2	Mouse Chordin-like 2
min	minute(s)

MTT	thiazolyl blue tetrazolium
MS	molecular standard
OD	optical density
PAGE	polyacrylamide gel electrophoresis
PCR	polymerase chain reaction
PEG	polyethylene glycol
pfu	plaque forming unit(s)
rpm	revolutions per minute
RT	room temperature
SDS	sodium dodecyl sulfate
SF9	<i>Spodoptera frugiperda</i> 9
ssDNA	single-stranded deoxyribonucleic acid
β -ME	β -Mercapoethanol
TB	Terrific Broth
TCA	trichloroacetic acid
TEMED	N,N,N',N'-tetramethylethylenediamine
TFA	trifluoroacetic acid
TGF- β	Transforming Growth Factor β

2.2 Chemicals

Basic chemicals of highest purity were purchased from Amersham, Biorad, Biolabs, Fluka, Gibco-BRL, Merck, NEB, Pharmacia, Promega, Pharmingen, Roth, Sigma. All solutions were prepared using deionized water of millipore quality.

2.3 Enzymes

Restriction endonucleases	MBI Fermentas
RNase	Roth/Sigma
Shrimp alkaline phosphatase (SAP)	Roche

T4-DNA Ligase MBI Fermentas

DNA Polymerases MBI Fermentas

2.4 Kits

DNA Preparation QIAGEN[®] Plasmid Kits, QIAGEN

Gel Extraction Wizard[®] SV Gel and PCR Clean-Up System, PROMEGA

DNA Sequencing CEQ[™] DTCS-QUICK Start Kit, BECKMAN

2.5 Vectors and oligonucleotides

2.5.1 Expression vector QKA for *E.coli*

QKA is a modified expression vector based on two old vectors, pQE-80L and pET-24a, for the cloning and expression of recombinant proteins in *E.coli*. It was constructed by replacing ampicillin resistance encoding sequence of pQE-80L vector with kanamycin resistance encoding sequence which came from pET-24a vector.

2.5.2 Baculovirus transfer vector pAcGP67-B/Th

The Baculovirus transfer vector pAcGP67-B/Th (PharMingen) provides a gp67 signal peptide, a thrombin cleavage site and C-terminal a 6x His-tag in frame with Bam HI. After co-transfection with Baculovirus DNA into SF9 cells, the cloned gene is expressed as a gp67 signal peptide fusion protein under the control of the strong Baculovirus polyhedron promoter.

2.5.3 Oligonucleotides

Oligonucleotides were synthesized and purchased by the MWG-Biotech Inc. in HPLC quality. Primers used for PCR mutagenesis, sequencing and PCR reactions are listed in the Table 2.1.

Table 2.1: Function and sequence of the used Oligonucleotides

Cloning of mCHL2 and mCHL2-VWC2, VWC3 to pAcGP67-B/Th/m	
EXM-s	5'-GTTGCTGATATCATGGAGATAA-3'
PAC-a	5'-TCCCAGGAAAGGATCAGATCTG-3'
PAC-Gs	5'-TCTAGAGCTGAGCAGGCCTTTGGTCCCTCGAGGAAGC-3'
PAC-Ga	5'-AGGCCTGCTCAGCTCTAGAAAGATCCGCCGCAAAGGC-3'
CHL-s	5'-GCGTCTAGACGATCCCGCTCGGGCAAAG-3'
CHL-a	5'-GCGAGGCCTTAATGTCTTGGTCACTTTG-3'
P-CR2s	5'-GACTCTAGAGTGGATCCTCATGTCCCC-3'
P-CR2a	5'-CTCAGGCCTCTCTCCATGCTGCAGCTG-3'
P-CR3s	5'-GACTCTAGATCAGTAGGAATGGGCAGC-3'
P-CR3a	5'-CTCAGGCCTCCGGGTGGAAATGACCTC-3'
Cloning of mCHL2-VWC1, VWC3 to QKA	
QKA-5'	5'-GGCTCATAACACCCCTTG-3'
Q-CR1-Sa	5'-TTTGCCCGAGCGGGATCGAGCCATGGTTAATTTCTC-3'
Q-CR1-Ss	5'-GAGAAATTAACCATGGCTCGATCCCGCTCGGGCAAA-3'
Q-CR1-a1	5'-GCCAGAGGGGACATGAGGGTCCACACACCT-3'
Q-CR1-a2	5'-TCTGGATCCCTATTAGCCAGAGGGGACATGAGG-3'
Q-CR3-Sa	5'-AGCTTTTTTATGTTTCTCCATGGTTAATTTCTCCT-3'
Q-CR3-Ss	5'-AGGAGAAATTAACCATGGAGAAACATAAAAAAGCT-3'
Q-CR3-a	5'-ACTGGATCCCTATTACGCCTCGTCCTCAGGGCA-3'
Site directed Mutagenesis of mCHL2	
CHL-1s	5'-TGCTCACAGCCTGTGATG-3'
CHL-2s	5'-CTGCCAGCTCCAGGAGACCACA-3'
CHL-3a	5'-TGTGGTCTCCTGGAGCTGGCAG-3'
CHL-4s	5'-CACAGAAGAACAGTTGACACAG-3'
CHL-5a	5'-CTGTGTCAACTGTTCTTCTGTG-3'

CHL-6a 5'-TGGCGTGCTGGGGCCTCT-3'

Site directed Mutagenesis of mCHL2-VWC3

CR3-M1s	5'-GGAGGTGTGGGACCCCACTGT-3'
CR3-M1a	5'-ACAGTGGGGTCCCACACCTCC-3'
CR3-M2s	5'-GTGTGGCACCGCACTGTGCTC-3'
CR3-M2a	5'-GAGCACAGTGCGGTGCCACAC-3'
CR3-M3s	5'-ACACAATGGGGACACATACTCCC-3'
CR3-M3a	5'-GGGAGTATGTGTCCCCATTGTGT-3'
CR3-M4s	5'-CACCCCACTGACCTCTCCTTTG-3'
CR3-M4a	5'-CAAAGGAGAGGTCAGTGGGGTG-3'
CR3-M5s	5'-CACTGTGCTCGCCTTTGGCCC-3'
CR3-M5a	5'-GGGCCAAAGGCGAGCACAGTG-3'
CR3-M6s	5'-CTCTCCTTTGCCCCCATGCC-3'
CR3-M6a	5'-GGGCATGGGGGCAAAGGAGAG-3'
CR3-M7s	5'-AAAGTGGCTGACAAGTGCTGCA-3'
CR3-M7a	5'-TGCAGCACTTGTCAGCCACTTT-3'

2.6 Bacterial strain

The following genotype *E. coli* was used:

MM294: ATCC 39607 F- supE44 hsdR17 endA1 thi-1 lambda

2.7 Cell line

SF9 cell line - a cell line, which was originally established from ovarian tissues of *Spodoptera frugiperda* larvae (Vaughn et al., 1977). SF9 cells may be grown in a monolayer or in a suspension.

2.8 BMP-2

BMP-2: Recombinant BMP-2 was a generous gift from Prof. W. Sebald, Wuerzburg.

2.9 Antibodies

For detection of Western Blot, the following antibodies were used:

Anti-His-tag McAb (QIAGEN)

Pod goat-Anti-mouse (Sigma)

2.10 Microbiological methods

2.10.1 Sterilization

Glasswares and other experimental materials were sterilized at 180 °C for 6 hours in a hot-air-cabinet (Heraeus, ST5060). Buffers, media and plastic containers were autoclaved (Sterico Vapoclav steam-steriliser) at 121 °C and 1.1 bar for 20 min. Solutions of temperature-unstable substances were sterilized by filtering through Millipore-Filter (MILLEX[®] GP, 0.22 µm, MILLPORE).

2.10.2 Culture media

LB-medium

10 g/L Peptone
5 g/L Yeast extract
10 g/L NaCL
Sterilized by autoclaving

LB-antibiotic plate

10 g/L Peptone
5 g/L Yeast extract
10g/L NaCL
15% Agar

The final concentration of antibiotics:
Ampicillin: 50ug/ml
Kanamycin: 30ug/ml
Tetracycline: 12.5ug/ml

Sterilized by autoclaving. When the agarose solution was cooled to 50°C, the antibiotics were added. After mixing, the agarose solution was filled into plates, cooled at RT and kept at 4°C

TB-medium		10x Pi Buffer	
13.3 g/L	Peptone	0.17 M	KH ₂ PO ₄
26.6 g/L	Yeast extract	0.72 M	K ₂ HPO ₄
4.4 ml/L	Glycerin		
Sterilized by autoclaving		Sterilized by autoclaving	

2.10.3 Culturing of bacteria

Glycerin stock-culture was spread over an agar plate and incubated at 37°C overnight. A colony was picked up and incubated in 2 ml of medium at 37°C for a day. This culture was further used for making larger culture.

2.10.4 Storage of bacterial culture

For short-term bacterial storage, 10 µl of glycerin stock-culture of bacteria was spread over an agar plate and incubated at 37°C overnight until colonies appeared. Such a plate can be kept for 4 to 6 weeks at 4°C.

For long-term bacterial storage, a single bacterial colony was cultivated in 50 ml of LB-medium with antibiotics at 37°C until the suspension reached OD₅₅₀ of 0.5. The following centrifugation was carried out at 4000 rpm for 10 min at 4°C. Then the pellet was washed with 40ml cold LB-medium for 2 times and resuspended in 1ml of LB-medium/antibiotics mixed with 1ml of sterilized glycerol. This culture can be kept at -20°C for several years.

2.10.5 Preparation of competent *E.coli* cells

Materials

Clean Bench	Heraeus LaminAir [®] HBB 2448 S
Millipore-Filter	MILLEX [®] GP, 0.22 µm, MILLPORE

TBS buffer 85% LB medium, 10% PEG8000, 5% DMSO, 50mM MgCL₂
(pH6.5). TBS was treated by Millipore-Filter, and pre-cooled at 4°C.

Procedure

E.coli MM294 colonies were picked off a freshly streaked plate derived from a frozen stock stored at -20°C and put into 2ml of LB medium in clean bench and incubated at 37°C for 2h. Then the 2ml of LB medium was added to 100ml LB medium and incubated at 37°C to OD 0.5. The culture was kept on ice for 5 min, and then transferred to two sterilized 50 ml Falcon-tubes followed by a centrifugation at 4000 rpm for 10min. For each tube the pellet was resuspended carefully in 10ml of TBS buffer. The competent cell suspension was aliquoted 200µl into the polypropylene tubes and put into liquid nitrogen for 20 sec. At the last the competent cell was kept at -80 °C.

2.11 Molecular biological methods

2.11.1 Site directed mutagenesis by PCR

Most of the mutations were generated by using a two-step polymerase chain reaction. The first step was performed in two different reactions - reaction 1a and reaction 1b. In reaction 1a (Figure 2.1; Table 2.2) the primer 2 carries the target mutation and the primer 1 is external. The primer 3, which was used in reaction 1b, was mutated and complementary to the primer 2 in reaction 1a. The primer 4 in reaction 1b was external.

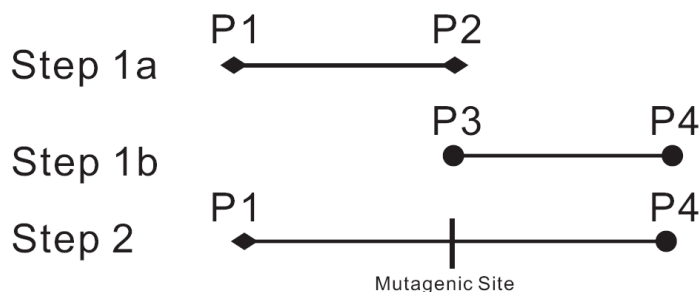


Figure 2.1: Two-step PCR procedure. Two-step PCR was used to generate a mutational cDNA which was synthesized during the second step of the PCR to gain the target mutation. P1 - P4, primer 1-4.

Table 2.2: PCR - reaction la and reaction lb

	Reaction la	Reaction lb
template	50 ng	50 ng
mutant primer	50 pmol (primer 2)	50 pmol (primer 3)
external primer	50 pmol (primer 1)	50 pmol (primer 4)
dNTPs	10 nmol	10 nmol
10 x Pfu polymerase buffer	5 μ l	5 μ l
Pfu polymerase	2.5 U	2.5 U
H ₂ O	to 50 μ l	to 50 μ l

The synthesized products from reaction la and lb were analyzed by an agarose gel and directly used as a template during the second step of the PCR generated mutagenesis. This recombinant PCR was performed with the two external primers used in the first step: the primer 1 from reaction la and the primer 4 from reaction lb (Figure 2.1; Table 2.3).

Table 2.3: Second step of PCR generated mutagenesis

	Reaction 2
template } reaction product la	2 μ l
} reaction product lb	2 μ l
primer 1 (from reaction la)	100 pmol
primer 4 (from reaction lb)	100 pmol
dNTPs	20 nmol
10 x Pfu polymerase buffer	10 μ l
Pfu polymerase	5 U
H ₂ O	to 100 μ l

All reactions were performed in safe-lock Eppendorf tubes with the following program (Table 2.4):

Table 2.4: PCR Program

Step	PCR-Program	
	Temperature, Time	Cycles
Initial denaturation	95 °C, 6 min	1
Melting	94 °C, 1 min	
Annealing	55 °C, 1 min	25-30
Elongation	72 °C, 1 – 2 min	
Final extension	72 °C, 10 min	1
Soak	4 °C, ∞	1

The product which was synthesized during the second step of the PCR contains the mutation of choice. After visualization on agarose gel, it was purified by Phenol/chloroform extraction and Ethanol precipitation for the further experiments.

2.11.2 Determination of the concentration of nucleic acids

The concentration of DNA can be roughly estimated by using an agarose gel electrophoresis. For amounts less than 200 ng, the fluorescence of the ethidium bromide, incorporated in the DNA fragments is proportional to the concentration of DNA. The intensity of the examined bands was compared to this of the DNA standards with known concentrations.

The concentration of nucleic acids also can be measured by spectrophotometry in the absorption spectrum range 240-320 nm. (CARY 50 Bio, UV-visible Spectrophotometer, VARIAN). Considering an extinction value of 1, the relation between A₂₆₀ and the concentrations is shown as follows:

Nucleic acids	Concentration
dsDNA	50ug/ml
ssDNA	33 ug/ml
Oligonucleotide	20ug/ml

2.11.3 Purification of DNA

2.11.3.1 Phenol/Chloroform extraction of DNA

The DNA containing fraction was mixed with the phenol (2:1 Vol.) adequately and later treated with chloroform (2:1 Vol.). After centrifuged at 15000 rpm for 5 min, the aqueous phase was transferred to a new tube. The aqueous phase was mixed with chloroform (1:1 Vol.), and the new aqueous phase was transferred to a new tube after centrifuged at 15000 rpm for 5 min.

2.11.3.2 Ethanol precipitation of DNA

DNA solutions were precipitated by adding 3M NaOAc/pH 8.0 (10:1 Vol.) and 100% cold ethanol (1:2.5 Vol.). The sample was thoroughly vortexed, incubated for 60 min at -20°C and centrifuged (10min, 15000 rpm). The pellet was washed with 70% cold ethanol and dried under vacuum. The pellet was dissolved in desired volume sterile dH₂O or TE buffer.

2.11.3.3 Gel extraction kit for DNA purification

After 2% agarose gel electrophoresis, the target DNA band was cut off on UV light panel and treated with the standard protocol of the Wizard[®] SV Gel and PCR Clean-Up System kit (PROMEGA).

2.11.4 Digestion of DNA

All restriction reactions were performed in the presence of recommended 10x reaction buffer. For analytical purposes, 100-500 ng DNA were digested in reaction volume of 10 µl, using 1-10 U restriction endonucleases. The reaction mix was incubated for 1 h at 37°C and stopped by incubated at 65°C for 30 min. Then 2-4 µl were examined by agarose gel electrophoresis. The DNA was purified by agarose gel electrophoresis and gel extraction kit, before it was used for ligation reaction.

2.11.5 Ligation of DNA to the vector

Materials

T4 DNA ligase, 10x T4 DNA ligase buffer (MBI)

Procedure

The vector/insert's molar ration of 1:3 was determined to be optimal. The total amount of DNA for cloning was 200ng per 10µl reaction volume. The reaction mixture, containing 1-5 U of T4 DNA ligases was incubated for 12-16 h (or overnight) at RT. The reaction was stopped by incubated at 65°C for 30 min. 10% samples from the ligation mixture

were loaded on an agarose gel to examine the reaction efficiency. The other recombinant plasmid DNA was directly used to transform to competent *E.coli*. Otherwise, it can be stored at -20°C.

2.11.6 Transformation of recombinant plasmid DNA to competent *E.coli*

10µl of DNA solution (DNA 50-100ng) were added to 200 µl aliquot of competent cell suspension and this mixture was incubated on ice for 30 min. A heat-shock was made at 42°C for 90 sec. After kept on ice for 2 min., 800 µl of LB medium was added and the mixture was continually incubated at 37°C for 1h. Then the transformed cell suspension was plated separately to antibiotic-plates with both a positive control and a negative control. The positive control was 0.1µg recombinant plasmid DNA transformed *E coli* cells and the negative control was 1-10ng linear vector transformed cells. The plates were incubated at 37 °C overnight to develop colonies of the transformed cells.

2.11.7 Mini-preparation of recombinant plasmid DNA

Materials

P1-Buffer: 50 mM, Tris/HCl, pH 8.0; 10 mM, EDTA

P2-Buffer: 0.2 M NaOH; 1 % (w/v) SDS

P3-Buffer: 2.8 M KAc, pH 5.1

Procedure

1. Inoculate a single colony in 5ml LB-Medium and incubate at 37°C overnight with shaking.
2. Collect cells by centrifugation at 10000 rpm for 5 min at RT and remove supernatant.
3. Resuspend bacterial pellet in 200µl P1-Buffer and then mix 300µl of P2-Buffer gently by inverting tube 6-8 times and incubate on ice for 5 min. Do not vortex to prevent the release of chromosomal DNA from the cell debris. Bacterial cells are

lysed by a NaOH/SDS solution. Chromosomal and plasmid DNA are denatured under this alkaline condition. It is important to control the duration of this step thoroughly.

4. Add 300µl of P3-Buffer for neutralization and mix like described above until a homogenous suspension is formed. Incubate on ice for 5 min. This step results in a precipitation of SDS, chromosomal DNA and other cellular compounds. Plasmid DNA stays in solution and reanneals to its supercoiled structure.
5. Centrifuge at 15000 rpm for 15 min at 4°C.
6. Transfer supernatant to a new cap and use Phenol/Chloroform Extraction method to purify the Plasmid DNA.
7. Precipitate DNA by adding 700µl of 2-propanol and centrifuge for 10 min at RT, 15000 rpm.
8. Rinse pellet twice with 70% Ethanol.
9. Briefly dry pellet (about 5 min at RT) with vacuum.
10. Resuspend DNA in 20µl water or suitable buffer.

2.11.8 Maxi-preparation of recombinant plasmid DNA

Materials

QIAGEN[®] Plasmid Kits, QIAGEN

Procedure

1. Inoculate a single colony in 2ml LB medium and incubate at 37°C overday with shaking. Then transfer the 2ml bacterial solution to 200 ml LB medium and incubate at 37°C overnight with shaking.
2. Collect cells by centrifugation at 10000 x g for 5 min at RT and remove supernatant.
3. Bacterial pellet was treated by the protocol of QIAGEN[®] Plasmid Kit.
4. Rinse pellet with 70% Ethanol and dry the pellet with vacuum pump.
5. Resuspend DNA in 100µl water or suitable buffer.

2.11.9 DNA sequencing

Materials

CEQ™ DTCS-QUICK Start Kit, BECKMAN

Procedure

According to manufacturer's protocol, sequencing PCR was performed with the Quick Start Mix of the CEQ™ DTCS-QUICK Start Kit followed the programs:

98 °C	96 °C	50 °C	65 °C	4 °C
2 min	0.2 min	0.2 min	4 min	Keep
30 cycles				

The DNA sequencing was performed by Beckman CEQ2000 automated DNA sequencer. The used method, according to Sanger, relies on the base-specific termination of the DNA chain elongation by random integration of labeled ddNTPs at the end of the chain. Four independent sequencing reactions were carried out for each analyzed DNA sample. Each reaction contained different chain-terminating ddNTP coupled to a corresponding fluorescent dye. Due to the different fluorescence, the single DNA fragments could be detected by an argon laser beam.

2.12 Protein chemical methods

2.12.1 Determination of the protein concentration

The concentration of a protein solution can be measured by spectrophotometry at the absorption spectrum range 250-320 nm (CARY 50 Bio, UV-visible Spectrophotometer, VARIAN). The absorbency value A at 280 nm was used for calculation. The concentrations of mCHL2, mCHL2-VWC1, VWC2, and VWC3 proteins per absorbency unit ($A_{280}=1$) and the path length equal to 1 cm are shown in the Table 2.5.

Table 2.5: Molar absorbency factor and concentration of mCHL2 and mCHL2-VWC1, VWC2, VWC3

Protein	Extinction coefficients (280nm) [$\text{mol}^{-1} \cdot \text{cm}^{-1}$]	Concentration per absorbency unit 1 [mg/ml]
mCHL2	41320	1.13
mCHL2-VWC1	12085	0.74
mCHL2-VWC2	3605	3.02
mCHL2-VWC3	10130	0.79
BMP-2	25791	0.68

2.12.2 Lyophilization of proteins

The purified protein was extensively dialysed against H_2O and frozen at -70°C overnight. The frozen protein were then transferred to the Lyophilizator (LDC-1, CHRIST), which was pre-cooled to -55°C and vacuum pumped to 0.02 bar overnight.

2.12.3 SDS - polyacrylamide gel electrophoresis

Materials

acrylamide solution	30% acrylamide, 0.8% N,N'-methylenebisacrylamide
4 x lower Tris	1.5M Tris-HCl, 0.4% SDS, pH 8.8
4 x upper Tris	0.5M Tris-HCl, 0.4% SDS, pH 6.8
glycerol	87% glycerol
Free radicals catalyst	TEMED
polymerization initiator	40% APS
SDS running buffer	25mM Tris-HCl pH 8.6, 190mM glycine, 0.15% SDS
SDS sample buffer	62.5mM Tris-HCl pH 6.8, 2% SDS, 20% glycerol. 2% BPB, 2% β -mercaptoethanol
staining solution	0.25% Coomassie Brilliant Blue R250 in destaining solution
destaining solution	1 Vol. acetic acid, 1 Vol. isopropanol, 8 Vol. H_2O

Procedure

In SDS-polyacrylamide gels, the proteins were separated by their molecular weight. The electrophoresis was performed in a vertical gel electrophoresis system Mini-V 8.10 (Gibco BRL). Different acrylamide concentrations can be used for different gel preparations depending on the size of the separated proteins. The separating gel solution was decanted between two vertical glass-slabs (layer thickness 0.75 mm) with a Pasteur pipette to 2/3 of the glasses upper edge and then covered with a water layer. After polymerization, the water was poured out, the stacking gel solution was filled on the top and a comb was immediately inserted.

The protein samples and SDS sample buffer (1:1) were mixed and boiled at 100°C for 5 min. A microlitre syringe was used to place the protein solutions in the wells of the slab. For each well 0.5-2 µg of protein was loaded. In the first lane, parallel to the samples, the protein standard was loaded. Until the samples were concentrating, the gels were running at 170 -200V.

After the end of the electrophoresis, the gel was placed for 30 min in a coomassie solution for staining. The destaining was done for more than 2h. The ready gel was kept 1 h in 20 % methanol and dried between two pieces of cellophane.

2.12.4 Concentration of protein samples by TCA

Materials

50% TCA, 100% ethanol, 1 M Tris-HCl (pH 8.0)

Procedure

When the protein concentration was low, concentration by 50% TCA was done before the sample was loaded on SDS-PAGE. 50% TCA (4:1 Vol.) and 100% ethanol (4:1 Vol.) was added to the protein sample. After mixing, the protein solution was incubated for 10 min on ice and then centrifuged for 10 min at 15000 rpm (Eppendorf Centrifuge). The pellet was dissolved in desired volume of SDS sample buffer. The yellow color of the solution indicates an acidic pH condition. Then 1µl of 1M Tris-HCl (pH 8.0) was added to

neutralize the acidic pH.

2.12.5 Protein mass spectroscopy

The precise molecular weight of protein was determined with a help of Dr. Werner Schmitz and Pro. Ernst Conzelman by the method of Fourier Transform-Ion Cyclotron Resonance mass spectroscopy. A detailed description of the method is available from Dr. Werner Schmitz upon request.

2.13 Western-Blot

Western blotting was used to verify the expression of mCHL2 by SF9 cells, after the second step of virus amplification.

Material:

Transfer buffer	25 mM Tris, 192 mM glycine, 20% methanol
3% milk solution	3g Skim Milk Powder (Fluka), 100µl Tween
	100 ml TBS: 100 mM Tris, 150 mM NaCl, pH 7.5
Primary antibody	Anti-His-tag McAb (QIAGEN)
Secondary antibody	Pod goat-Anti-mouse (Sigma)
Buffer A	5ml 0.1M, Tris, pH 8.5, 6 µl H ₂ O ₂
Buffer B	5ml Luminol (2.5 mM 3-Aminophthalhydrazide in 0.1 mM, pH8.5 Tris and 1% DMSO) , 22µl Enhancer (90 mM P-cumaric acid in 100% DMSO)
Nitrocellulose membrane	, Whatman paper
Blotting apparatus	Blot Module Mini-V8.10, Gibco BRL

Procedure

1. Collect virus solution of Second virus amplification (A2). Then centrifugate at 1000 rpm for 5 min and collect the supernatant.
2. 10 μ l of A2 virus supernatant mixed with equal volume of protein loading buffer was electrophoretically separated on a SDS polyacrylamide gel. The negative control was used a sample of equal volume, which contained only the medium for SF9 cells. The positive control was a sample of Chordin VWC1 with His tag (which was expressed by SF9 cell before) with known concentration.

Wet a Nitrocellulose membrane in water for 2 min and then in transfer buffer for 5 min with two pieces of Whatman papers and transfer pads. The gel and its attached Nitrocellulose membrane were sandwiched between two pieces of Whatman papers and two transfer pads. To be sure there were no air bubbles between gel and nitrocellulose membrane. The blotting apparatus, containing the 'sandwich', was placed in electrophoresis chamber filled with transfer buffer. The nitrocellulose membrane was toward to anode. Then transfer for 1 hour at 150 V. At this step, the proteins were transferred from gel to the nitrocellulose membrane.

3. Block
 - 3.1 Wash the nitrocellulose membrane 2 times with TBS buffer for 10 min.
 - 3.2 Incubate the nitrocellulose membrane in 10 ml milk solution for 1 hour at RT or alternatively overnight at 4°C (Remain shaking).
4. Primary antibody

Incubate the nitrocellulose membrane in 7 ml milk solution with 7 μ l primary antibody (diluted 1: 1000-2000 in milk solution) for 1 hour at RT or alternatively overnight at 4°C (Remain shaking).
5. Secondary antibody
 - 5.1 Wash the nitrocellulose membrane 3 times with 10 ml milk solution for 10 min.
 - 5.2 Incubate the nitrocellulose membrane in 7 ml milk solution with 3.5 μ l secondary antibody (diluted 1: 5000-10000 in milk solution) for 1 hour at RT (Remain shaking).
 - 5.3 Wash the nitrocellulose membrane 3 times with 10 ml milk solution for 10 min and dry.

6. In dark room, mix buffer A and buffer B. Then incubate the nitrocellulose membrane in the mixed solution for 3 min at RT. The nitrocellulose membrane was shortly dried, exposed to an X-ray film for 5 seconds. At the last the film was developed.

2.14 Expression of recombinant protein in *E.coli*

2.14.1 Analytical protein expression

Analytical protein expression should be used prior to large-scale purification to check clones for expression of the desired protein with help of SDS-PAGE analysis.

Materials

LB-medium (Antibiotics are added depends on expression vector and bacterial host.)

100 mM IPTG stock solution, 2x SDS loading buffer

Procedure

1. Inoculate a single, well isolated colony of *E. coli* transformed with the recombinants into separate tubes containing 2 ml of LB-medium plus necessary antibiotics.
2. Grow liquid cultures to an OD₅₅₀ of 0.6-0.8 (3-5 hours) with vigorous agitation at 30-37 °C.
3. Take 1ml of non-induced bacterial culture for later control in SDS-PAGE analysis.
4. Induce protein expression by adding 10 µl of 100 mM IPTG (final concentration is 1 mM) to 1ml bacterial culture.
5. Continue incubation for an additional 3 h.
6. Centrifuge 100µl control and induced sample in a microcentrifuge for 1 min. at 15000 rpm, discard the supernatants.
7. Dilute the disrupted cells in 30µl 2x SDS loading buffer.
8. The protein expression rate was investigated with SDS-PAGE analysis and could be quantitatively evaluated by scanning densitometry.

2.14.2 Preparative protein expression

Materials

LB-medium, TB-medium (antibiotics are added depending on expression vector and bacterial host)

Procedure

1. Overday culture

1.1 Inoculate a single, well isolated clone of *E.coli* transformed with the recombinant into glass tube containing 2 ml of LB-medium plus necessary antibiotics.

1.2 Incubate for 3-4 hours at 37°C with vigorous shaking.

2. Overnight culture

Dilute the overday culture into 240 ml LB-medium plus necessary antibiotics at 37°C with shaking over night.

3. Fermentation

3.1 Add 720 ml TB medium, 80 ml 10xPi, 20-40 ml Overnight culture and necessary antibiotics into an Erlenmeyer flask.

3.2 Cultivate the cells at 37°C until they reach early states of logarithmic growth phase (OD₅₅₀ 0.5-0.7).

3.3 Add IPTG (1mM) to cells and cultivate continuously for an additional 3-4 hours.

4. Harvest

4.1 Transfer the culture to JA-10 centrifuge beakers and Centrifugate at 6000 rpm for 20 min at 4°C.

4.2 Resuspend the pellet with TBSE buffer plus β-ME (1:1000 dilute) and Centrifugate at 6000 rpm for 20 min at 4°C again.

4.3 Freeze the cells at -20°C.

2.14.3 Preparation of inclusion bodies

Materials

TBSE Buffer 10 mM Tris, 150 mM NaCl, 1 mM EDTA, pH 8.0

PMSF stock 100 mM PMSF (Phenylmethylsulphonylfluoride) in isopropanol

Procedure

1. Resuspend 20g cell pellet in 200 ml $TBSE_{\beta-ME}^{PMSF}$ (1mM PMSF, 1:1000 diluted β -ME), and sonicate the cells for 5 min at 300 Watt on ice.
2. Centrifugate in JA-14 beakers at 11500 rpm for 30 min at 4°C.
3. Resuspend the pellet with $TBSE_{\beta-ME}^{PMSF}$ again.
4. Sonicate the cells for 3 min at 300 Watt on ice.
5. Resuspend and wash the inclusion bodies with $TBSE_{\beta-ME}$ and centrifugate in JA-14 beakers at 11500 rpm for 30 min at 4°C.
6. Remain the sediment (inclusion bodies) at -20°C.

2.14.4 Denaturation and refolding of protein

Materials

6 M GuHCl 6 M Guanidin HCl, 50 mM NaOAc, 1 mM EDTA, pH 5.0

8 M GuHCl 8 M Guanidin HCl, 50 mM NaOAc, 1 mM EDTA, pH 5.0

50 mM NaOAc pH 5.0

DTT stock 0.5M, DTT (1,4-Dithiothreit) in ethanol

Refolding Buffer 2 M LiCl, 50 mM Tris, 25 mM Chaps, 5 mM EDTA, 3 mM L-Glutathion red., 1 mM L-Glutathion ox.

S300 size exclusion chromatography Pump: LKB 2232 Microperpex S peristaltic Pump
Collector: LKB 2211 Superrac
Detector: LKB 2238 Uvicord SII
Recorder: LKB 2210 Recorder
Column: 2.6 x 63 cm (Pharmacia)
Column material: SephacrylTM S-300 High Resolution (Pharmacia)

Procedure

1. Weight inclusion bodies and resuspend them in 8 vol. (v/w) 50 mM NaOAc, pH5.0.

Add 1 vol. (v/w) 6M GuHCl plus β -ME (1:1000 dilute) and stir for 30 min at room temperature. The inclusion bodies were washed in 0.6M GuHCl in this step.

2. Centrifugate in JA-14 beakers at 11500 rpm for 20 min at 4°C.
3. Denaturation of protein
 - 3.1 Weight the pellets and resuspend them in 2.5 vol. (v/w), 50mM NaOAc, and pH5.0. Add 7.5vol. (v/w), 8M GuHCl plus β -ME (1:1000 dilute) and stir for 30min at RT. The final concentration of GuHCl was 6 M.
 - 3.2 Centrifugate in 45Ti rotor at 30000 rpm for 60 min at 18°C, and collect the supernatant.
 - 3.3 Purify the extract by size-exclusion chromatography on Sephacryl S300. Apply not more than 20 ml of the extract per run.
 - 3.4 Analyze every peak fraction by SDS-PAGE, and select the target peak fraction.
 - 3.5 Concentrate the denatured protein solution on Amican[®] to the final absorbency of 20 OD.
4. The denatured protein was diluted 100 times with the refolding buffer and incubated at 4°C for 7 days.
5. Dialyse the refolding protein with 20 mM Tris, 20 mM NaCl, pH 7.4 for the next step.

2.15 Expression of protein in SF9 cells

2.15.1 Co-transfection of BaculoGold DNA and a transfer vector into SF9 cells

Materials

BaculoGold Transfer Kit	Linearized BaculoGold Baculovirus DNA
(BD Biosciences Pharmingen):	Transfection buffer A
	Transfection buffer B
FCS (Biochrom KG)	
SF9-medium (Hyclone [®] , Perbio Science Company)	
Confluent monolayer culture of SF9 cells	
Transfer vector	

6-well tissue culture plate (Greiner Bio-One)

Procedure

1. Ethanol Precipitation of a transfer vector
 - 1.1 Mix 5µl of a transfer vector (about 5ug), 40µl H₂O, 5µl 3M NaOAc (pH 4.8) and 100µl ethanol, and incubate at -20 °C for 1 hour.
 - 1.2 Centrifugate at 15000 rpm for 10 min and Wash the pellet with 200 µl of 70% ethanol.
 - 1.3 Centrifugate at 15000rpm for 5 min and Dry in clean bench.
2. Adjust SF9 cell density to 0.8×10^6 cells/ml with 10% FCS SF9-medium.
3. Add 1 ml cell and 1 ml medium to each well of 6-well tissue culture plate, and incubate at 27 °C for 1 hour until the cells attach firmly to the bottom.
4. Remove the medium, and add 500µl of buffer A to each well.
5. The transfer vector is mixed with 2.5µl of Linearized BaculoGold Baculovirus, and then incubated for 5 min at RT. After 5 min of incubation, 500µl of buffer B is added to the co-transfection mixture.
6. Drop by drop, the co-transfection mixture is added to each well of 6-well tissue culture plate containing 500µl of buffer A slowly.
7. The plate is incubated at 27 °C for 4 hours.
8. Remove the medium and wash the cells with 1.5-2 ml fresh medium for 2 times.
9. The plate is incubated at 27 °C for 5 days containing 1 ml fresh medium.
10. Collect the virus solution and Centrifugate at 1000 rpm for 5 min.
11. Collect the supernatant, and store at 4°C in dark.

2.15.2 Plaque-assay for getting single virus clone

Materials

2.7 %, Plaque Agarose: low melting temperature agarose (Biozym),
dissolved in H₂O, autoclaved and kept at 65°C

Confluent monolayer culture of SF9 cells

FCS (Biochrom KG)

SF9-medium (Hyclone[®], Perbio Science Company)

2x Xpress Medium (GIBCO[™])

1 mg/ml, MTT dissolved in distilled water and filtered through 0.22µm filter

6-well tissue culture plate (Greiner Bio-One)

Procedure

1. Count cells, and adjust cell density to 1.2×10^6 cells/ml by 10% FCS SF9-medium
2. Apply 1 ml of cell solution and 1 ml of medium per well. Incubate for 1 hour at 27°C.
3. Dilute virus solution according to the following ratios (1ml per well required): 1×10^{-2} , 1×10^{-3} , 1×10^{-4} , 1×10^{-5} , and 1×10^{-6} .
4. Add virus solution to cell (1 ml per well), and incubate for 1 hour at 27°C.
5. Mix 3.3 ml Agarose (2.7%) with 700µl FCS and 6.6 ml 2x Xpress Medium for each plate (6 wells).
6. Remove medium of step '4', and apply 1.5 ml mixture of step '5' to each well.
7. After Agarose becoming hardened, close the plate with parafilm and store on a wet tissue in a box at 27°C for 5 days.
8. Apply 1 ml of MTT (1mg/ml) to each well, and incubate for 1 hour at 27°C for visualizing single clone.

2.15.3 First virus amplification (A1)

Materials

Confluent monolayer culture of SF9 cells

FCS (Biochrom KG)

SF9-medium (Hyclone[®], Perbio Science Company)

6-well tissue culture plate (Greiner Bio-One)

Procedure

- 1 Select 6 clones from the plaque, and incubate in 1 ml medium for 1 hour at 27°C.

Then Centrifugate at 1000 rpm for 5 min and collect the supernatant.

- 2 Count cells and adjust cell density to 1.5×10^6 . Apply 1 ml of cell solution and 1 ml of medium per well in 6-well plate. Incubate for 1 hour at 27°C (cells attach to surface).
- 3 Remove medium of step '2', and apply the 1ml of virus solution of step '1' per well.
- 4 Incubate for 4 days at 27°C.

2.15.4 Second virus amplification (A2)

Materials

Confluent monolayer culture of SF9 cells

FCS (Biochrom KG)

SF9-medium (Hyclone[®], Perbio Science Company)

6-well tissue culture plate (Greiner Bio-One)

Procedure

- 1 Collect A1 and centrifugate at 1000 rpm for 5 min and collect the supernatant.
- 2 Count cells and adjust cell density to 1.5×10^6 . Apply 1 ml of cell solution and 1 ml of medium per well. Incubate for 1 hour at 27°C.
- 3 Remove medium of step '2', then apply the 1 ml of virus solution of step '1' and 1 ml of medium per well.
- 4 Incubate for 4 days at 27 °C.

2.15.5 Western-Blot for positive clone (See 2.13)

2.15.6 Third virus amplification (A3)

Materials

Confluent monolayer culture of SF9 cells

FCS (Biochrom KG)

SF9-medium (Hyclone[®], Perbio Science Company)

Tissue culture Flask, 175cm², 550ml (Greiner Bio-One)

Procedure

Add 2 ml virus solution of positive clone from A2 into flask (175 cm²) with 8×10^7 cells/ in 30 ml medium, and incubate for 4 days at 27 °C.

2.15.7 Forth virus amplification (A4)

Materials

Confluent monolayer culture of SF9 cells

FCS (Biochrom KG)

SF9-medium (Hyclone[®], Perbio Science Company)

Roller-bottle (Greiner Bio-One)

Procedure

1. Collect A3. Then centrifugate at 1000 rpm for 5 min and collect the supernatant.
2. Add 7.5 ml of A3 into 30 ml cells (1.5×10^6 cells/ml) in roller-bottle, and incubate for 4 days at 27 °C.
3. Determination of A4 virus titers by plaque assay. To be sure the virus titers are above 5×10^7 virus /ml.

2.15.8 Expression

Materials

Confluent monolayer culture of SF9 cells

FCS (Biochrom KG)

SF9-medium (Hyclone[®], Perbio Science Company)

Roller bottle (Greiner Bio-One)

Procedure

Add 15 ml A4 (the titers are $5-10 \times 10^7$) to 200 ml cells (1.5×10^6 cells/ml) in roller bottle, and incubate for 4 days at 27°C. The virus/cell ratio was 2-5:1.

2.16 Purification of proteins by chromatography

2.16.1 Ni-NTA chelating chromatography

Materials

Loading and Wash-buffer	50 mM NaH ₂ PO ₄ , 300 mM NaCl, 10 mM Imidazol, pH 8.3
Elution buffer	50 mM NaH ₂ PO ₄ , 300 mM NaCl, 300 mM Imidazol, pH 8.3
Column material	Ni-NTA Agarose (QIAGEN [®])

Procedure

1. Mix Ni-NTA solution, and apply 10 ml of Ni-NTA to centrifugate at 500 rpm for 5 min at RT and remove the supernatant. Then wash the precipitate with 50 ml of wash buffer for 2 times.
2. Mix 5 ml Ni-NAT and 1 liter protein solution together, and stir for 1 hour at 4°C.
3. Transfer the mixture to column, and wash the column with 20 vol. (v/v) wash buffer.
4. Elute the column with elution buffer, and collect 5 ml per fraction. Analyse the collected fractions with SDS-PAGE and select those containing potential target protein.
5. Dialyse the collected protein solution with 20 mM Tris, 20 mM NaCl, and pH 7.4 for the next purification step.

2.16.2 Cation exchange chromatography on SP sepharose

Materials

Buffer A	20 mM Tris, pH 7.4
Buffer B	20 mM Tris, 1M NaCl, pH 7.4
Column	2 x25 cm (GE Health Care)
Column material	SP sepharose [™] , Fast Flow (GE Health Care)
FPLC system	Detector: L-4200 UV-VIS Detector (Merk-Hitach) Pump: L-6200 Intelligent Pump (Merk-Hitach) Collector: FC 203B Fraction Collector (GILSON) Recorder: LR 66920 Recorder (Pharmacia)

Procedure

1. Equilibrate the column with Buffer A with flow rate 1.5 of ml/min.
2. Apply protein solution to the SP sepharose and wash the column with Buffer A until the baseline is constant with flow rate of 1.5 ml/min.
3. Elute the protein with a linear salt gradient: 0 -1 M NaCl, achieved through mixing with Buffer B with flow rate of 1.0 ml/min. Collect 1.5 ml per fraction. Follow the elution profile with UV flow photometer, monitoring at wave length of 280 nm.

Gradient:

Time (min)	% NaCl
0	0
20	30
80	50
90	100
100	0

4. Analyze the flow through and peak fractions by SDS-PAGE and select those containing potential target protein.
5. Dialyse the collected protein solution with 10 mM HEPES, 500 mM NaCl, pH 7.4 for next purification step.

2.16.3 BMP-2 affinity chromatography

Materials

Buffer A	10 mM HEPES, 500 mM NaCl, pH 7.4
Buffer B	10 mM HEPES, 150 mM NaCl, pH 7.4
Elution buffer	4 M MgCl ₂
Affinity Matrix	BMP-2 immobilized CNBr-Sepharose 4B
Column	1x10 cm (Biorad)
Instruments	Pump: 2232 Microperpex S peristaltic Pump (LKB) Detector: 2238 Uvicord SII (LKB) Collector: 203 Collector (GILSON) Recorder: 2210 Recorder (LKB)

Procedure

1. Equilibrate the affinity column with Buffer A.
2. Apply protein solution to column and wash the affinity column with Buffer A until the baseline is constant.
3. Elute active protein which binds to immobilized BMP-2 with 4 M MgCl₂.
4. Collect 8 ml per fraction and measure their OD on UV spectrophotometer. Combine fractions carrying active protein and dialyse them against 50 vol. 10 mM HEPES, 500 mM NaCl for the next purification step.

2.16.4 Size exclusion chromatography on Superdex™ 200

Materials

Running buffer	10 mM HEPES, 700 mM NaCl, pH 7.4
Column	Superdex™ 200 HR 10/30, prepack (Pharmacia) Total bead volumn: 24ml

Column material Superdex™ 200 High Resolution (Pharmacia)

FPLC system Detector: L-4200 UV-VIS Detector (Merk-Hitach)

Pump: L-6200 Intelligent Pump (Merk-Hitach)

Collector: FC 203B Fraction Collector (GILSON)

Recorder: 2210 Recorder (LKB)

Centrifuge Filter Amicon® Ultra-4 Centrifuge Filter Device (Millipore)

Procedure

1. Equilibrate the column with elution buffer with a flow rate of 0.5ml/min.
2. Apply the protein sample to the column. For better chromatographical resolution, apply not more than 500 µl of every probe.
3. Run the chromatography with a flow rate of 0.5ml/min. Collect 0.5 ml per fraction. Follow the elution profile with UV flow photometer, monitoring at wave length 280 nm.
4. Analyse the collected fractions with SDS-PAGE and select those containing protein in certain size.
5. Concentrate fractions containing the purified target protein on Amicon® Ultra-4 to the final concentration of about 1 mg/ml and store at -20°C.

2.16.5 Reversal phase HPLC

Materials

Buffer A 0.1% Trifluoroacetic acid

Buffer B Acetonitrile

Column Vydac-214TP; C4; 10µM pore size; 0.46 x 25cm, analytical; 1 x 25 cm, preparative

HPLC system Detector: L-4200 UV-VIS Detector (Merk-Hitach)
Pump: L-6200 Intelligent Pump (Merk-Hitach)
Collector: FC 203B Fraction Collector (GILSON)
Recorder: LR 66920 Recorder (Pharmacia)

Procedure

1. Equilibrate the column with Buffer A.
2. Apply protein solution to C4 column, equilibrated with buffer A. Apply not more than 20mg of protein to preparative column and 100ug to analytical column.
3. Elute the protein with 0 -100% acetonitrile linear gradient, achieved through mixing with buffer B. Program flow rate for preparative column to 3 ml/min with fraction size 4.5ml, and respectively for analytical column to 0.7 ml/min with fraction size 1ml. Follow the elution profile with UV flow photometer, monitoring at wave length 280 nm.

Gradient:

Time (min)	% Acetonitrile
0	0
5	25
40	30
50	100

4. Collect the fractions of the peak and store at -80°C for the lyophylization.

2.17 Analysis of Protein-Protein interaction by BIAcore technology

The kinetic and thermodynamic analysis of protein-protein interaction between CHL2 or its VWC domains and BMP-2 was performed in BIAcore™ 2000.

BIA technology enables detection of biomolecules and monitoring of binding events between two or more molecules, in real time, without the use of labels. This technology relies on phenomenon of surface plasmon resonance (SPR) which occurs when surface plasmon waves are excited at a metal/liquid interface. The SPR phenomenon occurs in the

gold film at the tip of a sensor probe. White light passed into the optical fibre of the probe is totally internally reflected at the surface interfaces. Biomolecular binding events cause changes in the refractive index close to the surface and the wavelength of the reflected light intensity minimum shifts. By monitoring the output spectrum of the reflected light BIAcore probe is able to detect biomolecular binding occurring at the probe surface.

During a binding analysis SPR changes occur as a solution is passed over the surface of a sensor chip. The sensor surface forms one wall of a flow cell. A sample containing the other interactant(s) is injected over this surface in a precisely controlled flow, light at a fixed wavelength, in a fan-shaped form, is directed at the sensor surface and biomolecular binding events are detected as changes in the particular angle where SPR creates extinction of light. This change which reflects the progress of an interaction is measured continuously to form a sensorgram, which provides a complete record of the progress of association or dissociation of the interactants.

The analyte binds to the surface-attached ligand during sample injection, resulting in increase in signal. At the end of the injection, the sample is replaced by a continuous flow of buffer and the decrease in signal now reflects dissociation of interactant from the surface-bound complex. Binding events cause changes in the refractive index at the surface layer, which are detected as changes in the SPR signal. In general, the refractive index change for a given change of mass concentration at the surface layer is practically the same for all proteins and peptides, and also similar for glycoprotein, lipids and nucleic acids. Resonance signal is measured in so called Refractive Units (RU) - a response of 1000 RU corresponds to a change in surface concentration of 1 ng/mm².

After the measurement cycle, the added regeneration buffer causes an immediate dissociation of non-covalently bound substances from the matrix without affecting binding activity of covalently linked immobilized binding partner. In this way the sensor chip is regenerated for new measurement cycle.

2.17.1 Immobilizing of proteins through biotin-streptavidin coupling

Materials

EDC	50 mM N-Ethyl-N'-(dimethylaminopropyl) carbodiimid
NHS	200 mM N-hydroxysuccinimid
HBS	10 mM Hepes pH 7.4, 150 mM NaCl, 3.4 mM EDTA, 0.005% Surfactant P20
Streptavidin solution	100 ug/ml Streptavidin in 10 mM NaOAc pH 4.5
Regeneration buffer	100 mM HOAc, 1 M NaCl, pH 3.0

Procedure

Biotinylated BMP-2, mCHL2 or its VWC domains or Tsg immobilized on the dextran matrix of the sensor chip (CM5, BIAcore) by covalently conjugated with streptavidin. Immobilization was performed according to the recommendation of the supplier (BIAcore Handbook). For the immobilization biotinylated protein was applied at concentration of 1-3 ug/ml.

2.17.2 Measurement of binding of analytes

Materials

Buffer	10mM HEPES, pH 7.4; 500mM NaCl; 3,4mM EDTA, 0,05% P20
System	Biosensor BIAcore 2000 TM (BIAcore)

Procedure

The sensorgram obtained on BIAcoreTM 2000 could be characterized by the following three phases:

1. Association of CHL2 or its VWC domains with immobilized interaction partner after injection.
2. Equilibrium between processes of association and dissociation: a plateau on the sensorgram.
3. Dissociation of CHL2 or its VWC domains upon switch on running buffer. Association and dissociation phases carry information about kinetic of binding, whereas the level of the plateau yields the thermodynamic affinity of binding.

Calculations of kinetic and thermodynamic constants are performed with BIAevaluation 2.0 program.

4. For dissociation constants (K_D) of <50 nM, kinetic constants (k_{on} and k_{off}) were evaluated. For K_D values of >50 nM, dose-dependent equilibrium binding was evaluated. K_D values or rate constants k_{off}/k_{on} were evaluated from one experiment determined for 6–9 different concentrations of the analytes.

2.18 Biological activity in cell line

Inhibition of BMP-2 induced Alkaline Phosphatase (ALP) activity by CHL2 or its VWC domains was assessed by ALP assay in C2C12 cell line.

Materials

75 cm² culture flasks, 50 ml Falcon Tubes, Sterile pipette-syringe for Gilson, Multichannel pipette, 10 ml transfer pipette, 96-well plates sterile, 100 μ l comptips for multipipette, 1.5 ml Eppicaps

45g Glucose /100 ml H₂O, PBS, 2 x trypsin in PES, PCS, CS, Penicillin/Strap, Glutamine 200 mM, DMEM medium

Paranitrophenylphosphat (PNPP, store -20°C) (20 mg/ml H₂O).

freshly prepared C2C12 cells

Alkaline lysis butter 1 0.1M Glycine pH9.6; 1 % Nonidet P40 substitute (Fluka); 1mM MgCl₂; 1 mM ZnCl₂

Alkaline lysis butler 2 0.1 M Glycine pH9.6; 1 mM MgCl₂ 1 mM ZnCl₂

Procedure

1. Remove medium from confluent cells.
2. Trypsinize cells using 2 ml of 2 x trypsin for 5 min at RT. Stop trypsinization by adding 4 ml of 10% FCS-medium.

3. Spin down cells by 1200 rpm centrifugation for 2 min. Resuspend cells in 10 ml of 10% FCS-medium and count cells. Then dilute cells to 1.5×10^5 cells/ml and add 100 μ l/well in 96-well plates (1.5×10^4 cell/well).
4. Incubate for 24 h at 37°C with 10% CO₂.
5. Suck out medium. Add 100 μ l/well of 2% FCS-medium starting from second well.
6. Dilute protein to 10 x concentration and 1:10 dilution in 2% FCS-medium.
7. Add protein solution in first well and dilution until well11 and well 12 used as negative control.
8. Incubate for 72 h at 37°C /10% CO₂.
9. Suck out medium and wash with 100 μ l PBS.
10. Add 100 μ l alkaline lysis buffer 1/well and 1 h at RT shaking.
11. Mix 10 ml alkaline lysis buffer 2 with 1ml PNPP and add 100 μ l/well.
12. Wait for colour reaction for 20-30 min and measure absorbance at 405nm in the ELISA reader.

2.19 Crystallization of proteins

2.19.1 Preparation of protein samples for crystallization

The purified CHL2 or CHL2-VWC3 (1mg/ml, in 10 mM HEPES, 700 mM NaCl, pH 7.4) was mixed with BMP-2 (1mg/ml, in H₂O) at molar ratio of 2.5 or 2.2:1 respectively on ice. The mixture was incubated for 30 min at 0°C. Then the sample was centrifuged at 4000x g for 10 min at 4°C to sediment precipitated proteins. The 2:1 of CHL2/BMP-2 or CHL2-VWC3/BMP-2 complex was purified by size exclusion chromatography on Superdex™ 200 column. At the last for the crystallization, the purified protein complex was concentrated to 8-11 mg/ml by Amicon® Ultra-4 Centrifuge Filter.

2.19.2 Crystallization of proteins by vapour diffusion method

Materials

Crystal research Kits (Hampton Research; Emerald BioSystems; QIAGEN; European Molecular Biology Laboratory, Hamburg); Baysilone paste (Roth); 96-well sitting drop plate; 24-well hanging drop plat; siliconized glass, circle cover slides, 22mm (Hampton)

Procedure

Sitting-drop technique

The initial crystallization trials were performed by using crystal research Kits with Sitting-drop technique in 96-well plates. The sitting-drop vapor diffusion technique is a method for the crystallization of macromolecules. A sitting droplet composed of a mixture 1 μ l each of protein sample and reagent is placed in vapor equilibration with 100 μ l of reagent in reservoir. Typically the droplet contains a lower reagent concentration than the reservoir. To achieve equilibrium, water vapor leaves the droplet and eventually ends up in the reservoir. As water leaves the droplet, the sample undergoes an increase in relative supersaturation and forms crystal step by step. Both the sample and reagent increase in concentration as water leaves the droplet for the reservoir. At the last equilibration is reached when the reagent concentration in the drop is approximately same as that in the reservoir (Figure 2.2).

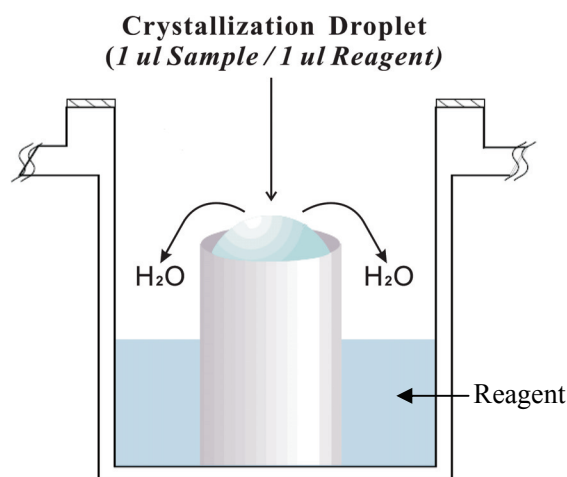


Figure 2.2: Sktch map showing process of vapor diffusion of sitting-drop technique.

(Modification from Hampton Research Web site: <http://www.hamptonresearch.com/support/pdf101/4.pdf>)

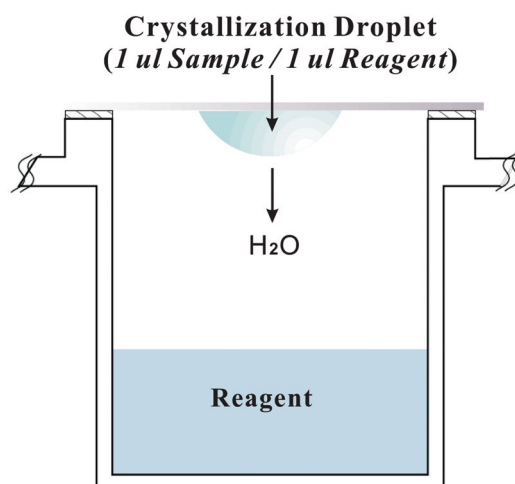


Figure 2.3: Sktch map showing process of vapor diffusion of hanging-drop technique.

(Modification from Hampton Research Web site: <http://www.hamptonresearch.com/support/pdf101/3.pdf>)

Hanging-drop technique

The fine screen experiments were set up with 24-well plates, siliconized glass cover and silicon grease. The hanging drop vapor diffusion technique is also a popular method for

the crystallization of macromolecules. A hanging droplet is prepared by mixing 1 μ l each of protein sample and reservoir reagent and placed in vapor equilibration with 500 μ l of reagent in reservoir. The principle of hanging-drop technique is same as sitting-drop technique. The hanging droplet has a lower reagent concentration than the reservoir. Water vapor leaves the droplet and ends up in the reservoir for achieving equilibrium. Equilibration is reached when the reagent concentration in the drop is approximately same as that in the reservoir (Figure 2.3).

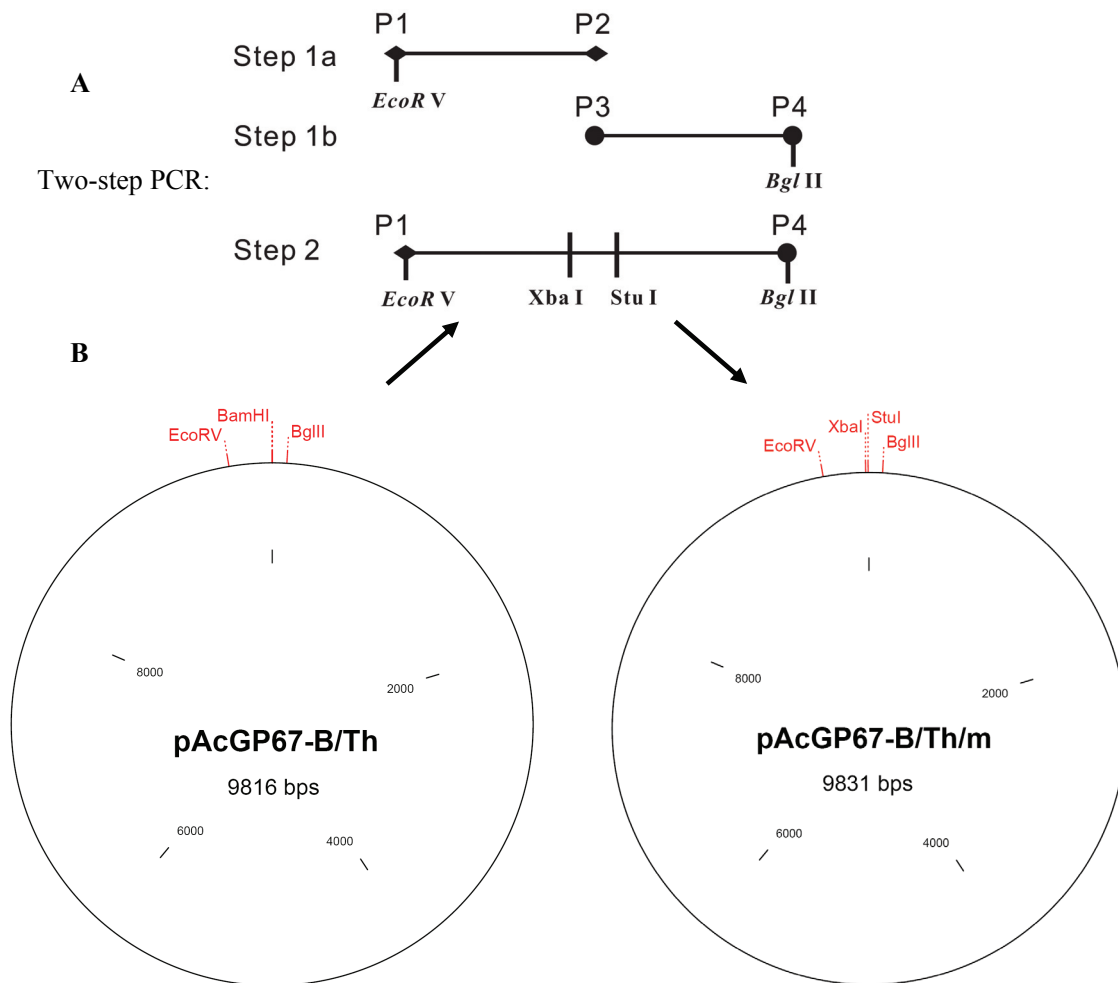
3 Results

3.1 Preparation of mCHL2 and its mutants in SF9 cells

In this experiment, the wild type mouse CHL2 (mCHL2) was first expressed in SF9 cells for the further functional and structural analysis of mCHL2/BMP-2 interaction. The mCHL2 is a secreted glycosylated protein of 67 KDa. There are two potential glycosylation sites which reside at N89 and N180. To facilitate the crystallization of BMP-2/CHL2 complex, three mCHL2 mutants were constructed to prevent glycosylation. In two single mutants (mCHL2-N89Q, mCHL2-N180Q) each of the two glycosylation sites was mutated singly and in one double mutant (mCHL2-N89Q/N180Q) both glycosylation sites were simultaneously removed.

3.1.1 Modification of pAcGP67-B/Th vector.

pAcGP67-B/Th vector is a transfer plasmid for expression of His-tag proteins in SF9 cells. As the mCHL2 cDNA contains BamHI restriction endonuclease site which is the cloning site in the vector, we modified pAcGP67-B/Th to *pAcGP67-B/Th/m* by replacing BamHI site with StuI and XbaI sites. The mutation was generated by using a two-step PCR. The cDNA synthesized during the second step of the PCR contained the target mutation: BamHI site was replaced by StuI and XbaI sites (Figure 3.1, A). This mutant cDNA as an insert and the original pAcGP67-B/Th plasmid as a vector were respectively digested by EcoRV and *Bgl*III. The digested pAcGP67-B/Th vector was purified by Gel Extraction Kit and the amounts of insert and vector were roughly estimated by checking the bands in agarose gel. Finally the insert was ligated into vector (Figure 3.1, B). The recombinant plasmid DNA of pAcGP67-B/Th/m was transformed into competent *E.coli* MM294 and the positive clone were identified by checking the EcoRV/*Bgl*III digestion products of the DNA from different colonies. After sequence determination, the new pAcGP67-B/Th/m plasmid was used for the further experiments.



P1 and P4: External primer EXM-s and PAC-a
 P2 and P3: Mutational primer PAC-Ga and PAC-Gs (See table 2.1)

Figure 3.1: **A**, Two-step PCR procedure. Two-step PCR was used to generate a mutational cDNA which was synthesized during the second step of the PCR to gain the target mutation: BamHI was replaced by StuI and XbaI. The mutational cDNA was inserted into the pAcGP67-B/Th between EcoRV and BglII to form a new transfer vector pAcGP67-B/Th/m. **B**, Maps of Baculovirus transfer vector pAcGP67-B/Th and pAcGP67-B/Th/m.

3.1.2 Cloning of mCHL2 and its mutants into pAcGP67-B/Th/m

The cDNA of mCHL2 (Figure 3.2-1/-2) encoding the residues 1-401 of the mature mCHL2 was inserted into the transfer vector pAcGP67-B/Th/m between StuI and XbaI restriction sites (Figure 3.3).

Then the plasmid carrying mCHL2 and mutant mCHL2 cDNA were used for transformation of competent *E.coli* MM294. The first selection of plasmid containing

1 atggttcccg gggtaggat catcccctct ttgctgggac tegtgatgtt ctggctcccg
M V P G V R I I P S L L G L V M F W L P
61 ttgactcac aagcacgata ccgctcgggc aaagtctgcc ttttcgggtga aaagatatat
L D S Q A R⁻¹ S R S G K V C L F G E K I Y⁻¹⁵
121 acccccgccc agagctggca cccctacttg gaaccacaag gcacgatata ctgcgtgcgc
T P G Q S W H P Y L E P Q G T I Y C V R⁻³⁵
181 tgtacctgct ctgagaatgg acatgtgaat tgttaccgcc tccgtgcccc acccctteac
C T C S E N G H V N C Y R L R C P P L H⁻⁵⁵
241 tgetcacage ctgtgatgga gccacagcaa tgctgtceca ggtgtgtgga tectcatgtc
C S Q P V M E P Q Q C C P R C V D P H V⁻⁷⁵
301 ccctctggcc tccgagttcc cctaaagtcc tgccagctca atgagaccac ataccaacat
P S G L R V P L K S C Q L N E T T Y Q H⁻⁹⁵
361 ggagagatct tcagtgccca ggagctgttc cctgcccgcc tgtccaacca gtgtgtcctg
G E I F S A Q E L F P A R L S N Q C V L⁻¹¹⁵
421 tglagctgta ttgaaggcca cacttactgt ggtctcatga cctgtcctga acccagctgc
C S C I E G H T Y C G L M T C P E P S C⁻¹³⁵
481 cccaccacac tccctctgcc tgattcctgc tgtcagacct gcaaaagacag gacaactgag
P T T L P L P D S C C Q T C K D R T T E⁻¹⁵⁵
541 agtccacag aagaaaactt gacacagctg cagcatggag agagacatte ccaggatcca
S S T E E N L T Q L Q H G E R H S Q D P⁻¹⁷⁵
601 tgctcggaga ggagaggccc cagcacgcca gccccacca gcctcagctc ccctctgggc
C S E R R G P S T P A P T S L S S P L G⁻¹⁹⁵
661 ttcatecctc gccacttcca gtcagtagga atgggcagca caaccatcaa gattatcttg
F I P R H F Q S V G M G S T T I K I I L⁻²¹⁵
721 aaggagaaac ataaa^{aaage} ttgcacacac aatgggaaga catactcecca tggggaggtg
K E K H K K A C T H N G K T Y S H G E V⁻²³⁵
781 tggcacecca ctgtgetete ctltggcccc atgceetgca tceetgtcac atgtategat
W H P T V L S F G P M P C I L C T C I D⁻²⁵⁵
841 ggetaccagg actgccaccg tgtgacctgc cccacceaat atccctgcag tcaaccecaag
G Y Q D C H R V T C P T Q Y P C S Q P K⁻²⁷⁵
901 aaagtggctg ggaagtgtg caagatctgc ccagaggacg aggcggaaga tgaccacagt
K V A G K C C K I C P E D E A E D D H S⁻²⁹⁵
961 gaggtcattt ccaccgggtg tccaaggta ccaggccagt tccatgtgta cacgttgcca
E V I S T R C P K V P G Q F H V Y T L A⁻³¹⁵
1021 tetccaagcc cagacagcct acaccgcttt gtcttgagc atgaagcctc tgaccaggta
S P S P D S L H R F V L E H E A S D Q V⁻³³⁵
1081 gagatgtaca tttggaagct ggtgaaagga atctaccact tggttcagat caagagagtc
E M Y I W K L V K G I Y H L V Q I K R V⁻³⁵⁵
1141 aggaagcaag atttccagaa agagctcag aacttccggc tgetcaccgg cacccatgaa
R K Q D F Q K E A Q N F R L L T G T H E⁻³⁷⁵
1201 ggtaactgga ccgtcttctt agccagact ccagagctga aagttacage cageccagac
G Y W T V F L A Q T P E L K V T A S P D⁻³⁹⁵
1261 aaagtacca agacattata g
K V T K T L -⁻⁴⁰¹

█ : Signal peptide █ : VWC1 █ : VWC2 █ : VWC3

Figure 3.2-1: The complete nucleotide and amino acid sequence of mCHL2. The colored boxes indicate the signal peptide and three VWC domains. The red letters are two potential N-glycosylation sites.

A: Mature mCHL2 (Expressed in Sf9 insect cell with pAcGP67-B/Th/m vector, 401 amino acids)

¹-RSRSGKVCLFGEKIYTPGQSWHPYLEPQGTYCVRCTCSENGHVNCYRLRCP
PLHCSQPVMEPQQCCPRCVDPHVPSGLRVPLKSCQLNETTYQHGEIFSAQELFP
ARLSNQCVLCSIEGHTYCGLMTCPEPSCPTTLPLPDSCCQTCKDRTTESSTEE
NLTQLQHGERHSQDPCSERRGPSTPAPTSLSPLGFIPRHFQSVGMGSTTIKIL
KEKHKKA¹CTHNGKTYSHGEVWHPTVLSFGPMP¹CILCTCIDGYQD¹CHRVT¹CPT
QYPCSQPKKVAGK¹CKICPEDEAEDDHSEVISTRCPKVPGQFHVYTLASPSDS
LHRFVLEHEASDQVEMYIWKLKGIYHLVQIKRVRKQDFQKEAQNFRLLTGTH
EGYWTVFLAQTPELKVTASPKVTKL⁴⁰¹RPLVPRGSHHHHHHGA--

B: mCHL2-VWC1 (Expressed in *E.coli* with QKA vector, 78 amino acids)

¹-RSRSGKVCLFGEKIYTPGQSWHPYLEPQGTYCVRCTCSENGHVNCYRLRCP
PLHCSQPVMEPQQCCPRCVDPHVPSG⁷⁸

C: mCHL2-VWC2 (Expressed in Sf9 insect cell with pAcGP67-B/Th/m vector, 99 amino acids)

⁷¹-VDPHVPSGLRVPLKSCQLNETTYQHGEIFSAQELFPARLSNQCVLCSIEGH
TYCGLMTCPEPSCPTTLPLPDSCCQTCKDRTTESSTEENLTQLQHGE¹⁶⁹

D: mCHL2-VWC3 (Expressed in Sf9 insect cell with pAcGP67-B/Th/m vector, 99 amino acids)

²⁰³-SVGMGSTTIKILKEKHKKA¹CTHNGKTYSHGEVWHPTVLSFGPMP¹CILCTC
IDGYQD¹CHRVT¹CPTQYPCSQPKKVAGK¹CKICPEDEAEDDHSEVISTR³⁰¹

E: mCHL2-VWC3-Short (Expressed in *E.coli* with QKA vector, 74 amino acids)

²¹⁷-EKHKKA¹CTHNGKTYSHGEVWHPTVLSFGPMP¹CILCTCIDGYQD¹CHRVT¹CPT
TQYPCSQPKKVAGK¹CKICPEDEA²⁹⁰

Figure 3.2-2: The amino acid sequence of mature mCHL2 (A) and its VWCs (B, C, D, E) expressed in this study. D and E are all VWC3, but have different numbers of residues in flanking sequences and expressed in different systems. Cysteines are highlighted in red.

MM294 was performed by plating on Ampicillin agar plate. Because the plasmid contains Ampicillin resistance gene, only bacterial cells carrying plasmid pAcGP67-B/Th/m-mCHL2 or pAcGP67-B/Th/m-mutant mCHL2 or empty pAcGP67-B/Th/m would be able to form colonies. The later selection procedure was completed by analytical restriction digestion of the purified cDNA. The intact circular plasmid was digested with *Stu*I and *Xba*I to confirm the presence of mCHL2 or mutant mCHL2 cDNA in the plasmid. The positive clones showed a band of 1203 bp after displaying the restriction digestion reaction on 1% agarose gel. The positive plasmid DNA was prepared and purified by DNA maxi preparation Kit (see 2.11.8) for sequencing. Sequence was verified to CHL2 wildtype and mutants. The plasmid DNA with correct sequence was used for storage and following co-transfection. The mutants of mCHL2 are shown below:

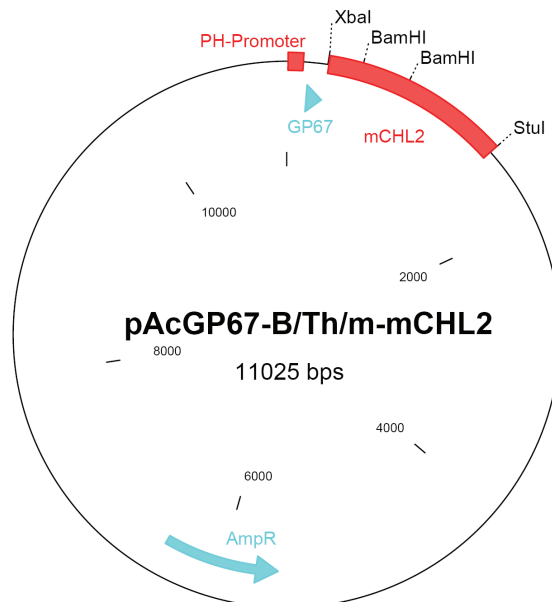
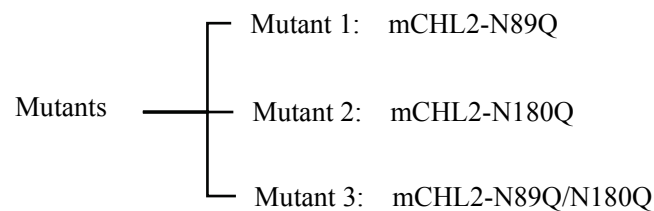


Figure 3.3: Map of transfer vector pAcGP67-B/Th/m-mCHL2. The cDNA of mCHL2 is cloned into the transfer vector pAcGP67-B/Th/m between *Stu*I and *Xba*I restriction sites

3.1.3 Co-transfection of BaculoGold DNA and the transfer vectors into SF9 insect cells and amplification of the recombinant virus

The first step necessarily to construct recombinant Baculoviruses was co-transfection of the transfer vector pAcGP67-B/Th/m containing mCHL2 or mCHL2 mutants cDNA and BaculoGold DNA into SF9 insect cells. BaculoGold DNA is a modified AcNPV Baculovirus DNA, which contains a lethal deletion and does not code for viable virus. Co-transfection of the BaculoGold DNA with a complementing Baculovirus Transfer Vector, such as pAcGP67-B, rescues the lethal deletion by homologous recombination. Since only the recombinant BaculoGold produces viable virus, a recombination frequency of 99 % is expected. To purify the stock of generated recombinant viruses during co-transfection, plaque purification was performed. Since each plaque represents a single virus, six individual plaques were randomly picked and used to generate clonal virus populations. Then the selected clonal virus populations were separately amplified twice. Finally a Western blot was performed with the virus supernatants to verify the protein production (Figure 3.4, 3.5, 3.6). In 23 of 24 tested supernatants expression of mCHL2 protein was detected. The virus clone, which showed the largest amount of recombinant mCHL2 or mutants, was selected for further amplification.

Two additional cycles of virus amplification were performed to produce a larger stock of recombinant virus with a high titer. Using a plaque assay the viral titer was determined to vary between 5×10^7 to 1×10^8 pfu/ml. An aliquot of the virus was stored at 4 °C for long-term storage and the rest was used to infect SF9 cells for expression of recombinant protein.

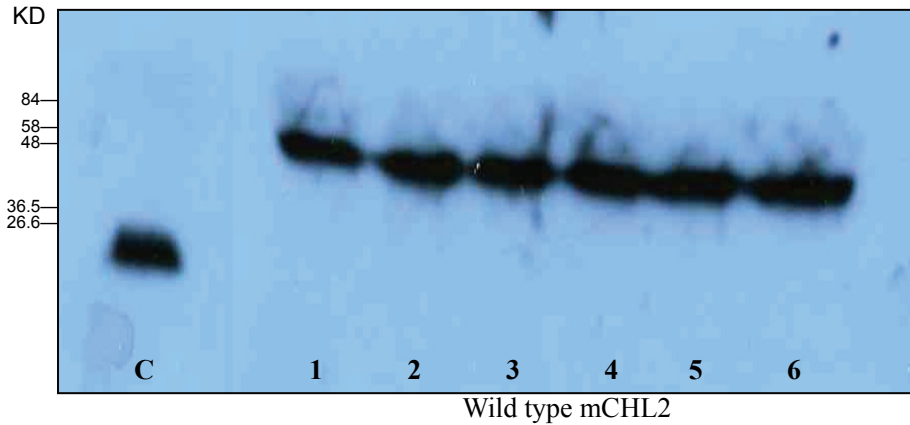


Figure 3.4: Analysis of mCHL2 expression in SF9 cells. Virus medium infected with Baculovirus containing mCHL2 cDNA was applied to western blot and detected by Anti-his tag antibody. C, Positive control (chordin VWC1-His-tag expressed in SF9 with Baculovirus transfer vector pAcGP67-B/Th); lines 1-6, examined recombinant virus clones of wild type mCHL2. The theoretical molecule weight of mCHL2 is 46.84 KD. The glycosylated proteins run at about 50 KD.

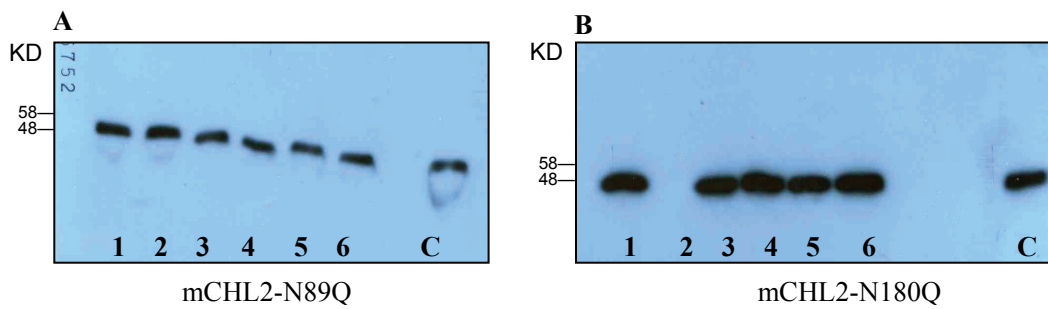


Figure 3.5: Analysis of the expression of mCHL2-N89Q (A) and mCHL2-N180Q (B) in SF9 cells. Virus medium infected with Baculovirus containing mCHL2 mutants cDNA was applied to western blot and detected by Anti-his tag antibody. C, Positive control (wild type mCHL-2 expressed in SF9 with Baculovirus transfer vector pAcGP67-B/Th/M); lines 1-6, examined recombinant virus clones. The theoretical molecule weight of mCHL2-N89Q and mCHL2-N180Q are both 46.85 KD.

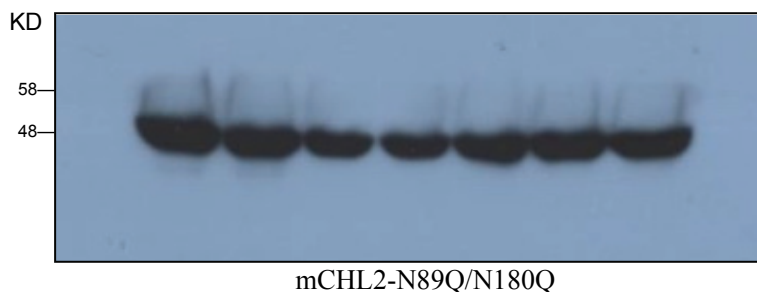


Figure 3.6: Analysis of mCHL2-N89Q/N180Q expression in SF9 cells. Virus medium infected with Baculovirus containing mCHL2 double mutant cDNA was applied to western blot and detected by Anti-his tag antibody. C, Positive control (wild type mCHL-2 expressed in SF9 with Baculovirus transfer vector pAcGP67-B/Th/M); lines 1-6, examined recombinant virus clones of mCHL2-N89Q/N180Q, The theoretical molecule weight of mCHL2-N89Q/N180Q is 46.87 KD.

3.1.4 Expression and purification of mCHL2 and its mutants

Recombinant proteins were expressed in SF9 insect cells after infection with high titer virus stock. The infected cells were incubated in roller-bottle with 10% FCS SF9-medium for 4 days at 27 °C. Protein expression was performed in serum-containing insect culture medium. The presence of serum increased the cell viability and the amount of expressed protein. Since it did not interfere with the purification procedure, serum was kept in the expression medium. Under these conditions, the expression of recombinant mCHL2 and its mutants from SF9 cells yielded 0.7-2 mg protein per liter of SF9 cells (see below). The mature recombinant proteins could be purified from the infection supernatant, which was collected at the end of the incubation period.

3.1.4.1 Purification of proteins by Ni-NTA chelating chromatography

The Ni-NTA Purification System is designed for purification of 6xHis-tagged recombinant proteins expressed in bacteria, insect, and mammalian cells. The mCHL2 and its mutants were expressed in SF9 cells with 6xHis-tag and thereby purified by Ni-NTA as a first step. After the expression, the culture supernatant was passed over the Ni-NTA chelating column and washed with wash-buffer to clean the column from non-specifically bound proteins. The specifically bound mCHL2 were eluted with elution-buffer (50 mM NaH₂PO₄, 300 mM NaCl, 300 mM Imidazol, pH 8.3). The protein amount and purity of the collected fractions were analyzed on SDS-PAGE (Figure 3.7, 3.8).

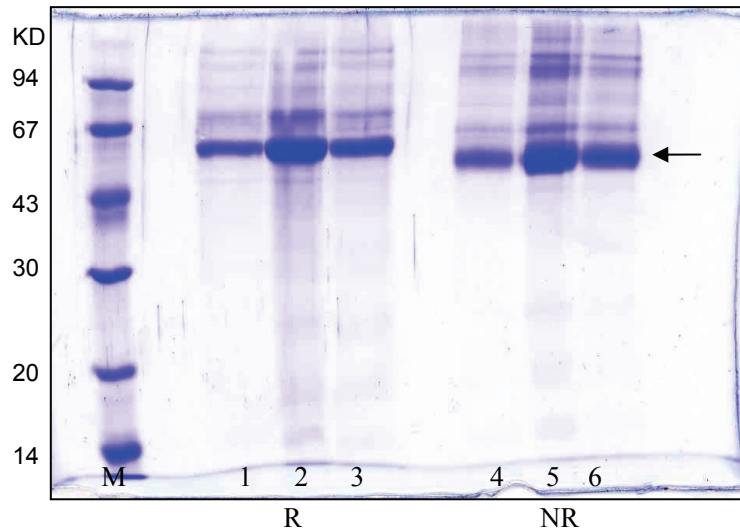


Figure 3.7: Purification of wild type mCHL2 by Ni-NAT chelating column. Lines 1-3, elution fractions 2-4, under reduced condition (R); Lines 4-6, fraction 2-4, under non-reduced condition (NR). Wild type mCHL2 is indicated by arrow. M, marker of protein molecular weight.

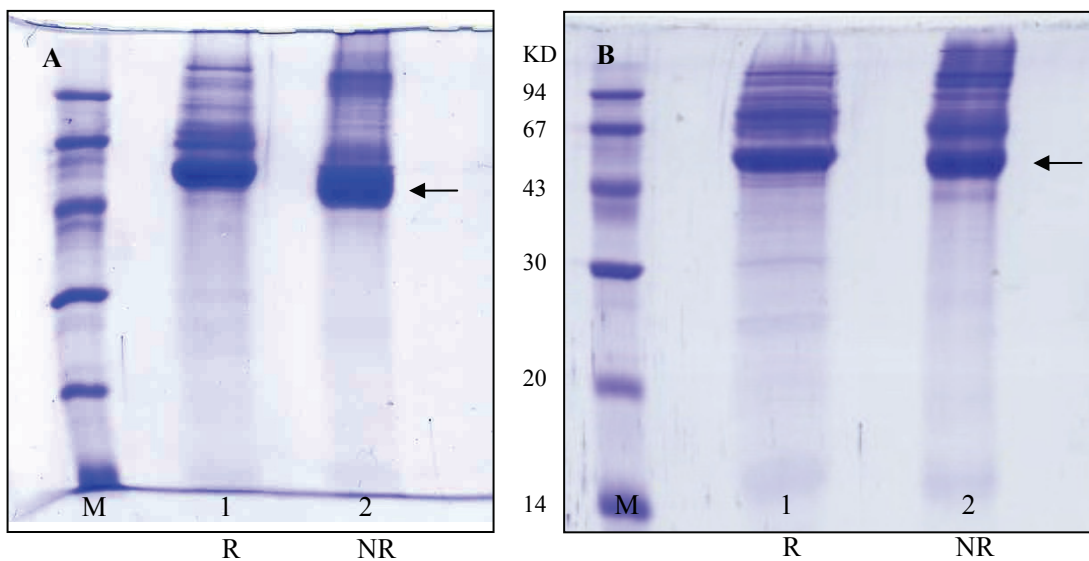


Figure 3.8: Purification of mCHL2-N89Q (A) and mCHL2-N89Q/N180Q (B) by Ni-NAT chelating column. Lines 1, elution fraction 3, under reduced condition (R); Lines 2, elution fraction 3, under non-reduced condition (NR). M, marker of protein molecular weight. The mutants mCHL2 are indicated by arrow.

3.1.4.2 Purification of proteins by cation exchange chromatography

Since the pI of mCHL2 and its mutants are around 8.14, the proteins were applied to SP-sepharose at pH7.4. During this cation exchange chromatography, the acidic and

neutral contaminating proteins could not bind to the column. Therefore the mCHL2 and its mutants could be effectively separated. The bound proteins were eluted with linear salt gradient from 0 M to 1 M NaCl. The protein amount and purity of the collected fractions were analyzed on SDS-PAGE (Figure 3.9, 3.10).

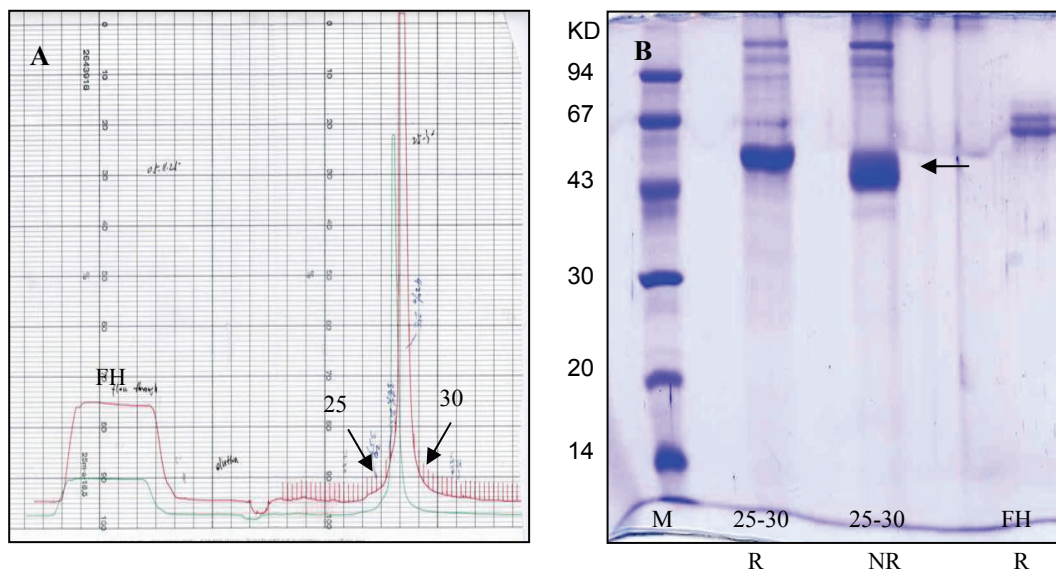


Figure 3.9: Purification of wild type mCHL2 by SP-sepharose cation exchange chromatography. **A**, The elution chart of wild type mCHL2. The samples are applied to SP-sepharose column equilibrating with 20mM Tris, pH7.4. The target protein is eluted by linear NaCl concentration gradient. **B**, SDS-PAGE analysis of collected elution fractions (25-30) for wild type mCHL2. M, marker of protein molecular weight; FH, Flow through; R, under reduced condition; NR, under non-reduced condition. The mCHL2 is indicated by arrow.

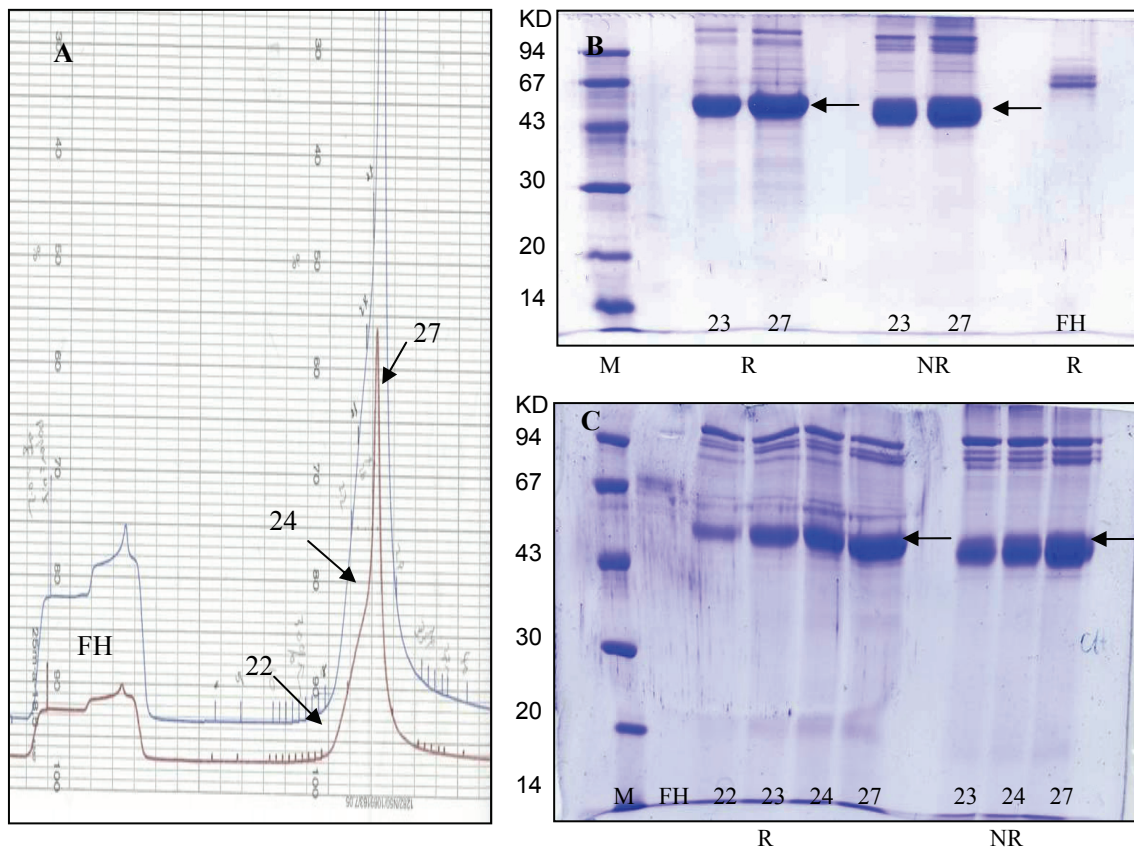


Figure 3.10: Purification of mCHL2 mutants by SP-sepharose cation exchange chromatography. **A**, The elution chart of mCHL2-N89Q/N180Q. The samples are applied to SP-sepharose column equilibrating with 20mM Tris, pH7.4. The target proteins are eluted by linear NaCl concentration gradient. The mCHL2-N89Q and mCHL2-N180Q are also purified by SP-sepharose cation exchange chromatography with the same protocol as the mCHL2-N89Q/N180Q. After the purification, the two mutants can get similar elution charts to mCHL2-N89Q/N180Q. **B**, SDS-PAGE analysis of collected fractions for mCHL2-N89Q. **C**, SDS-PAGE analysis of collected elution fractions for mCHL2-N89Q/N180Q. M, marker of protein molecular weight; FH, Flow through; R, under reduced condition; NR, under non-reduced condition. The mCHL2 mutants are indicated by arrows.

3.1.4.3 Purification of proteins by BMP-2 affinity chromatography

A column containing BMP-2-sepharose 4B gel was prepared and used for affinity chromatography. The protein solution after cation-exchange chromatography purification was passed over the BMP-2 affinity matrix and washed with wash buffer (10 mM HEPES, 500 mM NaCl, pH 7.4) to clean the column from non-specifically bound proteins. The specifically bound wild type mCHL2 and its mutants were eluted with 4M MgCl₂. The protein amount and purity of the collected fractions were analyzed on SDS-PAGE (Figure 3.11).

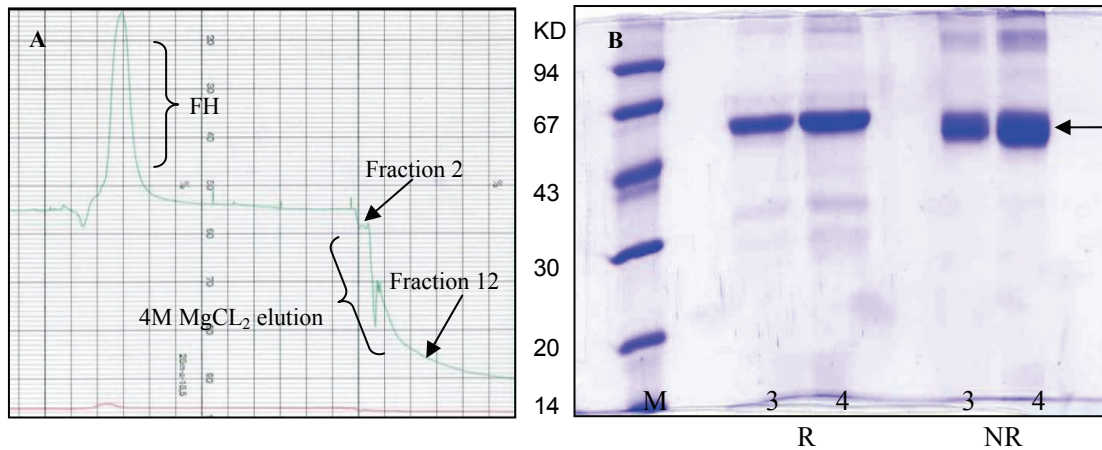


Figure 3.11: Purification of wild type mCHL2 by BMP-2 affinity chromatography. **A**, The elution chart of wild type mCHL2. The samples are applied to BMP-2 affinity column equilibrating with 10 mM HEPES, 500 mM NaCl, pH 7.4. The target proteins are eluted by 4M MgCl₂. **B**, SDS-PAGE analysis of collected fractions for wild type mCHL2. Line 3, 4, fraction 3 and 4; M, marker of protein molecular weight; R, under reduced condition; NR, under non-reduced condition. FH, flow through. The mCHL2 is indicated by arrow.

3.1.4.4 Purification of proteins by size exclusion chromatography

The protein solution which was purified by BMP-2 affinity chromatography was applied to Superdex™ 200 column. The separated fractions were analyzed with SDS-PAGE on purity and presence of possible structure isomers (Figure 3.12, 3.13). Finally the pure fractions were stored in -20 °C for further experiments.

After the purification of Ni-NTA affinity chromatography, cation exchange chromatography, BMP-2 affinity chromatography and size exclusion chromatography, the expression of recombinant mCHL2 and its double mutant (mCHL2-N89Q/N180Q) from SF9 cells respectively yielded 2-2.5mg and 0.7-0.9mg per liter of SF9 cell suspension.

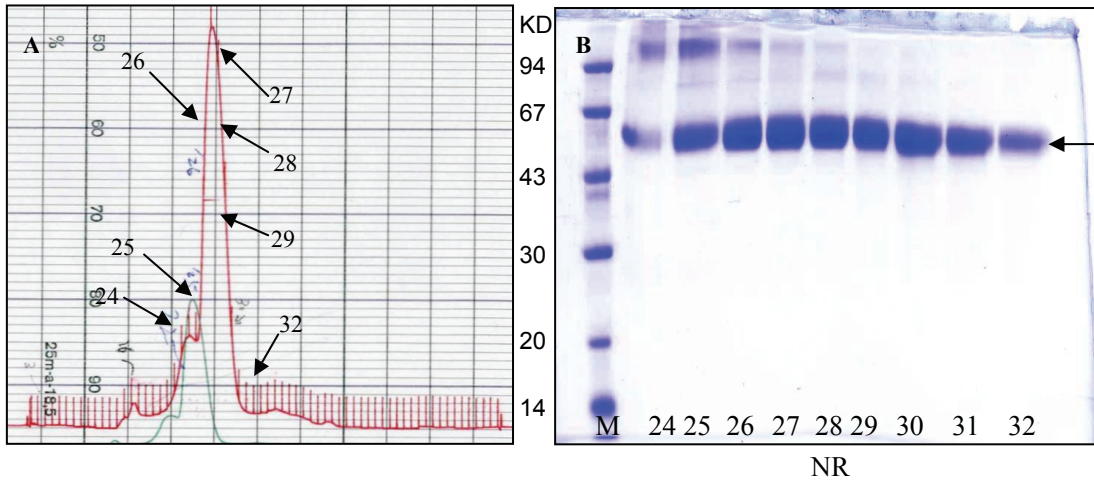


Figure 3.12: Purification of wild type mCHL2 by superdex 200 column. **A**, The elution chart of wild type mCHL2. The sample is running in 10 mM HEPES, 700 mM NaCl, pH 7.4. **B**, SDS-PAGE analysis of collected fractions for wild type mCHL2. Line 24-32, fraction 24-32; Wild type mCHL2 is indicated by arrow; M, marker of protein molecular weight; NR, under non-reduced condition.

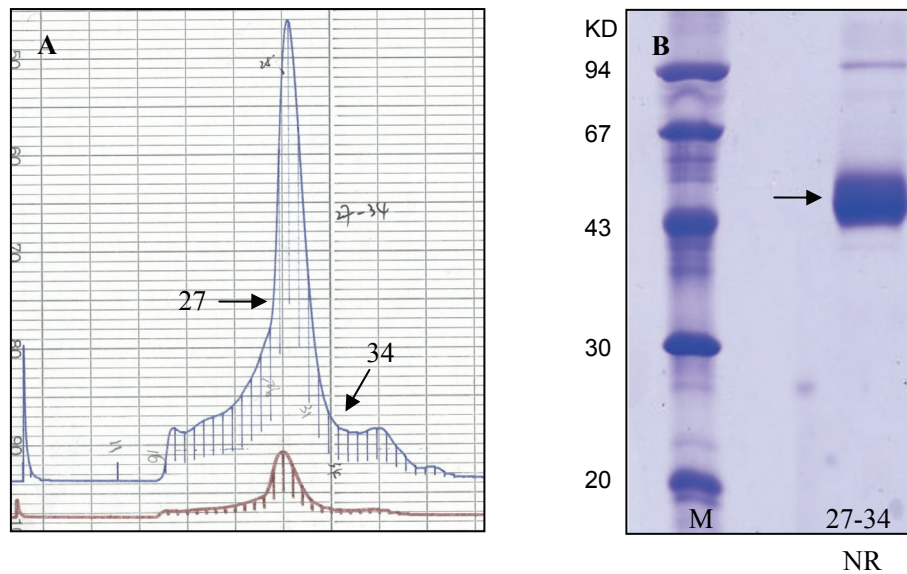


Figure 3.13: Purification of mCHL2-N89Q/N180Q by superdex 200 column. **A**, The elution chart of mCHL2-N89Q/N180Q. The sample is running in 10 mM HEPES, 700 mM NaCl, pH 7.4. **B**, SDS-PAGE analysis of collected fractions for mCHL2-N89Q/N180Q. mCHL2-N89Q/N180Q is indicated by arrow. M, marker of protein molecular weight; NR, under non-reduced condition.

3.2 Preparation of mCHL2-VWC1 in *E.coli*

3.2.1 Cloning of mCHL2-VWC1 into QKA vector

mCHL2-VWC1 cDNA encoding the amino acids 1-78 of the mature mCHL2 was ligated into the QKA expression vector between NcoI and BamHI restriction sites (Figure 3.14). The recombinant plasmid was transformed into competent *E.coli* MM294. Then the transformed cell suspension was plated separately to Kanamycin-plates which were incubated at 37 °C overnight to develop colonies of the transformed cells. Sequencing of plasmid DNA from positive colonies was confirmed the correct cDNA insert.

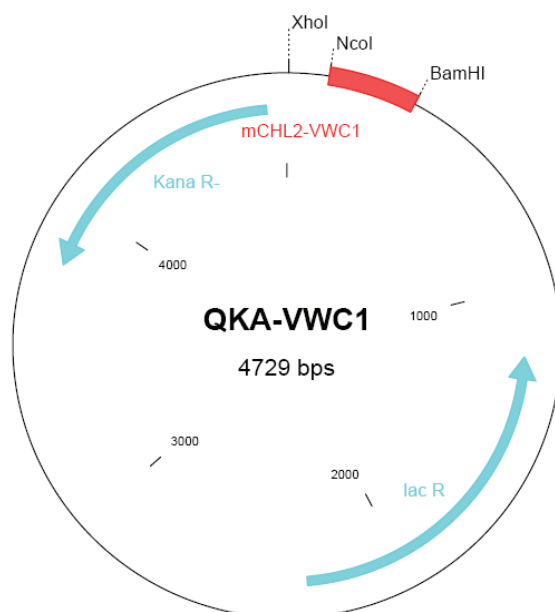


Figure 3.14: Map of expression vector QKA-VWC1. The cDNA of mCHL2-VWC1 is cloned into the expression vector QKA between NcoI and BamHI restriction sites.

3.2.2 Expression and purification of mCHL2-VWC1

For the expression of mCHL2-VWC1, *E.coli* was cultivated at 37 °C until reaching early states of logarithmic growth phase with OD₅₅₀ of 0.5-0.7 and then induced by 1mM IPTG for 4h. Under these conditions, the recombinant mCHL2-VWC1 was expressed as inclusion body in the cell cytoplasm. The induced and non-induced bacteria were analyzed by SDS-PAGE (Figure 3.15, A).

The inclusion bodies were completely dissolved in 6M GuHCl for denaturation and purified by size-exclusion chromatography on Sephacryl S300. Then every fraction was analyzed by SDS-PAGE (Figure 3.15, B). Later the target fractions containing denatured mCHL2-VWC1 protein were concentrated to a final absorbency of 20 OD/ml and refolded by the renaturation protocol.

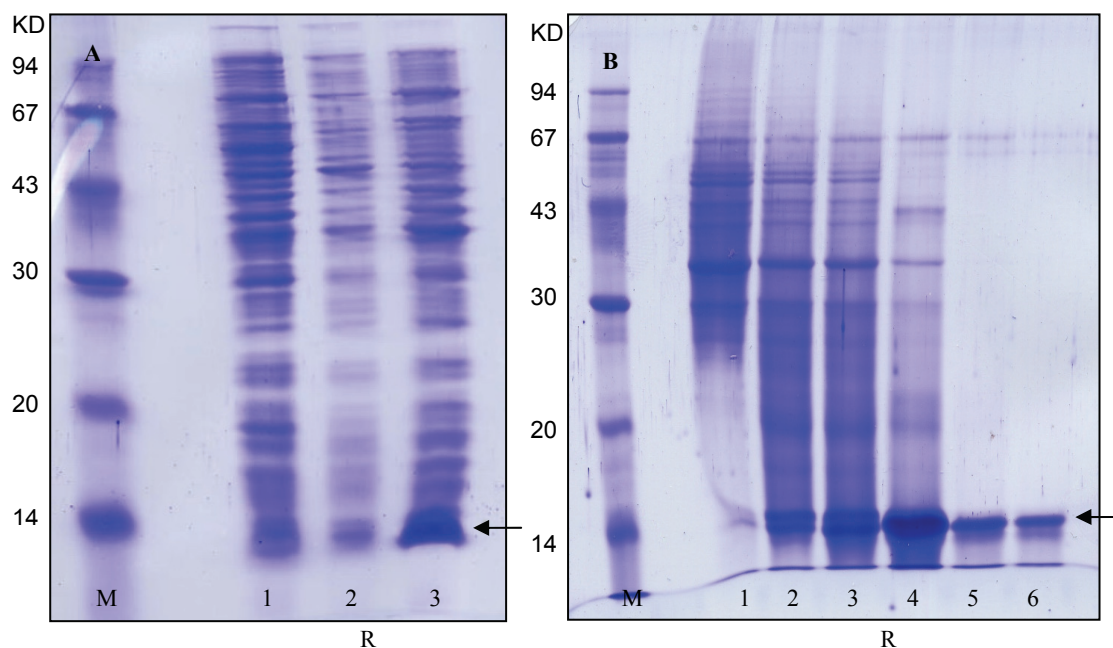


Figure 3.15: **A**, An analytical SDS-PAGE illustrating steps of mCHL2-VWC1 expression. 1, overnight culture; 2, OD 0.5 culture; 3, induced culture by IPTG. **B**, Purification of the denatured mCHL2-VWC1 by size-exclusion chromatography on Sephacryl S300 with 6 M Guanidin HCl, 50 mM NaOAc, 1 mM EDTA, pH 5.0. mCHL2-VWC1 is indicated by arrows. M, marker of molecular weight; R, under reduced condition

The refolded mCHL2-VWC1 was purified by cation exchange chromatography, BMP-2 affinity chromatography, size exclusion chromatography of Superdex 200 and then HPLC (Figure 3.16). The final purified mCHL2-VWC1 was analyzed by Mass Spectrometry (Figure 3.17). The mass result showed that the measured molecular weight of 8883.092 corresponds to the expected calculated molecular weight of 8883.036. This method can yield about 900 μ g VWC1 proteins per 10g wet cells.

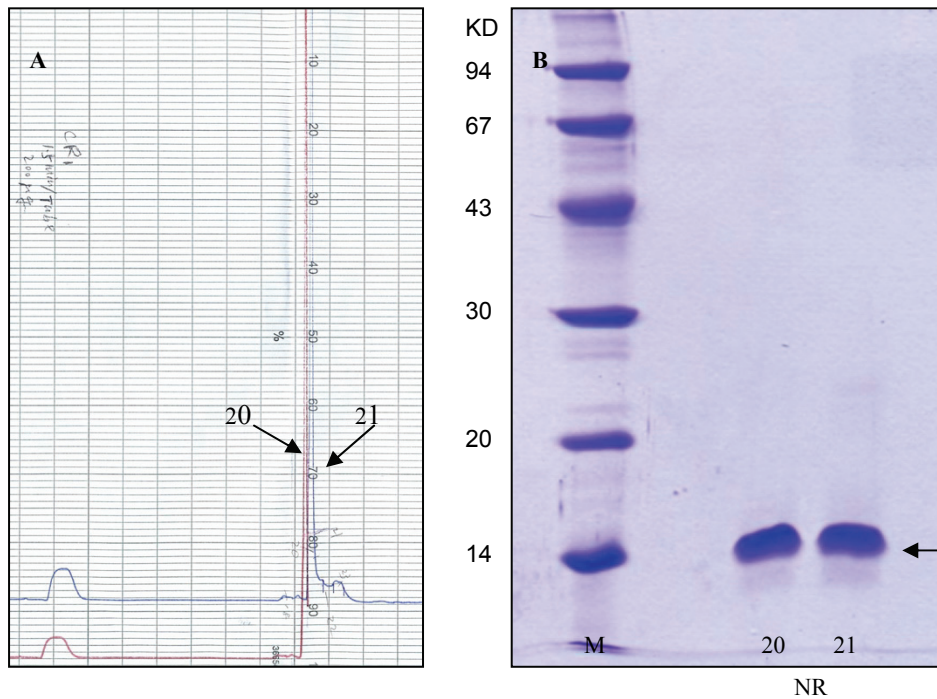


Figure 3.16: Purification of CHL2-VWC1 by HPLC. **A**, The elution chart of mCHL2-VWC1. The samples are applied to HPLC column equilibrating with 0.1% Trifluoroacetic acid. The target proteins are eluted at around 27% of acetonitrile. **B**, SDS-PAGE of the fractions 20 and 21 of HPLC. mCHL2-VWC1 is indicated by arrow. M, marker of molecular weight; NR, under non-reduced condition.

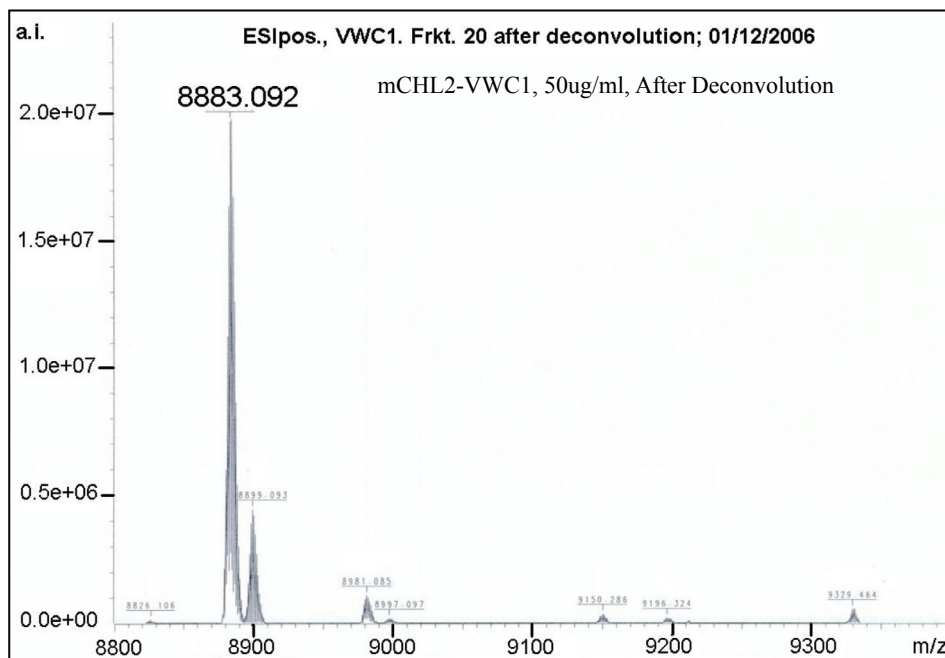


Figure 3.17: ESI/FT-ICR Mass spectrometry analysis of mCHL2-VWC1. Signal with average relative mass of 8883.092 corresponds to the expected mCHL2-VWC1 (calculated molecular weight is 8883.036)

3.3 Preparation of mCHL2-VWC2 in SF9 cells

3.3.1 Cloning of mCHL2-VWC2 into pAcGP67-B/Th/m

The cDNA of mCHL2-VWC2 encoding the amino acids 71-169 was inserted into the transfer vector pAcGP67-Bm between StuI and XbaI restriction sites (Figure 3.18).

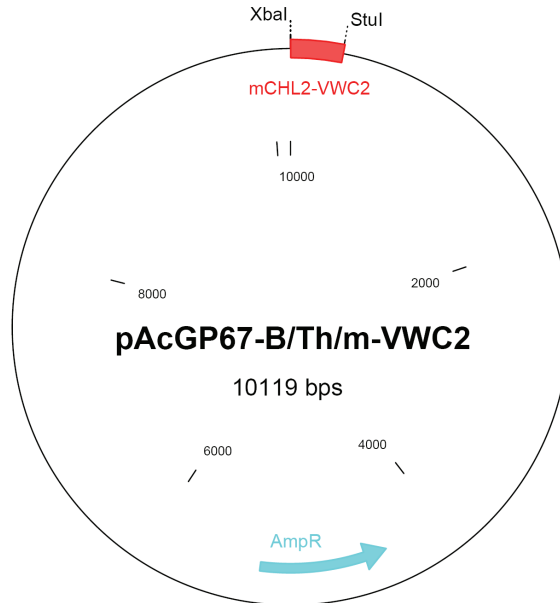


Figure 3.18: Map of transfer vector pAcGP67-B/Th/m-VWC2. The cDNA of mCHL2-VWC2 is cloned into the transfer vector pAcGP67-B/Th/m between StuI and XbaI restriction sites.

Then the plasmid carrying mCHL2-VWC2 was transformed into competent *E.coli* MM294, and first selected by plating transformation cell suspension on Ampicillin agar plate. The later selection procedure was performed by analytical restriction digestion. The intact circular plasmid was digested with StuI and XbaI to confirm the presence of mCHL2-VWC2 in the plasmid. The positive clones could show a band of 297 bp after the restriction digestion reaction visualized on 2% agarose gel. Then the positive plasmid DNA was prepared and purified by DNA maxi preparation Kit (see 2.11.8) for DNA Sequencing. The plasmid DNA with correct sequence was used for storage and the subsequent co-transfection.

3.3.2 Co-transfection of BaculoGold DNA and the transfer vector into SF9 insect cells

and amplification of the recombinant virus

The same protocol as the pAcGP67-B/Th/m-mCHL2 was used for the co-transfection and the amplification of the recombinant virus of pAcGP67-B/Th/m-mCHL2-VWC2 (see 3.1.3). A Western blot was performed with the virus supernatants to verify the protein production (Figure 3.19)

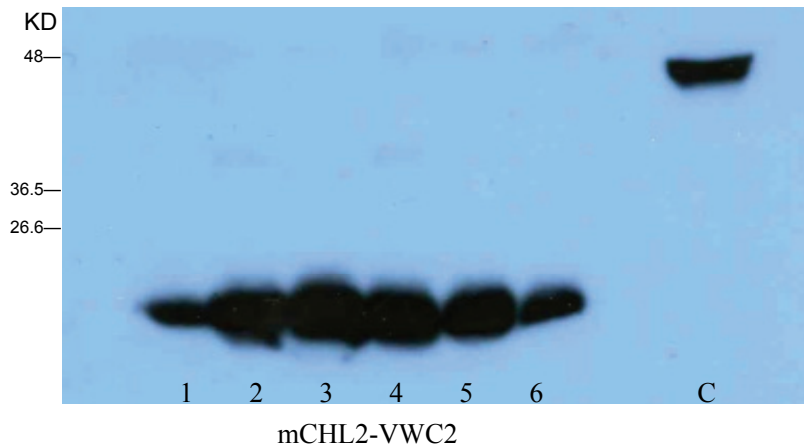


Figure 3.19: Analysis of mCHL2-VWC2 expression in SF9 cells. Virus medium infected with Baculovirus containing mCHL2-VWC2 cDNA was applied to western blot and detected by Anti-his tag antibody. C, Positive control (wild type mCHL-2 expressed in SF9 with Baculovirus transfer vector pAcGP67-B/Th/m); lines 1-6, examined recombinant virus clones of mCHL2-VWC2, molecule weight of the target protein is 10.89 KD.

3.3.3 Expression and purification of mCHL2-VWC2

After the expression step, the culture supernatant was purified by the Ni-NTA affinity column. Next the protein was applied to size exclusion chromatography- Sephacryl S-100 column. The protein purity of the collected fractions was analyzed on SDS-PAGE (Figure 3.20).

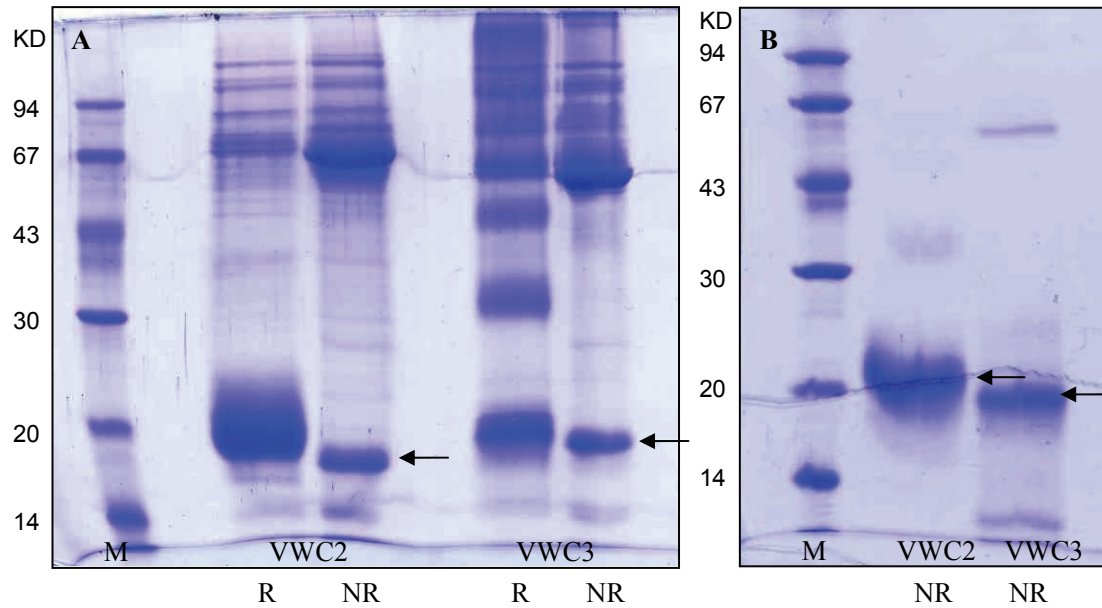


Figure 3.20: **A**, SDS-PAGE showing mCHL2-VWC2 and mCHL2-VWC3 purified by Ni-NAT affinity chromatography. **B**, SDS-PAGE showing mCHL2-VWC2 and mCHL2-VWC3 purified by size exclusion chromatography. M, marker of protein molecular weight; mCHL2-VWC2 and mCHL2-VWC3 were indicated by arrows. R, under reduced condition; NR, under non-reduced condition.

3.4 Preparation of mCHL2-VWC3 and its mutants

3.4.1 Preparation of mCHL2-VWC3 in SF9 cells

The same protocol as the preparation of mCHL2-VWC2 (its cDNA encoding 203-301 amino acids of mature mCHL2) in SF9 cells was used for the preparation of mCHL2-VWC3 (see 3.3) (Figures 3.21, 3.22). The protein purity of the collected fractions was analyzed on SDS-PAGE (Figure 3.20).

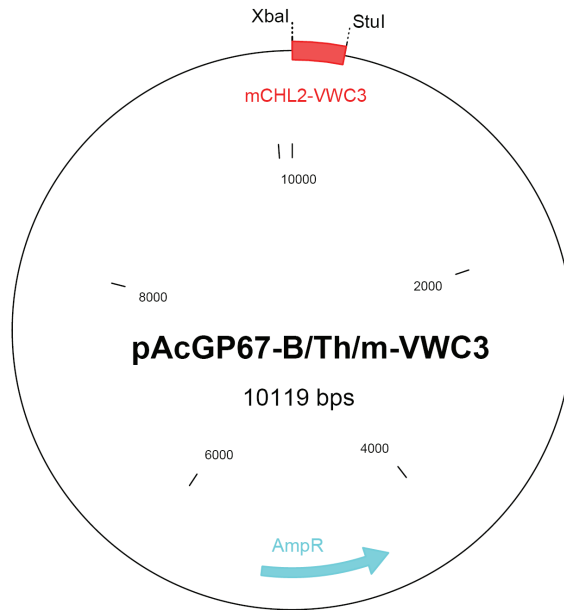


Figure 3.21: Map of transfer vector pAcGP67-B/Th/m-VWC3. The cDNA of mCHL2-VWC3 is cloned into the transfer vector pAcGP67-B/Th/m between StuI and XbaI restriction sites.

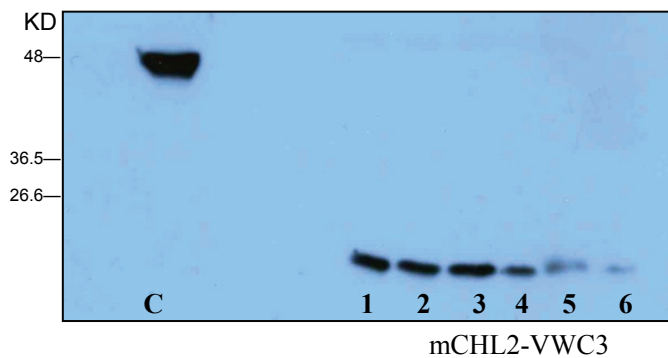


Figure 3.22: Analysis of mCHL2-VWC3 expression in SF9 cells. Virus medium infected with Baculovirus containing mCHL2-VWC3 cDNA was applied to western blot and detected by Anti-his tag antibody. C, Positive control (wild type mCHL-2 expressed in SF9 with Baculovirus transfer vector pAcGP67-B/Th/m); lines 1-6, examined recombinant virus clones of mCHL2-VWC3, molecule weight of the target protein is 10.94 KD.

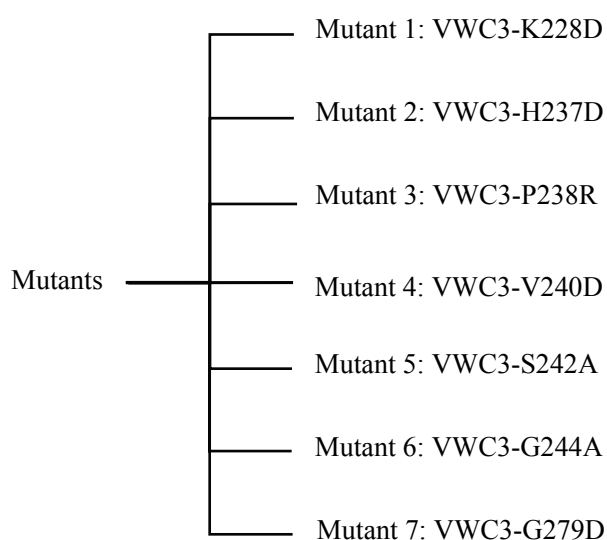
3.4.2 Preparation of mCHL2-VWC3 and its mutants in *E.coli*

3.4.2.1 Cloning of mCHL2-VWC3 and its mutants into QKA vector

mCHL2-VWC3 cDNA encoding amino acids 218-290 of the mature mCHL2 and its mutants cDNA were ligated to QKA expression vector between NcoI and BamHI

restriction sites (Figure 3.23). The nucleotide and amino acid sequence of mCHL2-VWC3 and its mutants are shown in Figure 3.24. The recombinant plasmids carrying mCHL2-VWC3 and mutant mCHL2-VWC3 cDNA were transformed into competent *E.coli* MM294. Then the transformed cell suspension was plated separately to Kanamycin-plates. The plates were incubated at 37°C overnight to develop colonies of the transformed cells. Because the plasmid contains Kanamycin resistance gene, only bacterial cells carrying plasmid QKA/mCHL2-VWC3 or QKA/mutant mCHL2-VWC3 or empty OKA would be able to form colonies. The later selection procedure was completed by analytical restriction digestion of the purified cDNA. The intact circular plasmid was digested with NcoI and BamHI to confirm the presence of mCHL2-VWC3 or mutant mCHL2-VWC3 cDNA in the plasmid. The positive clones showed a band of 222 bp after the restriction digestion reaction has been visualized on 2% agarose gel. The positive plasmid DNA was prepared and purified by DNA maxi preparation Kit (see 2.11.8) for DNA Sequencing. The plasmid DNA with correct sequence was used for storage and following expression.

To generate the mutants of mCHL2-VWC3, an alignment of mCHL2-VWC3 and col IIA VWC domain was performed. In the NMR structure of col IIA VWC, some residues expose to the surface, which are likely involved in BMP binding. The residues of mCHL2-VWC3 which corresponds to these amino acids of col IIA VWC were chosen for mutagenesis. The mutants of mCHL2-VWC3 are shown below:



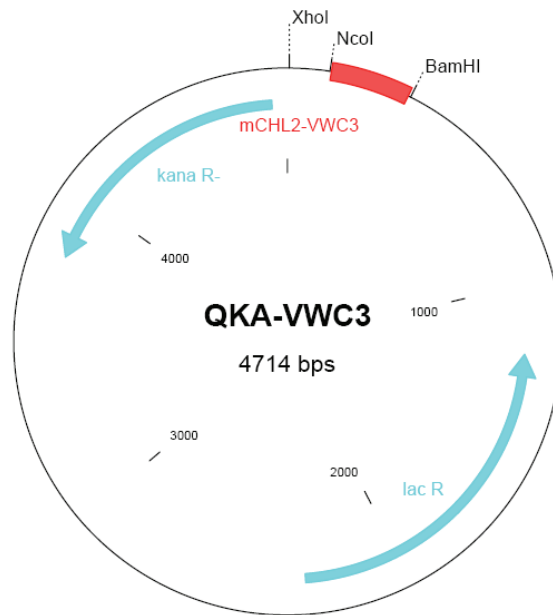


Figure 3.23: Map of expression vector QKA-VWC3. The cDNA of mCHL2-VWC3 is cloned into the expression vector QKA between NcoI and BamHI restriction sites.

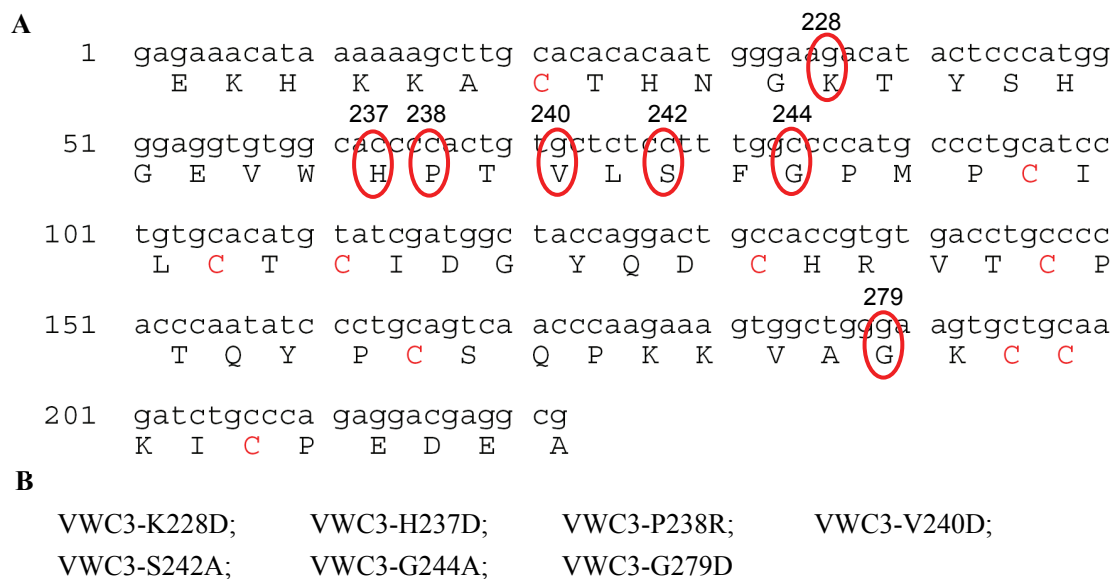


Figure 3.24: The nucleotide and amino acid sequence of mCHL2-VWC3 (A) and its mutants (B). The mutated residues were encircled. The 10 cysteines are highlighted in red.

3.4.2.2 Expression and purification of mCHL2-VWC3 and its mutants

a) Expression of proteins in *E.coli*

For the expression of mCHL2-VWC3 and its mutants, *E.coli* was cultivated at 37°C until

reaching early states of logarithmic growth phase with OD_{550} of 0.5-0.7 and then induced by 1mM IPTG for 4h. Under these conditions, the recombinant mCHL2-VWC3 and its mutants were expressed as inclusion body in the cell cytoplasm. The non-induced and induced VWC3 bacteria were analyzed by SDS-PAGE (Figure 3.25).

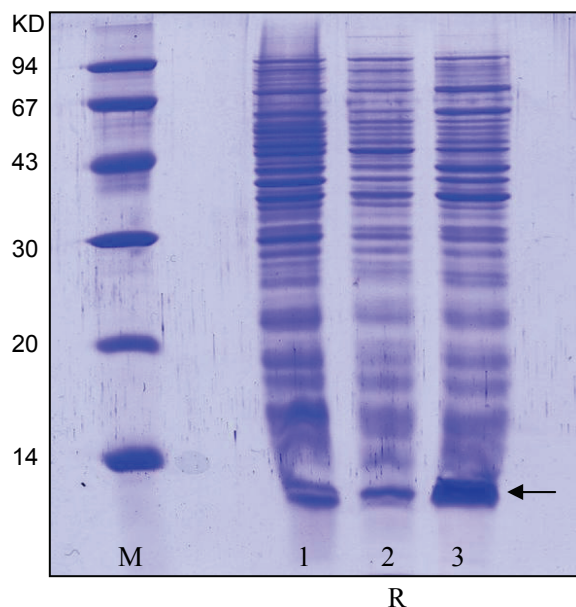


Figure 3.25: An analytical SDS-PAGE illustrating steps of mCHL2-VWC3 expression. 1, overnight culture; 2, OD 0.5 culture; 3, induced culture by IPTG. M, marker of molecular weight. R, under reduced condition. mCHL2-VWC3 is indicated by arrow.

b) Preparation of inclusion body of proteins

The bacterial cells were resuspended with $TBSE_{\beta-ME}^{PMSF}$ buffer and sonicated following the protocol (see 2.14.3). The sediment containing inclusion bodies, was washed with 0.67M GuHCl for 30 min at RT.

c) Denaturation and refolding of proteins

The inclusion bodies were completely dissolved in 6 M GuHCl for denaturation and purified by size-exclusion chromatography on Sephacryl S300. Then every fraction was analyzed by SDS-PAGE (Figure 3.26). Later the target fractions containing denatured mCHL2-VWC3 or its mutant protein were concentrated to the final absorbency of 20 OD/ml and refolded by diluting 100 times with the refolding buffer (see 2.14.4) and

incubating for 7 days at 4 °C.

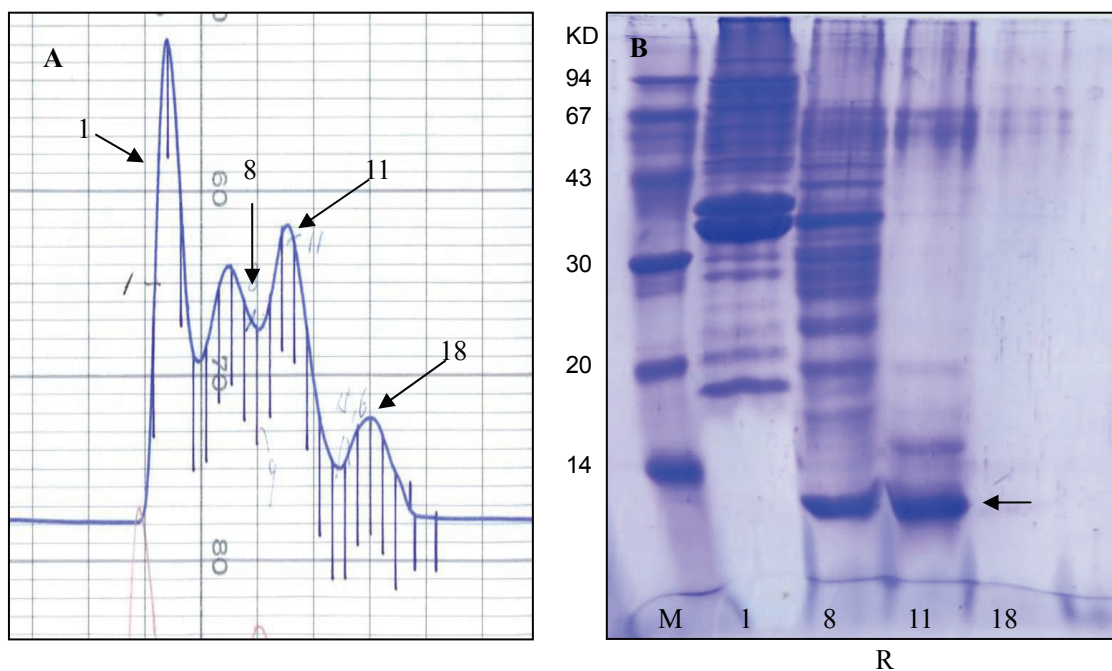


Figure 3.26: Purification of the denatured mCHL2-VWC3 by size-exclusion chromatography on Sephacryl S300 with 6 M Guanidin HCl, 50 mM NaOAc, 1 mM EDTA, pH 5.0. **A**, The elution chart of mCHL2-VWC3 on Sephacryl S300. **B**, SDS-PAGE analysis of collected fractions indicated by fraction numbers. The fractions 8 to 15 were combined for the further experiments. mCHL2-VWC3 is indicated by arrows. M, marker of molecular weight; R, under reduced condition.

d) Purification of proteins by cation exchange chromatography on SP-sepharose

The refolded mCHL2-VWC3 and its mutants were first purified by cation exchange chromatography. Since the pI of mCHL2-VWC3 and its mutants are around 8.12, the proteins could be applied to SP-sepharose at pH 7.4. During this cation exchange chromatography, the acidic and neutral contaminating proteins could not bind to the column. Therefore the mCHL2-VWC3 and its mutants could be effectively separated. The bound proteins were eluted with linear salt gradient from 0 M to 1 M NaCl. The protein purity of the collected fractions was analyzed on SDS-PAGE. The eluted proteins consist of monomer and multimers which appear as two unseparate peaks (Figure 3.27). The wild type mCHL2-VWC3 was further purified by BMP-2 affinity chromatography. The CHL2-VWC3 mutants were purified by HPLC directly.

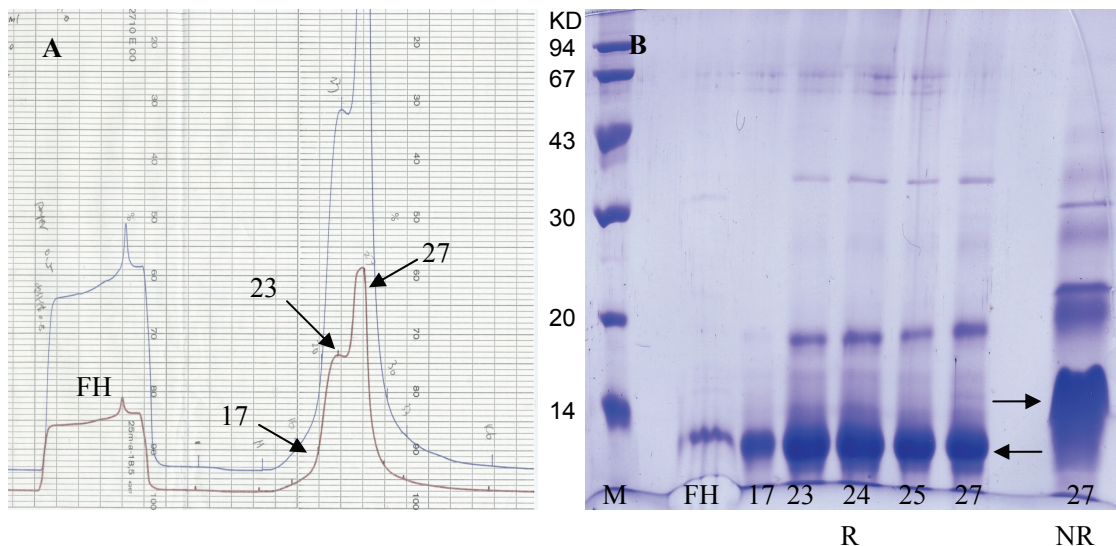


Figure 3.27: Purification of wild type mCHL2-VWC3 by SP-sepharose cation exchange chromatography. **A**, The elution chart of wild type mCHL2-VWC3. The samples are applied to SP-sepharose column equilibrating with 20mM Tris, pH7.4. The target protein is eluted by linear NaCl concentration gradient from 0-1 M. **B**, SDS-PAGE analysis of collected fractions for wild type mCHL2-VWC3. M, marker of molecular weight; FH, Flow through; R, under reduced condition; NR, under non-reduced condition. The fractions from 17 to 34 were combined for the further purification. mCHL2-VWC3 is indicated by arrows.

e) Purification of mCHL2-VWC3 by BMP-2 affinity chromatography

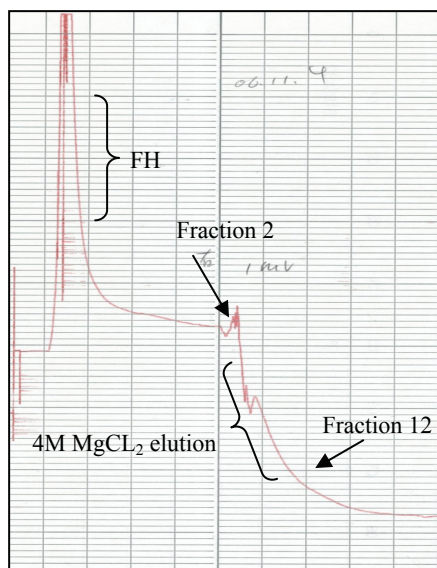


Figure 3.28: The elution chart of the purification of wild type mCHL2-VWC3 by BMP2 affinity chromatography. The samples are applied to BMP2 affinity column equilibrating with 10 mM HEPES, 500 mM NaCl, pH 7.4. The target proteins are eluted by 4M MgCl₂. FH: flow through.

The protein solution after the purification of cation-exchange chromatography was passed over the affinity matrix and washed with wash buffer (10 mM HEPES, 500 mM NaCl, pH

7.4) to clean the column from non-specifically bound proteins. The specifically bound wild type mCHL2-VWC3 was eluted with 4M MgCl₂ (Figure 3.28).

f) Purification of proteins by size exclusion chromatography

The protein solution which was purified by BMP-2 affinity chromatography was applied to Superdex™ 200 column. The separated fractions were analyzed with SDS-PAGE on purity and presence of possible structure isomers (Figure 3.29). Finally the proteins were purified by HPLC.

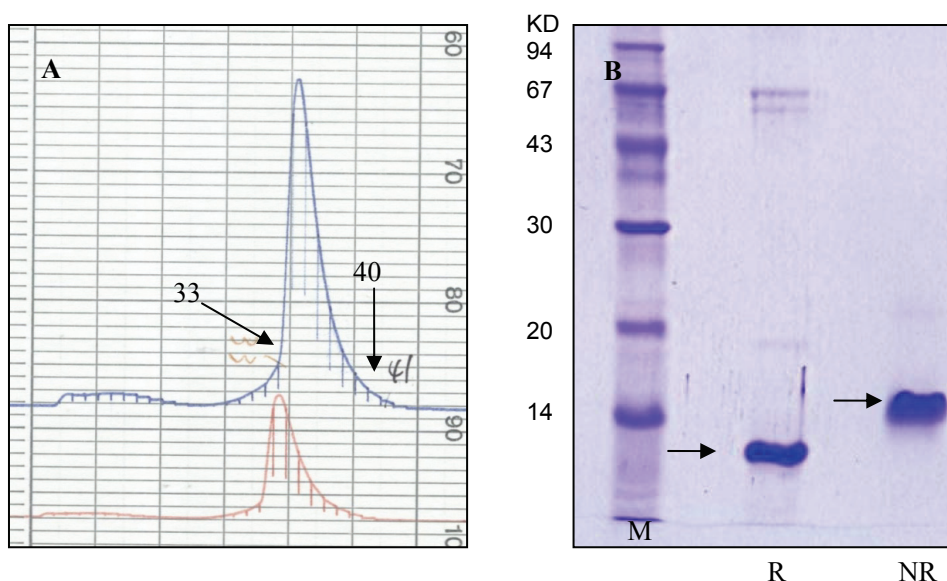


Figure 3.29: Purification of wild type mCHL2-VWC3 by size exclusion chromatography on superdex 200 column. **A**, The elution chart of mCHL2-VWC3. The sample is running in 10 mM HEPES, 700 mM NaCl, pH 7.4. **B**, SDS-PAGE analysis of collected fractions from 33 to 40 of wild type mCHL2-VWC3. The fractions from 33 to 40 were collected for further experiments. M, marker of molecular weight; R, under reduced condition; NR, under non-reduced condition. Wild type mCHL2-VWC3 was indicated by arrow.

g) Purification of proteins by HPLC

The protein purification was accomplished by reversed phase HPLC. Based on hydrophobic interactions, the protein bound to the chromatography matrix and the elution with increasing concentration of acetonitrile was performed. The mCHL2-VWC3 and its mutants were eluted at around 27% of acetonitrile. The collected fractions were analyzed by SDS-PAGE (Figure 3.30). The highly purified proteins were divided into aliquots, lyophilized and stored at -20 °C for following mass spectrometry analysis. This method can yield about 1.5-2.2 mg CR3

proteins per 10g wet cells.

The mass spectrometry showed the measured molecular weight of 8360.776 for wild type VWC3 corresponds to the expected calculated molecular weight of 8360.750 (Figure 3.31).

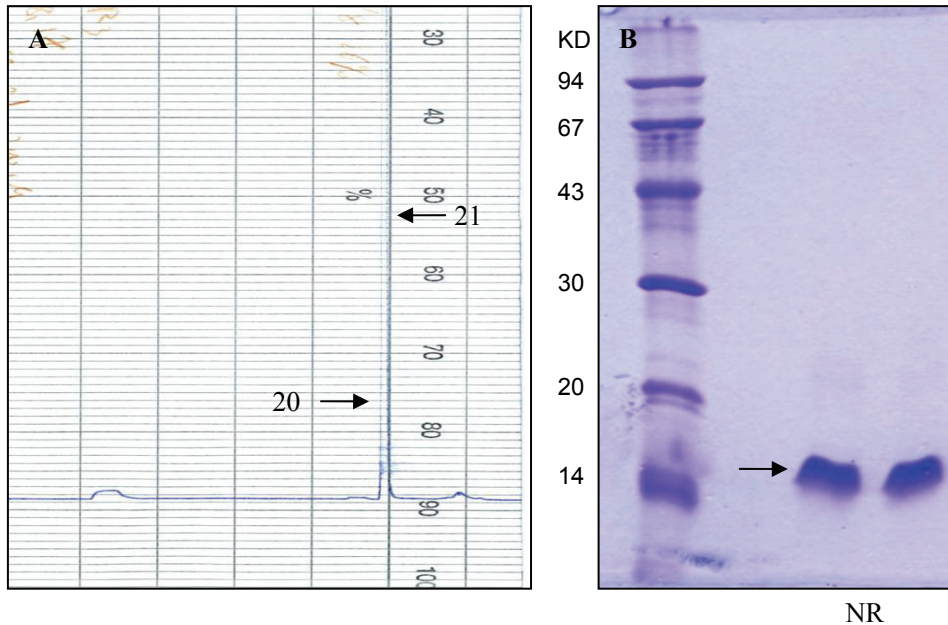


Figure 3.30: Purification of mCHL2-VWC3 by HPLC. **A**, The elution chart of mCHL2-VWC3. The samples are applied to HPLC column equilibrating with 0.1% Trifluoroacetic acid. The target proteins are eluted at around 27% of acetonitrile. **B**, SDS-PAGE of the fractions 20 and 21 of HPLC. mCHL2-VWC3 is indicated by arrow. M, marker of molecular weight; NR, under non-reduced condition.

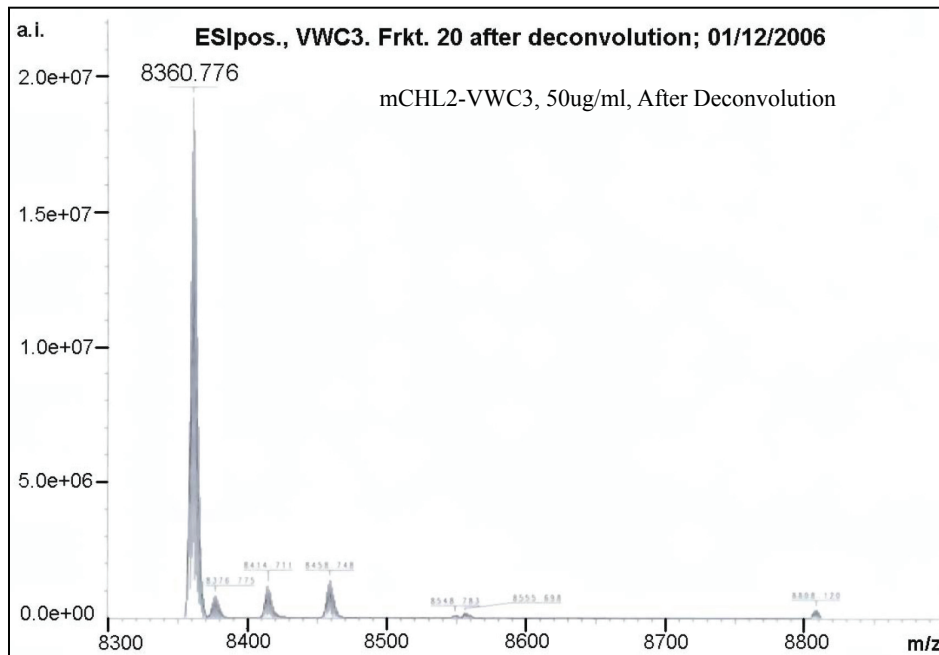


Figure 3.31: ESI/FT-ICR Mass spectrometry analysis of mCHL2-VWC3. Signal with average relative mass of 8360.776 corresponds to the expected mCHL2-VWC3 (calculated molecular weight is 8360.750)

3.5 Functional analysis of mCHL2 and its VWC domains

3.5.1 Binding of mCHL2 and its VWC domains to BMPs

The binding affinities of mCHL2 and its VWC domains to BMPs were analyzed by BIAcore technology with immobilized BMPs and mCHL2 respectively (Figure 3.32; Table 3.5, 3.6). mCHL2 bound to immobilized BMP-2 with a K_D of 10 nM, and BMP-2 bound to immobilized mCHL2 with an affinity of 1nM (Figure 3.32). These affinities are similar to those of BMP-2 for its high affinity type I receptor (Kirsch et al., 2000a; Keller et al., 2004). BMP-7 bound to immobilized mCHL2 with about 20 times lower affinity than BMP-2. GDF-5 bound to immobilized mCHL2 with lower affinity than BMP-2 and BMP-7.

mCHL2 contains three VWC domains. We found that mCHL2-VWC1 and mCHL2-VWC3 bound to BMP-2, BMP-7 and GDF-5, but mCHL2-VWC2 did not (Table 3.5, 3.6). Compared with full-length mCHL2, mCHL2-VWC1 and mCHL2-VWC3 domains bound to immobilized BMP-2 with about 100 and 20 times lower affinity separately. The results indicate that the high affinity of mCHL2 to BMP-2 results from the cooperative binding of these two VWC domains. mCHL2-VWC1 and mCHL2-VWC3 bound to BMP-7 with similar or slightly lower affinity as full-length mCHL2. mCHL2-VWC1 seems to account for most of the binding affinity for GDF-5 in the full-length mCHL2. Here again, the different binding affinities suggest that the single VWC domain has some selectivity for various BMP/GDF proteins.

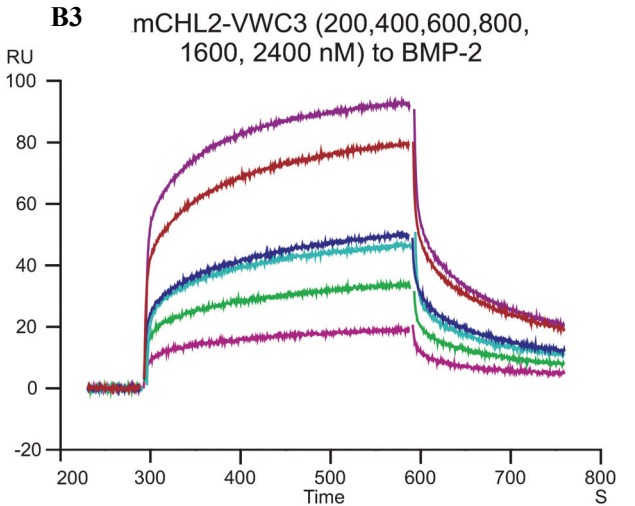
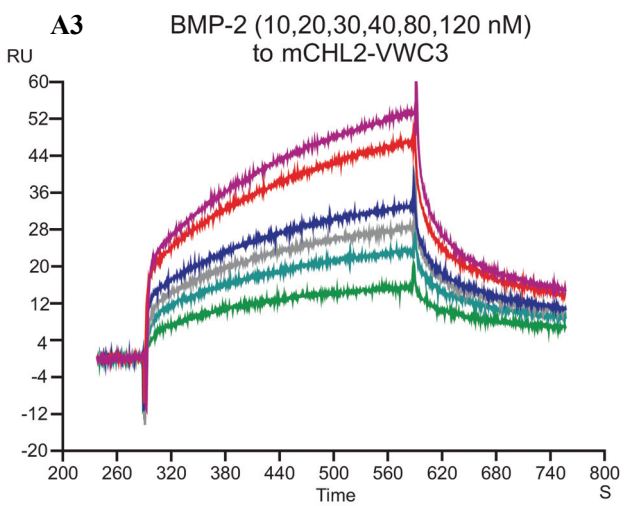
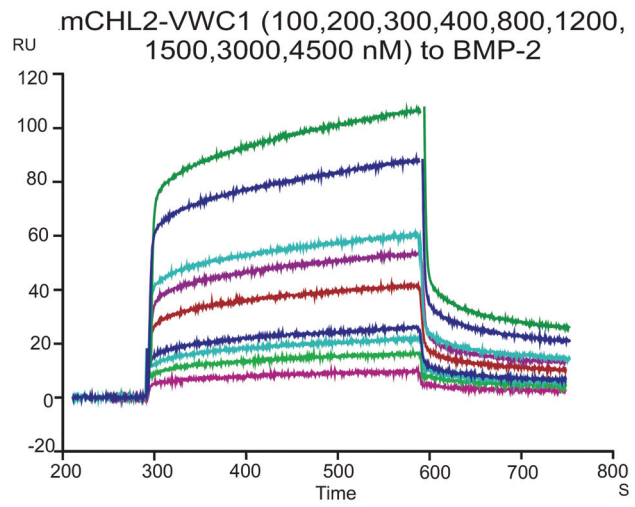
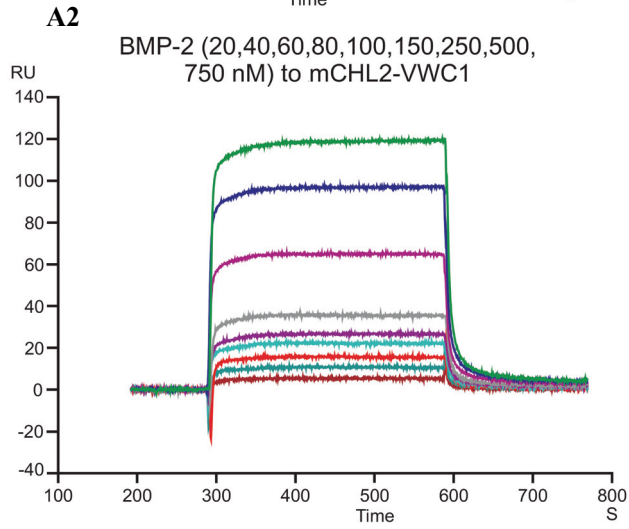
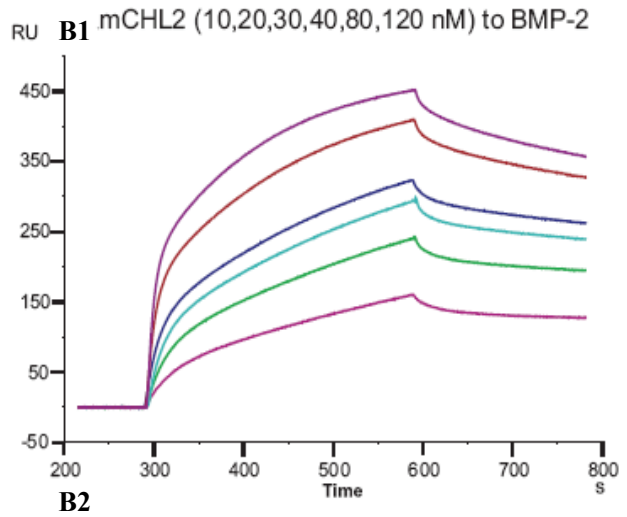
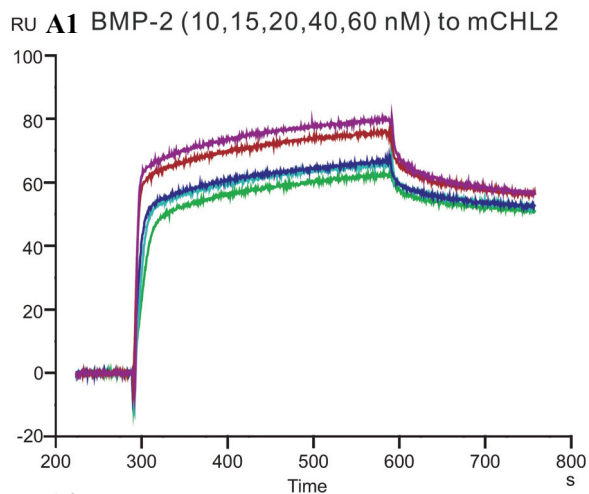


Figure 3.32: BIAcore analysis of mCHL2/VWCs and BMP-2 interaction **A1-A3**, overlay of sensograms showing the binding of BMP-2 to the immobilized full-length mCHL2, mCHL2-VWC1 or mCHL2-VWC3. BMP-2 at different concentrations was applied. **B1-B3**, overlay of sensograms showing the binding of full-length mCHL2, mCHL2-VWC1 or mCHL2-VWC3 to the immobilized BMP-2. Full-length mCHL2, mCHL2-VWC1 or mCHL2-VWC3 at different concentrations were applied.

Table 3.5: Binding analysis of BMPs and immobilized mCHL2/VWCs proteins (BIAcore)

	mCHL2			
	Full-length	VWC1	VWC2	VWC3
	Apparent K_D (nM)			
BMP-2	1.2	130	NB	20
BMP-7	21	32	NB	72
GDF5	44	70	NB	>1000

NB, No binding.

Table 3.6: Binding analysis of mCHL2/VWCs proteins and immobilized BMP-2 (BIAcore)

mCHL2	BMP-2
	Apparent K_D (nM)
Full-length	10
VWC1	2200
VWC2	NB
VWC3	300

NB, No binding.

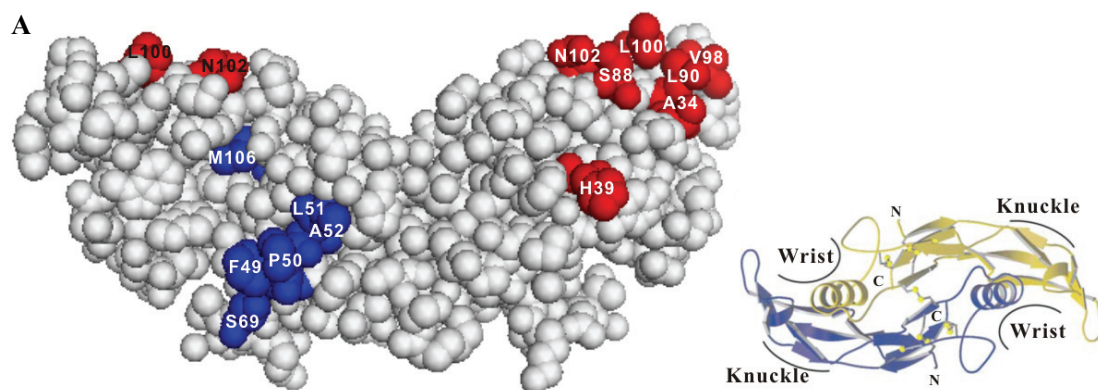
3.5.2 Binding epitopes of BMP-2 for mCHL2

A collection of BMP-2 mutants which were mutated in the wrist and knuckle epitopes was used to delimit binding epitopes of BMP-2 for mCHL2. The decreases of the binding affinities between BMP-2 mutants and immobilized mCHL2 and its VWC domains indicate the influences of the amino acid substitutions in the wrist and knuckle epitopes for binding. According to the structure of the ternary complex of BMP-2/BMPRII/ActRII (Weber et al., 2007), seven variants mutated in the wrist epitopes and eight variants mutated in the knuckle epitopes (Figure 3.33, A) in which single residues were substituted by alanine, charged residue or proline (Kirsch et al., 2000b; Keller et al., 2004), were selected for analyzing the interaction with mCHL2 and its VWC domains by Biacore. The mutants F49A, P50A, L51P, A52R, M106A, D53P, and S69R exhibited a reduced affinity for type I receptors. The mutants A34D, H39D, S88P, L90A, V98P, L100P, L100K and L100K/N102D bound type II receptors with reduced affinities (Kirsch et al., 2000b;

Keller et al., 2004; Zhang et al., 2007). mCHL2 bound many of the tested wrist and knuckle epitopes mutants with reduced binding affinity (Figure 3.33, B). The change of the affinity for the wrist epitope mutants was mild and for the knuckle epitopes mutants were relatively stronger. The results clearly indicate that mCHL2 binds to both the knuckle and wrist epitopes of BMP-2.

The binding of BMP-2 mutants for mCHL2-VWC1/-VWC3 was also measured (Figure 3.33, B). Almost all tested knuckle epitope mutants bound to mCHL2-VWC1 with significantly reduced binding affinity except mutant S88P. However, there was no difference of the binding affinities between wild type BMP-2 and the tested wrist epitope mutants to mCHL2-VWC1. In contrast, only wrist epitope mutants exhibited remarkable reduced binding affinity for mCHL2-VWC3 except mutant L51P. Together, the results indicated that the binding epitopes of BMP-2 for mCHL2 correspond with two different BMP-2 sites: the residues in the knuckle epitopes are involved in mCHL2-VWC1 binding and the residues in the wrist epitopes in binding to mCHL2-VWC3.

Moreover, the decreases of the affinities of the variants to full-length mCHL2 were lower than those to the VWC1 or VWC3 domain. This might be due to the compensating effects of two cooperative VWC domains in full-length CHL2 molecule (Figure 3.33, B).



B

Variants	Epitope	mCHL2					
		Full-length		VWC1		VWC3	
		K_D (nM)	V/W	K_D (nM)	V/W	K_D (nM)	V/W
BMP-2-Wild type		1.2	1.0	130	1.0	20	1.0
BMP-2-F49A	wrist	3.2	2.7	100	0.8	160	7.9
BMP-2-P50A	wrist	2.3	1.9	75	0.6	70	3.5
BMP-2-L51P	wrist	1.8	1.5	120	0.9	15	0.8
BMP-2-A52R	wrist	3.3	2.8	110	0.9	77	3.9
BMP-2-D53P	wrist	ND	-	ND	-	60	3.0
BMP-2-S69R	wrist	4.5	3.4	65	0.5	98	4.9
BMP-2-M106A	wrist	5.4	4.5	100	0.8	960	48
BMP-2-A34D	knuckle	10	8.3	28500	219	11	0.6
BMP-2-H39D	knuckle	1.8	1.5	280	2.1	15	0.8
BMP-2-S88P	knuckle	2.3	1.9	100	0.8	21	1.0
BMP-2-L90A	knuckle	11	9.2	4300	33	17	0.9
BMP-2-V98P	knuckle	6.2	5.2	1800	14	33	1.7
BMP-2-L100P	knuckle	3.6	3.0	1400	11	29	1.5
BMP-2-L100K	knuckle	4.3	3.6	700	5.4	28	1.4
L100K/N102D	knuckle	4.3	3.6	1300	9.8	37	1.9

ND, Not done; V/W, Ratio of K_D (Variant/Wild type)

Ratio of K_D (Variant / Wild type)



Figure 3.33: Mutational analysis of BMP2 interaction with mCHL2 and its VWC domains

A, Mutants in the wrist (Blue) and knuckle (Red) epitopes of BMP-2, which were selected for analysis. The small ribbon model presents a view of BMP-2 along the 2-fold axis and shows the location of the wrist and knuckle epitopes. **B**, The binding affinities of wild-type and mutant BMP-2 for immobilized full-length mCHL2 and its VWC domains. Relative affinities (Ratio of K_D) showing the influence of the mutations on binding. Values of relative K_D are classified into six categories according to the colour code shown at the bottom of the table.

3.5.3 Binding mode of mCHL2 and BMP-2

Previous study showed that binding affinities of BMP-2 for receptors are two orders of magnitude different when binding is measured by Biacore with immobilized ectodomain or with immobilized ligand, respectively (Kirsch et al., 2000b; Sebald et al., 2004). This difference has been explained by the assumption that the solute BMP-2 dimer binds simultaneously to two immobilized receptors on the chip (1:2 interaction), which results in an enhanced affinity, whereas the separate ectodomains bind immobilized BMP-2 in a

1:1 interaction, which results in a low affinity. Similarly the affinity of solute mCHL2 to immobilized BMP-2 was about 10-fold lower than that of solute BMP-2 to immobilized mCHL2 (Figure 3.33 and Table 3.5). Therefore, the binding of mCHL2 to BMP-2 may also follow the rule of BMP/ receptors interaction. In this case, two mCHL2 molecules bind to BMP-2 dimer in a 2:1 interaction. As two wrist and two knuckle epitopes exist in the BMP-2 dimer, this assumption of binding mode also fit to the result that VWC1 and VWC3 of mCHL2 bound respectively to the knuckle and wrist epitopes of BMP-2.

The 2:1 stoichiometry of the mCHL2/BMP-2 complex is further confirmed by the analysis of gel-filtration chromatography and SDS-PAGE. The free mCHL2, BMP-2 and mixtures of BMP-2 and mCHL2 in different molar ratios were chromatographed on a Superdex 200 HR 10/30 column. When a 2.5:1 mixture of mCHL2 and BMP-2 was chromatographed, a major peak with an apparent molecular weight of 140 kDa was separated from a minor peak corresponding to the excess mCHL2 (Figure 3.34, A, c). When a 2:1 mixture of mCHL2 and BMP-2 was chromatographed, the whole protein was eluted as a single peak of 140 kDa (Figure 3.34, A, d). The apparent molecular weight of 140 kDa agrees with the calculated molecular weight of 138 kDa for a 2:1 complex of mCHL2 and BMP-2. When a 1:1 mixture of mCHL2 and BMP-2 was chromatographed, the mixture was eluted with a major peak (140 kDa) and a second slight shoulder (Figure 3.34, A, e). The main peak with an apparent molecular weight of 140 kDa matches the molecular weight of the 2:1 complex. But the apparent molecular weight of 80 kDa of the second shoulder observed only after separation of the 1:1 mixture is similar to the molecular weight of a 1:1 complex (80 kDa). Probably, the surplus of free BMP-2 precipitated under this condition and was not recovered.

Finally the quantitative protein composition of the chromatographed fractions was determined by SDS-PAGE analysis and subsequent Integrated Density (ID) analysis of the Coomassie stained proteins by the software of *Scion Image* (Figure 3.34, B). On the same gel, 2:1 and 1:1 mixtures of mCHL2 and BMP-2 were analyzed as standard. PAGE of the gel filtration fractions of the 2.5:1 CHL2/BMP-2 mixture revealed the complex formation by co-elution of mCHL2 and BMP-2 from fractions 22 to 26 (Figure 3.34, A, c). The ratio of the ID of the mCHL2 band relative to the BMP-2 band clearly showed that

the complex corresponded to the 2:1 complex, because the ratio of the protein bands in fractions of 24 and 25, which were the peak fractions, were very close to the standard ratio measured for the 2:1 molar ratio of mCHL2 and BMP-2 (Figure 3.34, B, c1, c2), but clearly different from the ratio of 1:1 molar ratio. The composition of the major peak in Figure 3.34, A, e also corresponded to a 2:1 complex (Figure 3.34, B, e1, e2). The quantitative analysis for the second peak (shoulder) was difficult because the two peaks in Figure 3.34 (A, e) displayed no baseline separation.

According to the results of BIAcore and chromatography above, we can conclude that mCHL2 binds to BMP-2 with a 2:1 stoichiometry.

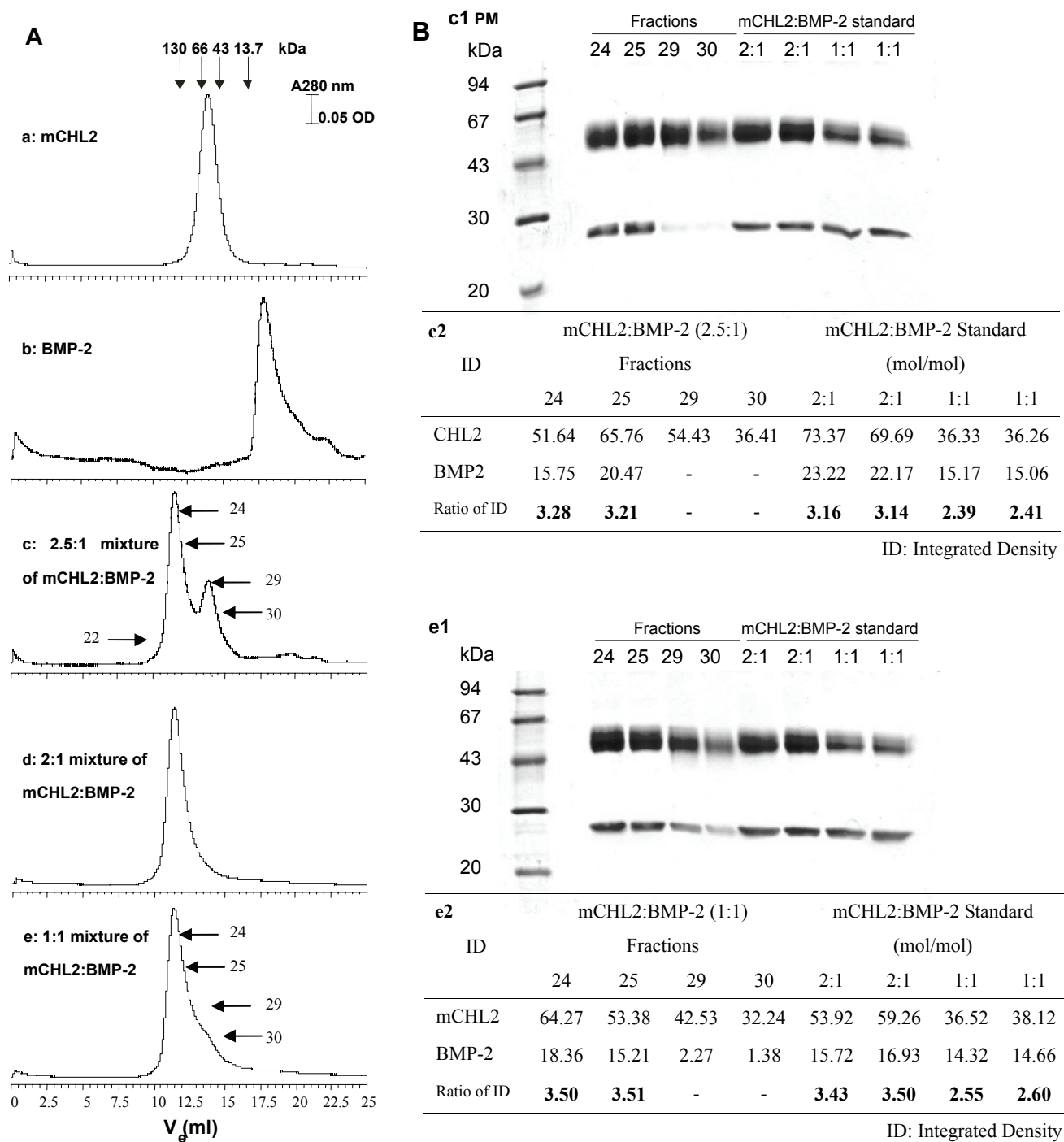


Figure 3.34: Stoichiometry of mCHL2/BMP-2 assembly. A, Chromatographs of the gel filtration runs with A280 on the y-axis and elution volume V_e on the x-axis. a: mCHL2; b: BMP-2; c: 2.5:1 mixture of mCHL2 and BMP-2; d: 2:1 mixture of mCHL2 and BMP-2; e: 1:1 mixture of mCHL2 and BMP-2. Protein samples were run at a flow rate of 0.5 ml/min on a Superdex 200 HR 10/30 column in 10 mM HEPES, pH 7.4, 700 mM NaCl. B, c1, e1: SDS-PAGE of the fractions of 2.5:1 or 1:1 mixture of mCHL2/BMP-2 from gel filtration chromatography under non-reducing condition; c2, e2: ID analysis of the fractions of 2.5:1 or 1:1 mixture. ID: Integrated Density, which is calculated by the software Scion Image to analyze the quantities of Coomassie stained proteins. mCHL2:BMP-2 standard: Standard mixtures of mCHL2/BMP-2 at a 2:1 and 1:1 molar ratios. Ratio of ID: The ratio of the ID of the CHL2 band relative to the BMP-2 band (ID mCHL2/ID BMP-2). PM, protein marker.

3.5.4 Competition of mCHL2/VWCs with receptors for BMP-2 binding

It has been shown that mCHL2 inhibited BMP activity in a competitive manner in vitro (Nakayama et al., 2004). Here we investigated whether mCHL2 inhibit binding of BMP-2 to type I or type II receptors by Biacore methodology. As shown in Figure 3.35, 100nM of mCHL2 prevented completely the binding of 50nM BMP-2 to immobilized BMPR-IA or ActR-IIB. These results demonstrated that mCHL2 could inhibit the binding of BMP-2 to both type I and type II receptors.

The knuckle epitope binding protein mCHL2-VWC1 displayed no inhibition on BMP-2/BMPR-IA interaction even at very high concentration, and could inhibit the BMP-2/ActR-IIB binding by 50% at this concentration (Figure 3.35, 3). The wrist epitope binding protein mCHL2-VWC3 inhibited the binding of BMP-2 to BMPR-IA at high concentration (Figure 3.35, 2), but the mixture of BMP-2 and mCHL2-VWC3 showed an increased response (resonance unit, RU) to ActR-IIB, compared to BMP-2 alone, probably due to the increased mass of the stable BMP-2/mCHL2-VWC3 complex in which the binding site for type II receptor is not occupied (Figure 3.35, B, 2). These results suggested that BMP-2 could simultaneously bind mCHL2-VWC3 and type II receptor.

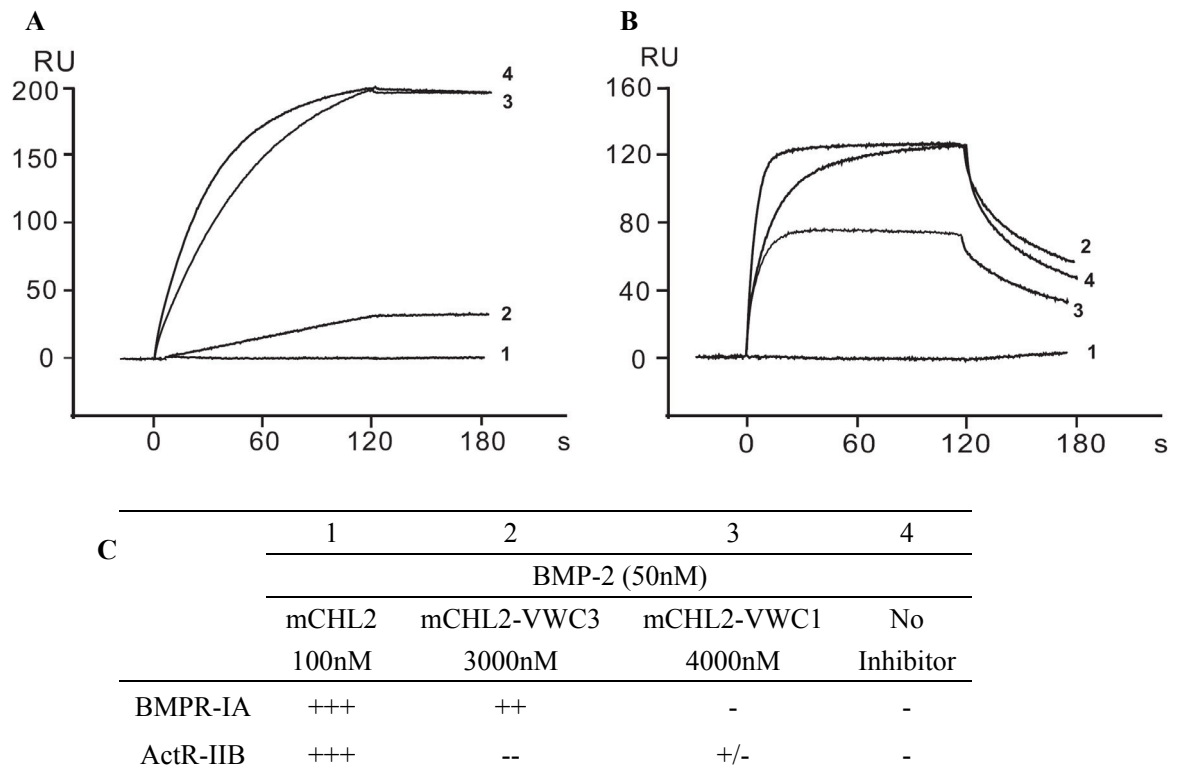


Figure 3.35: Inhibition of the binding of BMP2-type I or -type II receptor by mCHL2 and its VWC domains in Biacore. BMPR-IA (A) and ActR-IIB (B) were immobilized on the chip surface. 50nM BMP-2 plus 100nM CHL2 (1), 3000nM CHL2-VWC3 (2), 4000nM CHL2-VWC1 (3) and 50nM BMP-2 alone (4), were injected over the chip surface. C, summary of the results in A and B. +++: Binding was completely prevented; ++: Binding was blocked by 80-90%; +/-: binding was blocked by 50%. -: No inhibition; --: Increased resonance unit was obtained.

3.5.5 Biological activity in cell lines

The inhibitory effect of mCHL2 proteins on BMP signaling was assessed by measuring the BMP-2 induced alkaline phosphatase (ALP) activity in C2C12 cells. mCHL2 inhibited 10 nM BMP-2 induced ALP activity in a dose-dependent manner with a IC50 of 9 nM. In contrast, the single domain of mCHL2-VWC1 and mCHL2-VWC3 showed no inhibitory activity up to a concentration of 1 μ M (Figure 3.36).

In previous experiments the mutant BMP-2-L51P has been generated (Keller et al., 2004). This mutant does not bind BMPR-IA but binds to type II receptors normally. It does not induce measurable ALP activity in C2C12 cells and has no dominant-negative inhibitory effect. As the L51P mutant binds to mCHL2 normally (Figure 3.33, B), it can release

inhibition of BMP-2-induced ALP activity by mCHL2 in a dose-dependent manner (Figure 3.37). Now, five double or triple mutants of BMP-2 were generated, in which the knuckle epitope mutants A34D, L90A, V98P, L100P and L100K/N102D were introduced in the background of the L51P mutation. These mutants showed an obvious reduced affinity for BMPR-IA, decreased affinities for BMPR-II, ActR-II, ActR-IIB, normal or decreased affinities for mCHL2 in Biacore measurement as to expect from the property of the single mutants. The inhibition of BMP-2 activity by mCHL2 could be partially relieved to different extents by L51P/L100P, L51P/V98P, L51P/L90A, L51P/A34D and L51P/L100K/ N102D (PKD) (Figure 3.37). The biological activity of the mutants (i.e., release of CHL2 inhibition) correlates with their binding affinities to mCHL2 (See Figure 3.33, B).

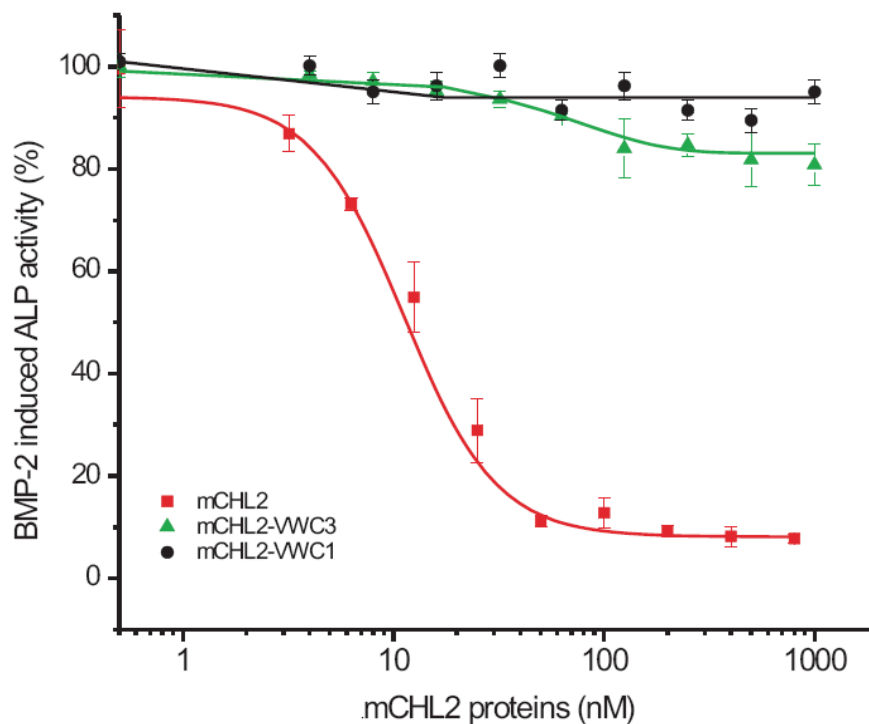


Figure 3.36: Inhibitory properties of mCHL2 and its VWC domains. Inhibition of the 10nM BMP2-induced alkaline phosphatase (ALP) activity by increasing doses of mCHL2, mCHL2-VWC1 and mCHL2-VWC3 was analyzed in serum-starved C2C12 cells.

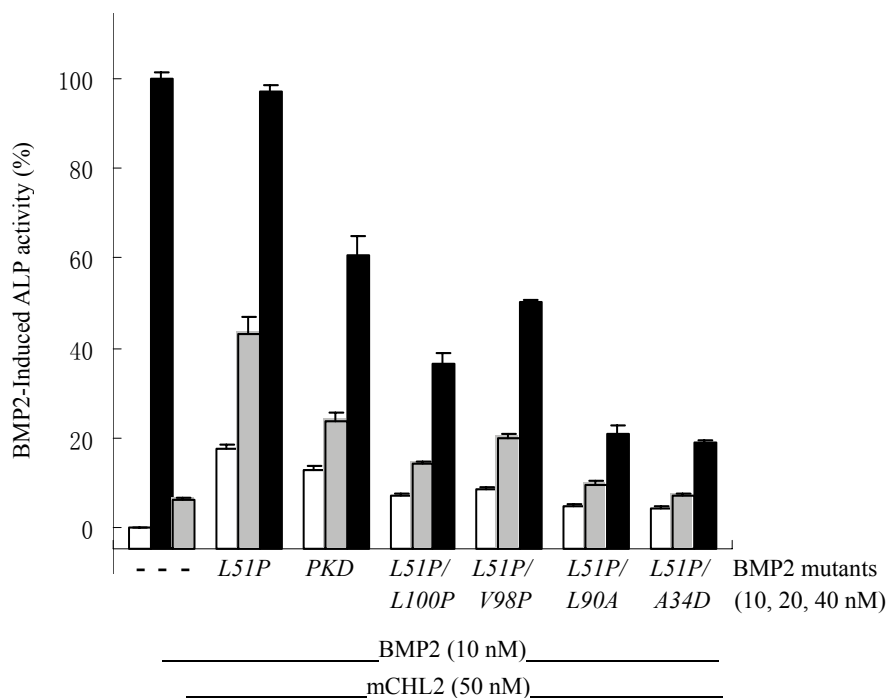


Figure 3.37: Release of mCHL2 inhibited BMP-2 activity by BMP-2 mutants. Induction of ALP by 10 nM BMP-2 in C2C12 cells was inhibited to 10% by 50 nM mCHL2. L51P and the compound mutants by themselves do not induce ALP activity. The release of mCHL2-inhibited BMP-2 activity was determined at the indicated mutant concentrations. PKD, L51P/L100K/N102D-BMP-2.

3.5.6 Analysis of mCHL2-VWC3 determinants for BMP-2 binding

Studies have shown that VWC domain is a versatile binding module. Most of the BMP binding VWC domains bind mainly the knuckle epitope of BMP-2. So far, only the VWC3 of mCHL2 is found to bind the BMP wrist epitope for type I receptor (Figure 3.35 and Zhang et al., 2007). To further characterize the binding properties of VWC3 domain, we conducted mutational analysis for this domain. Seven mutants of VWC3 were randomly generated (Figure 3.24) namely mutants VWC3-K228D, VWC3-H237D, VWC3-P238R, VWC3-V240D, VWC3-S242A, VWC3-G244A and VWC3-G279D. Four of the seven mutants VWC3-H237D, VWC3-P238R, VWC3-V240D, and VWC3-G244A showed decreased binding affinities for BMP-2 compared to wild type VWC3. Remarkably, the VWC3-P238R exhibited a 130-fold lower affinity (Table 3.7). These results indicated that these four amino acids contribute strongly to the binding of VWC3

to BMP-2 and might be the determinants of VWC3 for BMP-2.

Table 3.7: Binding affinity of CHL2-VWC3 mutants for immobilized BMP-2

	BMP-2	
	K_D (nM)	V/W
VWC3-wild type	300	1.0
VWC3-K228D	280	0.9
VWC3-H237D	12000	40
VWC3-P238R	40000	130
VWC3-V240D	9600	32
VWC3-S242A	320	1.1
VWC3-G244A	5300	18
VWC3-G279D	410	1.4

V/W, Ratio of K_D (Variant/Wild type)

3.5.7 Binding of mCHL2/VWCs to Tsg

It is known that Chordin binds simultaneously to BMP4 and Tsg, and the formation and dissociation of Chordin/Tsg/BMP complex correspond to the pro-and anti-BMP activity of Chordin and Tsg (De Robertis and Kuroda, 2004). Studies also showed that the pro-BMP activity of Tsg is independent of BMP binding but is specific for Chordin-like protein. Therefore, Tsg might bind other Chordin-like proteins and exert its pro-BMP activity independent of Chordin (Oelgeschlager et al., 2003). To discover more Tsg-binding Chordin-like proteins, we analyzed the possible interaction between mCHL2 and Tsg. We found that mCHL2 bound Tsg with high affinity, and the two BMP-binding VWC domain of mCHL2, VWC1 and VWC3, bound Tsg with 20-25 times lower affinity compared to full-length mCHL2 (Figure 3.38; Table 3.8). These results identify mCHL2 as a novel Tsg binding partner and show that the VWC1 and VWC3 domain of mCHL2 cooperatively generate a high binding affinity for Tsg. Furthermore, a stable Tsg/mCHL2/BMP-2 ternary complex could be isolated by gel-filtration chromatography (Figure 3.39, A). Biological assays showed that Tsg and mCHL2 synergistically inhibit

BMP-2-induced ALP activity (Figure 3.39, B). In summary, mCHL2 binds strongly to Tsg and forms a ternary complex with Tsg and BMP-2. This complex makes mCHL2 a better BMP-2 antagonist.

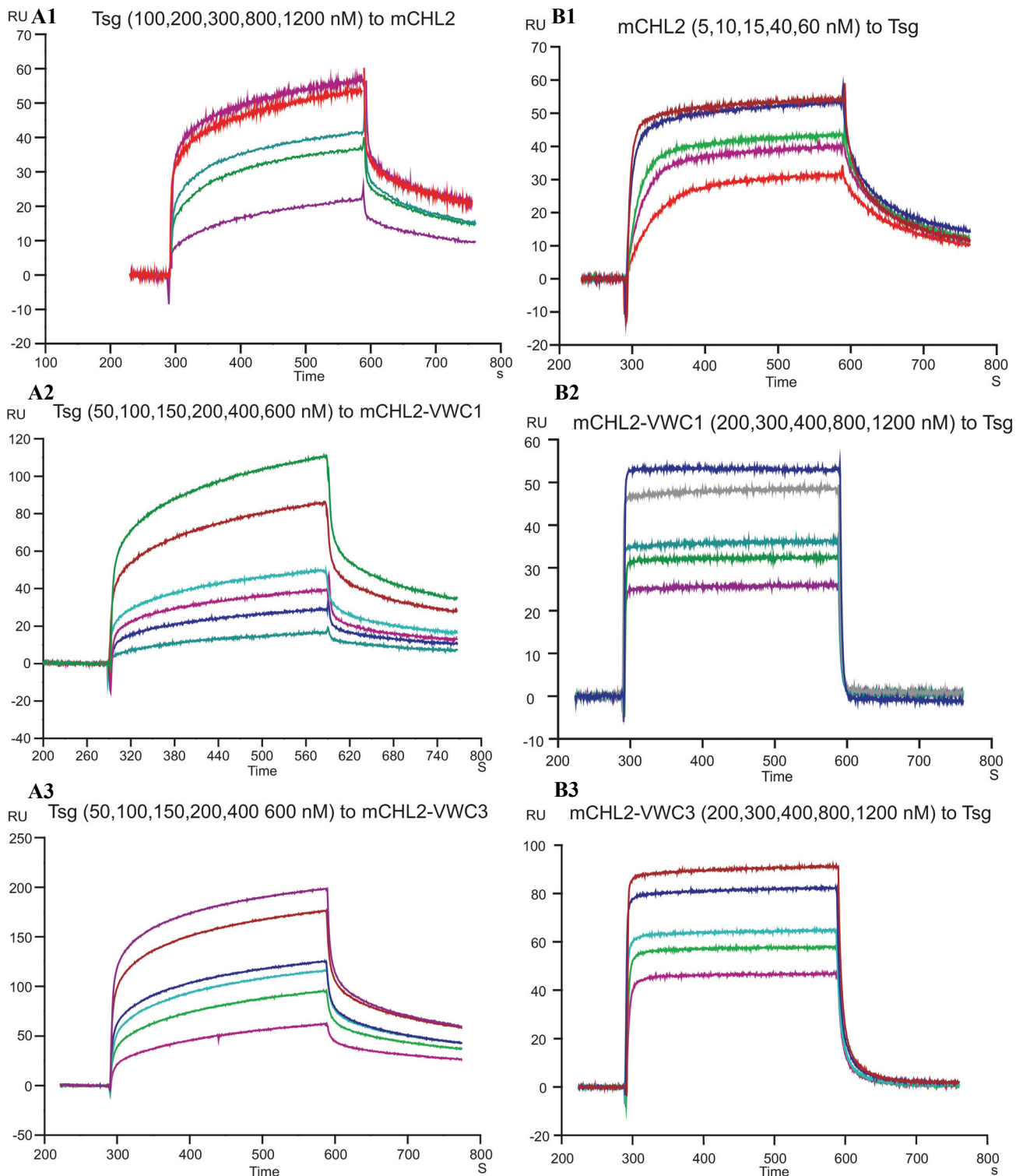


Figure 3.38: BIAcore analysis of mCHL2/VWCs and Tsg interaction **A1-A3**, overlay of sensograms showing the binding of Tsg to the immobilized full-length mCHL2, mCHL2-VWC1 and mCHL2-VWC3. Tsg at different concentrations were applied. **B1-B3**, overlay of sensograms showing the binding of full-length mCHL2, mCHL2-VWC1 and mCHL2-VWC3 to the immobilized Tsg. Full-length mCHL2, mCHL2-VWC1 and mCHL2-VWC3 at different concentrations were applied respectively.

Table 3.8: Binding analysis of Tsg for mCHL2/VWCs (BIAcore)

	mCHL2			
	Full-length	VWC1	VWC2	VWC3
Apparent K_D (nM)				
Tsg ^a	13	330	NB	280
Tsg ^b	24	870	NB	180

a: immobilized; b: perfused; NB, No binding.

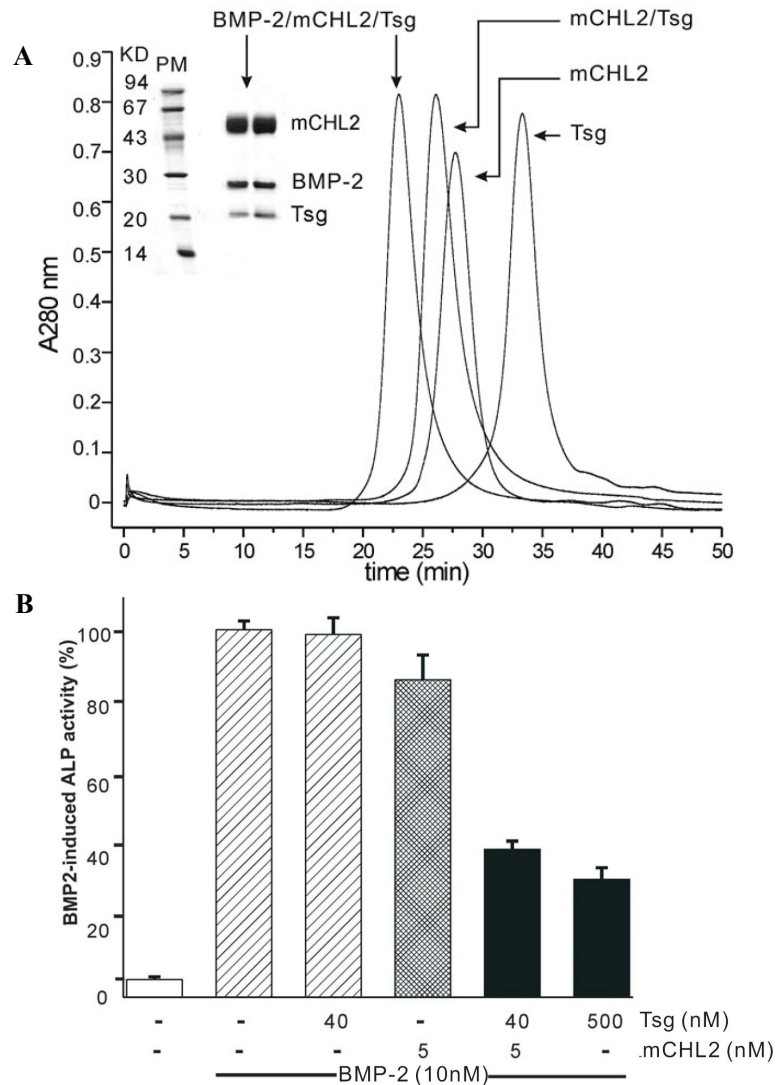


Figure 3.39: Formation of the ternary complex of BMP-2/mCHL2/Tsg and synergistic effect of Tsg and CHL2 for inhibition of BMP-2 activity. **A**, Free BMP-2, mCHL2, Tsg, binary and ternary complexes of BMP-2/mCHL2 and BMP-2/mCHL2/Tsg were chromatographed on a Superdex 200 HR 10/30 gel-filtration column. The ternary complex of BMP-2/mCHL2/Tsg was analyzed by SDS-PAGE under the non-reducing condition. **B**, Inhibition of BMP-2 activity (10 nM BMP-2) in serum starved C2C12 cells by different doses of Tsg, mCHL2 or Tsg plus mCHL2 was determined by analysis of the induced ALP activity.

3.6 Protein complexes formation and crystallizations of the complexes

3.6.1 Crystallization of mCHL2/BMP-2 complex

The purified wildtype mCHL2 was mixed with BMP-2 at a molar ratio of 2.5:1 on ice. The mCHL2/BMP-2 complex was isolated by size exclusion chromatography on Superdex™ 200 column. The fractions (22-26) containing the two components of the complex were pooled (Figure 3.40). The complex was concentrated to 8-11 mg/ml and submitted to crystallization.

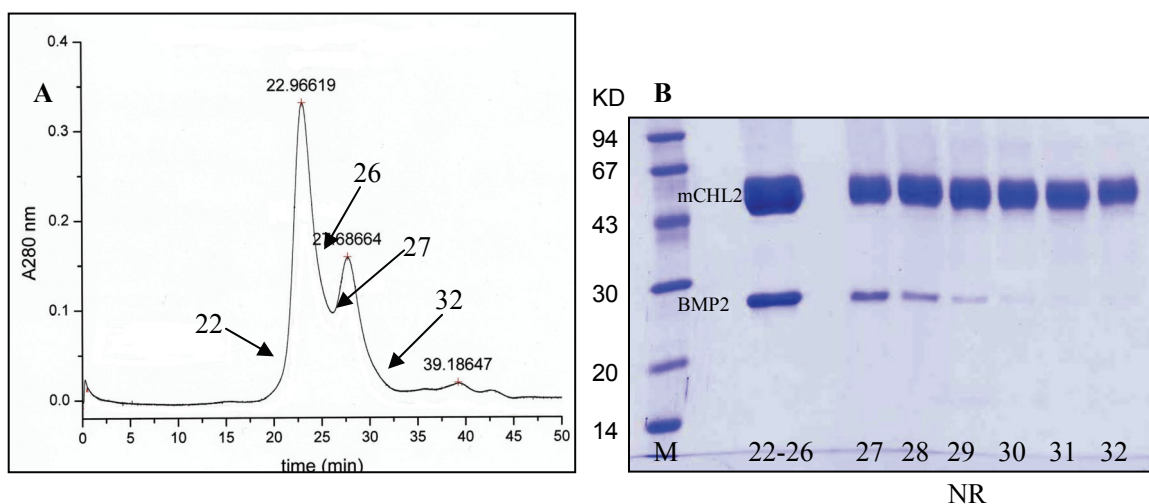


Figure 3.40: **A**, Chromatographs of the gel filtration on Superdex 200 for 2.5:1 mixture of mCHL2 and BMP-2; **B**, SDS-PAGE of the fractions from gel filtration chromatography. M, protein marker. NR, under non-reduced condition. Fractions 22-26 were combined for crystallization.

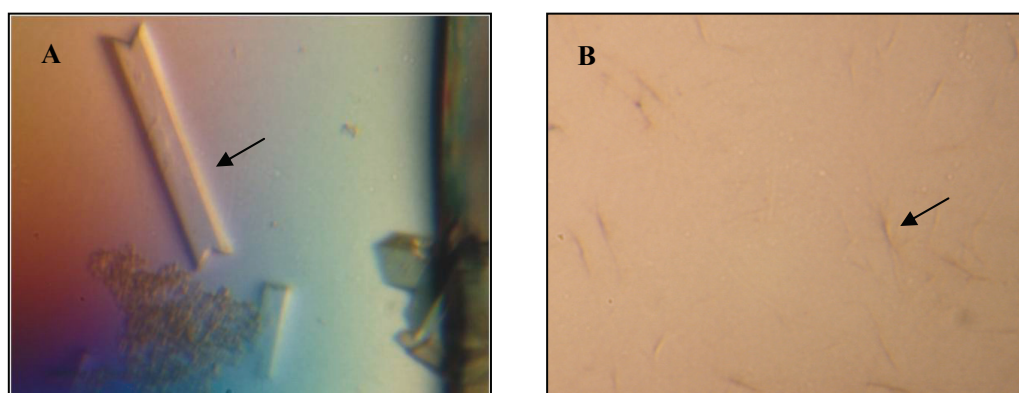


Figure 3.41: Initial screen of crystallization of mCHL2/BMP-2 complex. **A**, Single crystals growing in 0.1M Tris, pH 8.5, 25% w/v PEG3350; **B**, Needle crystals growing in 0.1M Tris, pH 8.5, 25% tert-Butanol. The arrows indicate the crystals.

Initial screening was performed in sitting drops with the kits of *Hampton 1 and 2*, *Hampton SaltRx*, and *Hampton Index* (Hampton Research). Two among the 288 conditions (Figure 3.41, A and B) were found to give crystals. The condition A served as a basis for further optimization and the following fine screen crystallization trials at different pH, precipitant concentration, and cryoprotectant (Table 3.9):

Table 3.9: Procedure of screening with pH, precipitant concentration, cryoprotectant reagents for the crystallization of mCHL2/BMP-2 complex.

Original condition	pH of buffer screening	Precipitant concentration screening	cryoprotectant reagents screening
A 0.1M Tris, pH 8.5, 25% w/v PEG3350	pH 7.5	20% w/v PEG3350	5% 10% 15% 20% 25% 30% } glucose } saccharose } Glycerin
	pH 8.0	25% w/v PEG3350	
	pH 8.5	30% w/v PEG3350	
	pH 9.0		
B 0.1M Tris, pH 8.5, 25% tert-Butanol.			

Single crystals could grow under the conditions of 0.1M Tris, 25% w/v PEG3350 with pH 7.5, pH 8.0, pH 8.5 and pH 9.0. However no crystal grew in the buffers with 20% and 30% w/v PEG 3350 (precipitant concentration screening) and in the buffers with different cryoprotectants.

Furthermore, the complex of BMP-2 and CHL2-N89Q/N180Q mutant, which exists as an unglycosylated protein, was applied to the initial screening in sitting drops with HR2-110 kit and crystal screen2 HR2-112 kit (98 buffers). However no crystal was found in all these conditions.

3.6.2 Crystallization of mCHL2-VWC3/BMP-2 complex

The purified mCHL2-VWC3 was mixed with BMP-2 at a molar ratio of 2.2:1 on ice. The mCHL2-VWC3/BMP-2 complex was isolated by size exclusion chromatography on Superdex™ 200 column. The fractions (28-33) containing the complex were pooled (Figure 3.42). The purified complex was finally concentrated to 8-11 mg/ml and applied

for initial screening in sitting drops.

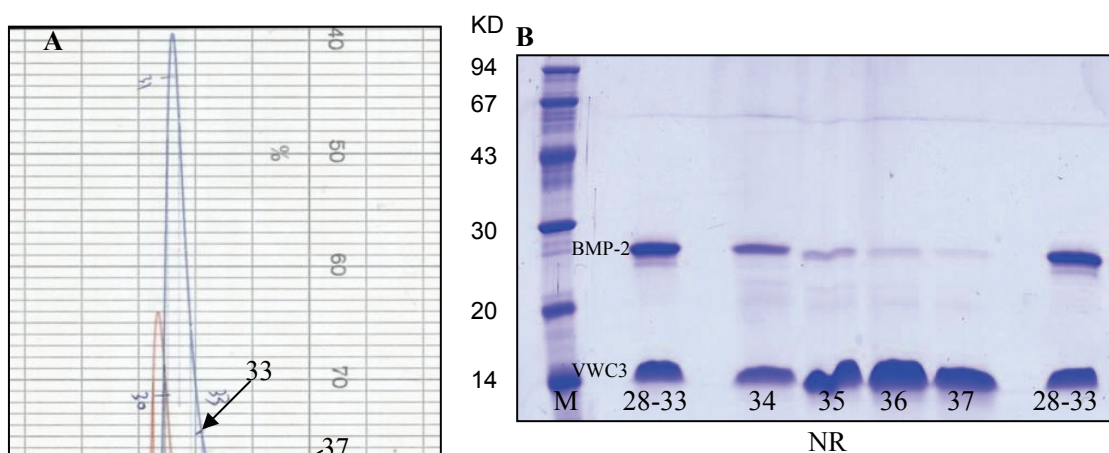


Figure 3.42: **A**, Chromatographs of the gel filtration on Superdex 200 for 2.2:1 mixture of mCHL2-VWC3 and BMP-2; **B**, SDS-PAGE of the fractions from gel filtration chromatography. M, protein marker. NR, under non-reduced condition Fraction 28-33 were combined for crystallization.

Crystals were found in 9 (A-I) conditions from the kits of *HR2-110*, *HR2-112*, *HR2-144*, *HR2-108*, *HR2-130*(Hampton Research); *Wizard™ I* and *Wizard™ II* screen, *Cryo I™* and *Cryo II™* screen (Emerald BioSystems); *JCSG crystallization suite* (Qiagen); *Classic 1-10 screen* (European Molecular Biology Laboratory, Hamburg) in initial screening (Figure 3.43):

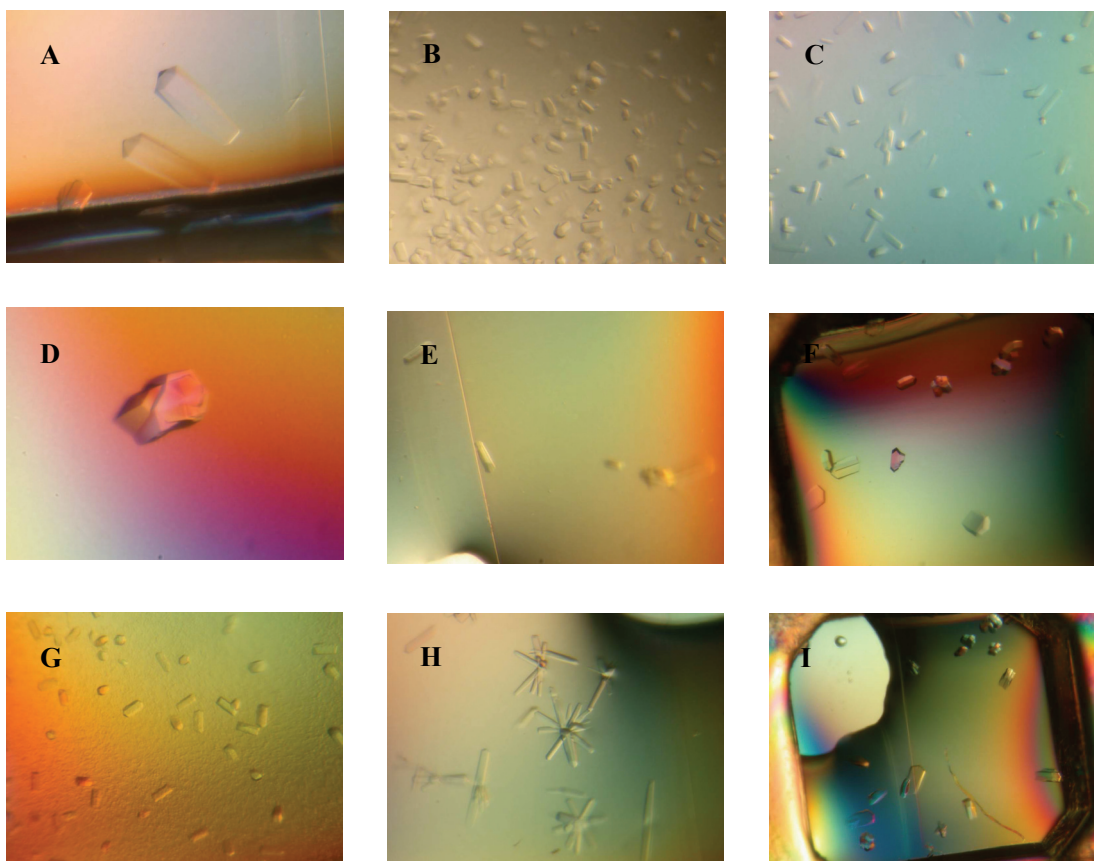


Figure 3.43: Initial screening of crystallization of mCHL2-VWC3/BMP-2 complex. Single crystals grow in these conditions below: **A**, 1.5M Sodium chloride, 10% v/v Ethanol; **B**, 0.1M MES, pH 6.5, 1.6 M Magnesium sulfate heptahydrate; **C**, 1.26M Sodium phosphate monobasic monohydrate, 0.14M Potassium phosphate dibasic, pH 6.0; **D**, 0.8M Succinic acid, pH 7.0; **E**, 1.1M Ammonium tartrate dibasic, pH 7.0; **F**, 35% v/v Tacsimate, pH 7.0; **G**, 0.1M Sodium chloride, 0.1M BIS-TRIS, pH 6.5, 1.5M Ammonium sulfate; **H**, 1.0M Ammonium sulfate, 0.1M BIS-TRIS, pH 5.5, 1% w/v Polyethylene glycol 3,350; **I**, 1.0M Ammonium sulfate, 0.1M HEPES, pH 7.0, 0.5% w/v Polyethylene glycol 8,000.

These conditions were served as a basis for optimization and subsequent fine screening trials (I, II, III) with pH, precipitant concentration, cryoprotectant reagents as follows (Figure 3.44).

A

Original condition	I: pH of buffer screening	II: Precipitant concentration screening	III: cryoprotectant reagents screening
A: 1.5M Sodium chloride, 10% v/v Ethanol		1.0M, 1.25M, 1.5M, 2.0M } NaCl	5% } 10% } Glycerin 15% } 20% } glucose 25% } 30% } saccharose
B: 0.1M MES, pH 6.5, 1.6 M Magnesium sulfate heptahydrate		1.2M, 1.6M, 1.8M } MgSO ₄	
C: 1.26M Sodium phosphate monobasic monohydrate, 0.14M Potassiumphosphate dibasic, pH 5.6	pH 6.0 pH 5.6	1.26M / 0.14M 1 M / 0.4 M } 0.71M / 0.29M } NaH ₂ PO ₄ /K ₂ HPO ₄	
D: 0.8M Succinic acid, pH 7.0		0.6M, 0.8M, 1.0M } Succinic acid	
E: 1.1M Ammonium tartrate dibasic, pH 7.0		0.8M, 1.1M } Ammonium tartrate dibasic	
F: 35% v/v Tacsimate, pH 7.0		20%, 25%, 30%, 40%, 45% } Tacsimate	
G: 0.1M Sodium chloride, 0.1M BIS-TRIS, pH 6.5, 1.5M Ammonium sulfate			
H: 1.0M Ammonium sulfate, 0.1M BIS-TRIS, pH 5.5, 1% w/v Polyethyleneglycol 3,350		1.0M, 1.5M } (NH ₄) ₂ SO ₄	
I: 1.0M Ammonium sulfate, 0.1M HEPES, pH 7.0, 0.5% w/v Polyethylene glycol 8,000	pH 7.0 pH 6.0	0.8M, 1.0M, 1.2M } (NH ₄) ₂ SO ₄	

B

A	1M NaH ₂ PO ₄ , 0.4M K ₂ HPO ₄ , pH6.0, 25% Glycerin
B	35% tacsimate, 15% glucose
C	1.0 M (NH ₄) ₂ SO ₄ , 0.1 M HEPES pH 7.0, 20% Glucose
D	1.5M NaCl, 10% ethanol, 25% Saccharose

C

A	1M NaH ₂ PO ₄ , 0.4M K ₂ HPO ₄ , pH6.0, 25% Glycerin
----------	--

Additive screening (72 additives from kits of Hampton Research)

Best diffraction was 15-20 Å

Figure 3.44: Procedure of screening with pH, precipitant concentration, cryoprotectant reagents and additive screening for the crystallization of mCHL2-VWC3/BMP-2 complex. **A**, 9 original conditions (A-I) gained from initial screening, were served as a basis for optimization screening trials I (pH), II (precipitant concentration) and III (cryoprotectant reagents). **B**, 4 optimized conditions (A-D) in cryo-condition were obtained from **A**. **C**, the selected condition A from **B** was performed for the further additive screening to improve the poor diffraction. However, the best diffraction was 15-20 Å.

Finally, large single crystals (50-200nm in the first dimension) grew in 4 conditions under cryo-conditions (Figure 3.45). However, these crystals showed only very weak diffraction with 15-20Å resolution. In order to improve the poor diffraction, the additive screening was performed later with the kits of *Addition Screen 1-3* (Hampton Research) in the condition A (1M NaH₂PO₄, 0.4M K₂HPO₄, pH6.0, 25% Glycerin). But the results showed no improvement. Further optimization steps for the conditions of crystallization and probably the protein constructs has to be done in the future experiments.

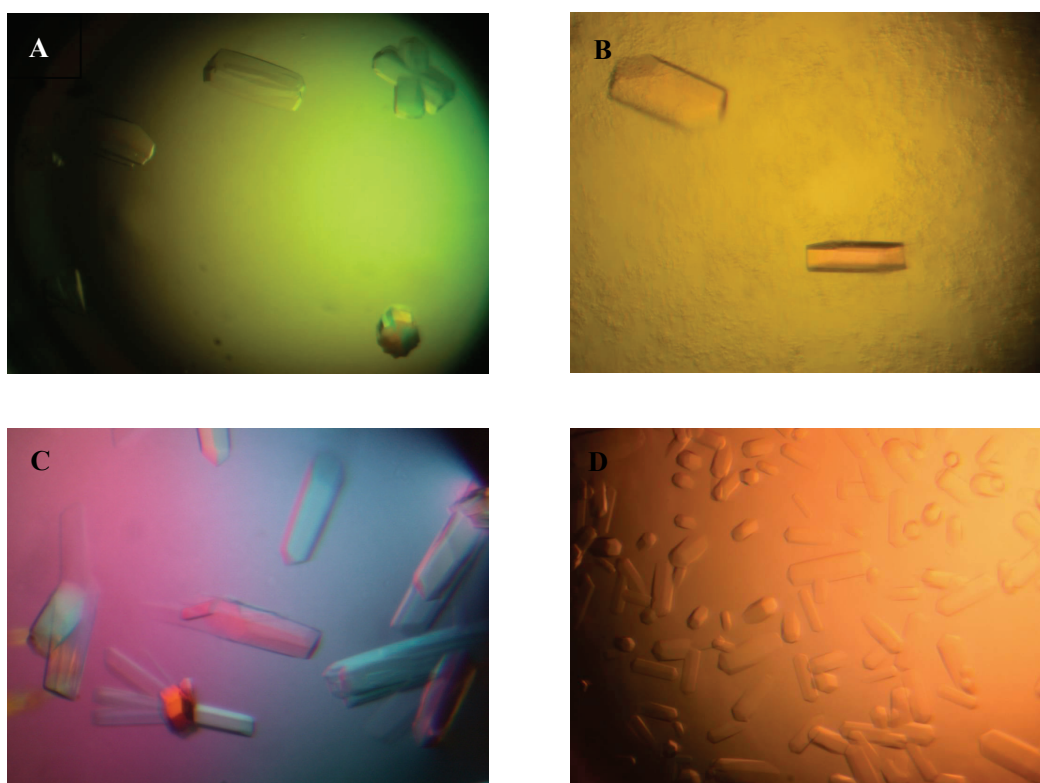


Figure 3.45: Optimization screening of crystallization of mCHL2-VWC3/BMP-2 complex with pH, precipitant concentration, cryoprotectant reagents. Single crystals grow in these conditions below: **A**, 1M NaH₂PO₄, 0.4M K₂HPO₄, pH6.0, 25% Glycerin; **B**, 35% tacsimate, 15% glucose; **C**, 1.0 M Ammonium sulfate, 0.1 M HEPES pH 7.0, 20% Glucose; **D**, 1.5M NaCl, 10% ethanol, 25% Saccharose.

4 Discussion

VWC-containing proteins act as extracellular modulators in the BMP/TGF- β signaling pathway and play important roles in development and diseases. CHL2, a novel BMP inhibitor, is a member of VWC-containing proteins and interacts with different BMPs, inhibiting their actions *in vitro* as well as *in vivo*. CHL2 is expressed preferentially in chondrocytes of developing cartilages of hip and knee joints and costochondral junction (Nakayama et al., 2004). The up-regulation of CHL2 transcripts specifically in middle zone cartilage of adult joints was observed with osteoarthritis patients. The significant inhibition of cartilage mineralization by up-regulated CHL2 suggested that in osteoarthritis cartilages, CHL2 might delay and/or reduce the degree of chondrocyte hypertrophy, thereby amending cartilage degeneration. CHL2 may thus play negative roles in the (re)generation and maturation of articular chondrocytes in the hyaline cartilage of both developing and degenerated joints (Nakayama et al., 2004).

Although the functions of CHL2 and other Chordin like proteins are extensively studied, the structural basis of the interactions of BMPs and CHL2 or other VWC domain-containing proteins are still poorly understood. Improving the knowledge of the features characterizing the binding mechanisms of CHL2 and BMP-2 interaction is not only of theoretical interest, but is important as well for the development of drugs for the treatment of degenerated bone diseases, such as osteoarthritis.

In order to understand the recognition mechanisms of CHL2 for BMPs and especially the characteristics of its VWC domains, we analyzed in detail the binding affinities, the binding specificities, the binding epitopes and the binding modes of BMP-2 for mCHL2 and its VWC domains. The interaction of mCHL2 and Tsg has been established for the first time in this study. The isolation and crystallization of the complexes of mCHL2/BMP-2 and mCHL2-VWC3/BMP-2 paved the way for solving the crystal structures of the complexes.

Binding of mCHL2/VWC domains to BMPs

CHL2 was demonstrated to inhibit ALP activity induced by BMP-2/4/6/7 and to prevent BMP-4 interaction with its BMPR-IB receptor (Nakayama et al., 2004). However, the binding affinity of CHL2 for BMPs has not been reported and which domain of CHL2 is involved in binding has not been analysed. In our study, we defined the binding affinities of mCHL2 for BMP-2, BMP-7 and GDF-5, which are representatives of three BMP subfamilies. Full-length mCHL2 bound to BMP-2 with high affinities, which is similar to those of Chordin, CV2 and BMPR-IA for BMPs. Two of the three VWCs of mCHL2, VWC1 and VWC3, were found to bind BMP-2, and VWC2 did not. Compared with full-length mCHL2, VWC1 and VWC3 bound to BMP-2 with about 100 and 20 times lower affinity respectively (Table 3.5). The results indicate that the affinity of mCHL2 for BMP-2 results from the cooperative binding of VWC1 and VWC3 domains. This is similar to Chordin, for which its VWC1 and VWC3 domain bind BMPs cooperatively, but different from CV2 which bind BMPs via its single VWC1 domain (Zhang et al., 2007). Surprisingly, our mutational analysis showed that VWC1 and VWC3 domain of mCHL2 bind to knuckle and wrist epitopes, respectively. This differs from the VWC domains of Chordin and CV2 which bind mainly to knuckle epitopes of BMP-2. Furthermore, even for the knuckle epitope-binding VWC domains, the binding determinants are different. These results suggest that the VWC domains exhibit different binding characteristics.

Consistent with the results of the mutational analysis, we found that mCHL2 inhibits the binding of BMP-2 to both the type I and type II receptors *in vitro*, and the single VWC1 or VWC3 domain can only inhibit the binding of BMP-2 to the type II or type I receptor respectively. Interestingly, the individual VWC domain is not able to inhibit BMP signaling in cell culture, which indicates that for inhibition of BMP signaling, the high-affinity binding of full-length mCHL2 containing both VWC1 and VWC3 domain is necessary. It is as yet unknown whether the full-length mCHL2 is proteolytically cleaved *in vivo*. Otherwise, the processing of the mCHL2 molecule would lead to decrease of its inhibitory potency as seen for Chordin protein (De Robertis and Kuroda, 2004).

Binding mode of mCHL2/BMP-2 interaction

Our results showed that the affinity of solute mCHL2 to immobilized BMP-2 was about 10-fold lower than that of solute BMP-2 to immobilized mCHL2. This difference could be explained by the assumption that the solute BMP-2 dimer binds simultaneously to two immobilized mCHL2 on the chip (1:2 interaction, Figure 4.1, A), which results in an enhanced affinity; and the separate mCHL2 binds immobilized BMP-2 in an 1:1 interaction, which results in a lower affinity (Figure 4.1, B). The similar situation has been reported for the BMP/receptor interaction in BIAcore measurement (Greenwald et al., 2003; Sebald et al., 2004). Furthermore, our mutational analysis has clearly demonstrated that mCHL2-VWC1 and VWC3 bound respectively to the knuckle and wrist epitopes of BMP-2. As two wrist and two knuckle epitopes exist in a BMP-2 dimer (Figure 4.2, C), it seems that mCHL2 binds BMP-2 dimer in a 2:1 interaction. Finally, the stoichiometry of mCHL2/BMP-2 interaction has been determined to be 2:1 by gel filtration chromatography (Figure 3.34); Tsg has been shown to bind mCHL2 via the cooperative binding of VWC1 and VWC3, and a Tsg/mCHL2/BMP-2 ternary complex could be isolated. Based on these results, we suggest a model for mCHL2/Tsg/BMP-2 interaction in Figure 4.2, A. However, the second possibility in Figure 4.2, B could not be excluded from our results. Notably, the binding mode of mCHL2/Tsg/BMP-2 interaction is different from those of BMP-2 interacting with the other Chordin family member CV2 and Chordin (Figure 4.3)(Zhang et al., 2007). CV2 binds BMP-2 also with 2:1 stoichiometry, but only one VWC domain participates in binding and Tsg is not involved in the interaction. In contrast, Chordin binds BMP-2 with an 1:1 stoichiometry, however, similar to mCHL2/BMP-2 interaction, two VWC domains and Tsg are involved in this binding. In summary, Chordin-like proteins modulate BMP signaling through different recognition mechanisms.

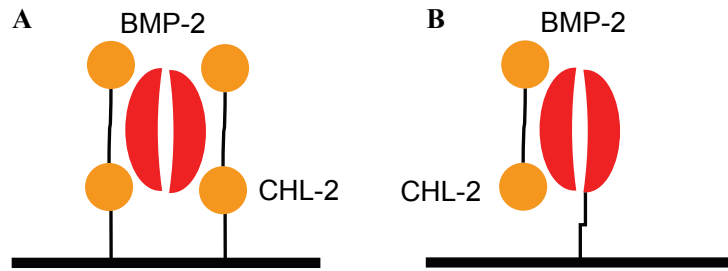


Figure 4.1: Scheme illustrates the 2:1 and 1:1 interaction of CHL2 and BMP-2. **A**, The immobilized CHL2 bind to BMP-2 dimer by 2:1 interaction. **B**, The CHL2 in solution binds to immobilized BMP-2 by 1:1 interaction. The second CHL2 in solution is omitted to emphasize the 1:1 interaction.

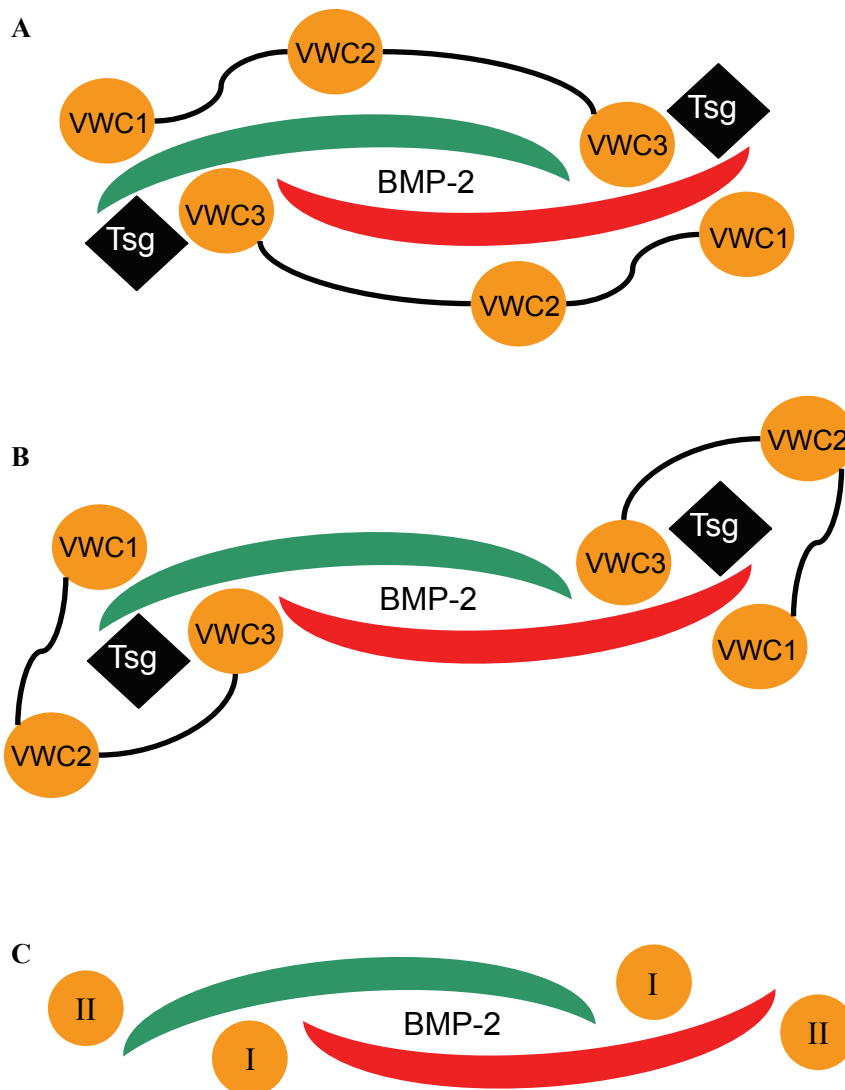


Figure 4.2: Model of binding mode of mCHL2/BMP-2/Tsg interaction. **A**, two mCHL2 monomers surround the BMP-2 dimer. The VWC1 and VWC3 domain of each mCHL2 monomer respectively -

- shares the knuckle epitopes and wrist epitopes of the BMP-2 monomers. Two Tsg bind mCHL2 via the cooperative binding of VWC1 and VWC3 of the different mCHL2 monomers and synchronously share the wrist epitopes of the BMP-2 monomers. **B**, VWC domains of CHL2 and Tsg bind to BMP-2 wrist and knuckle epitopes in the same way in model A, but each CHL2 monomer binds to one side of the butterfly shaped BMP-2. **C**, BMP-2 signaling complex with type I and type II receptors.

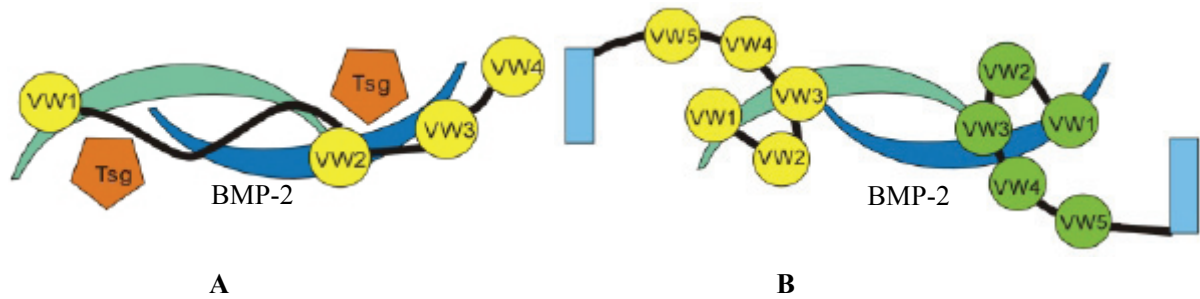


Figure 4.3: **A**, Model of BMP2/Chordin/Tsg ternary complex. One Chordin monomer binds the BMP-2 dimer. The VWC1 and VWC3 domains of Chordin monomer bind respectively the knuckle epitopes of the BMP-2 monomers. Two Tsg bind chordin via VWC1 and VWC3 of the chordin monomer and synchronously share the wrist epitopes of the BMP-2 monomers. **B**, Model of BMP-2/CV2 complex. Two CV2 monomers bind to each side of the BMP-2 dimer via the binding of two VWC1 domains to the knuckle epitopes of the different BMP-2 monomer. The cyan box in (B) indicates the C-terminal domain of CV2 (Zhang et al., 2007)

Interaction of Tsg and BMP-2/CHL2

Tsg plays important roles in Chordin regulation of BMP signaling. Previous study showed that Tsg has Chordin-independent activity which was speculated to be due to other Chordin-like proteins (Oelgeschlager et al., 2003). In this study we have established for the first time the novel interaction between mCHL2, Tsg and BMP-2. Tsg binds to VWC1 and VWC3 of mCHL2 and thereby strengthens the binding affinity. A study (Nakayama et al., 2004) showed that CHL2 inhibited BMP functions *in vitro* and *in vivo*. Our result indicates that this inhibition must be enhanced by the presence of Tsg. Recent results from Tsg-deficient mice indicated a critical role of Tsg in skeletal development of vertebrates (Gazzerro et al., 2006; Nosaka et al., 2003). Tsg has also been shown to be an important modulator of BMP-regulated cartilage development and chondrocyte differentiation (Schmidl et al., 2006). However, whether Tsg exerts its regulating function in cartilage

through the interaction with Chordin remains questionable, because Chordin is absent from all fetal bovine growth plate chondrocyte populations except for resting chondrocytes (Schmidl et al., 2006). In situ hybridization studies of the developing mouse skeleton showed the absence of Chordin from cartilage proper (Scott et al., 2000; Zhang et al., 2002). Thus, at least in the regulation of BMP activity by Tsg in cartilage, other modulator proteins might be at work. CHL2 could be one of these proteins, since CHL2 is co-expressed with Tsg in cartilage (Nakayama et al., 2004; Schmidl et al., 2006) and they bind each other with high affinity. Further studies will have to show the *in vivo* relevance of the Tsg/CHL2 interaction and whether it leads to a pro- or anti-BMP activity. It seems unlikely that mCHL2 is cleaved by Xolloid protease like Chordin, since no Xolloid cleavage site is found in the mCHL2 sequence. This could mean an important difference between the BMP-2/Tsg/Chordin and BMP-2/Tsg/mCHL2 complexes. It remains to be seen whether mCHL2 could be cleaved by other proteases. Otherwise, the formation of a BMP/CHL2/Tsg complex would only result in a strong anti-BMP activity differing from the formation of the BMP/Chordin/Tsg complex, which plays a role as transporter and thereby promotes BMP activity in this context (De Robertis and Kuroda, 2004; Eldar et al., 2002; Shimmi et al., 2005).

VWC domain is a versatile binding module

VWC-containing proteins play an important role in regulating BMP activity. In contrast to the extensive studies on the function of these proteins in development and diseases, the structural basis for the mechanisms of BMP regulation by these proteins is still poorly understood. The present results and data in the recent literature (Zhang et al., 2007) indicate that the VWC domains are versatile binding modules which can exhibit multiple binding characteristics as follows:

- 1) VWC domains show different affinities and specificities to different BMPs. Promiscuities exist in the interaction between different VWC domains and BMPs.
- 2) Many VWC domains bind mainly to knuckle epitope of BMP-2 (such as Chordin-VWC1/-VWC3, CV2-VWC1 (Zhang et al., 2007) and CHL2-VWC1), but

CHL2-VWC3 for instance, binds preferentially to the wrist epitope of BMP-2. Moreover even for the same epitope of BMP-2, different determinants are found for different VWCs.

- 3) VWC domain binds not only BMPs but also Tsg. Interestingly, only the BMP-binding VWC domains bind Tsg, indicating cooperation of these two binding proteins. Furthermore, the binding of individual VWC domain to Tsg could be independent (e.g. VWC1 and VWC3 of Chordin) or cooperative (e.g. VWC1 and VWC3 of mCHL2).
- 4) VWC domain plays not only a functional role such as BMP/Tsg binding, but also a purely structural role as many non-binding VWCs only function to space the different parts of the full-length proteins of the Chordin family.

Binding determinants of mCHL2-VWC3 for BMP-2

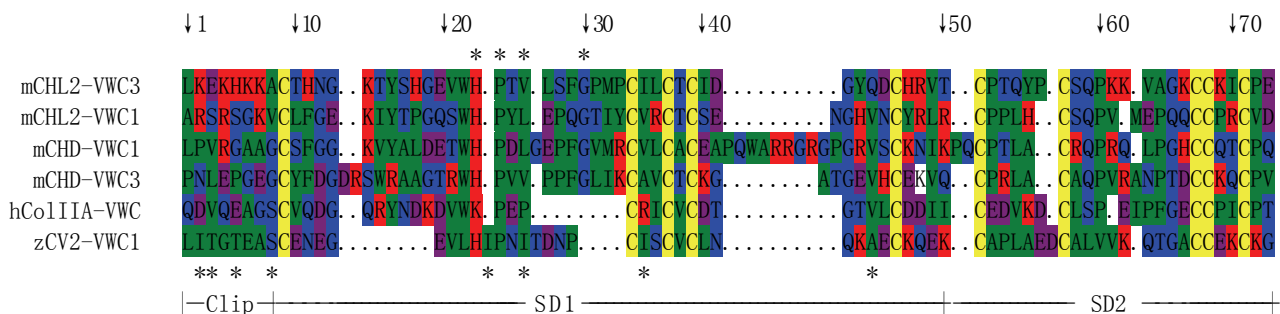


Figure 4.4: Sequence alignment of VWC domains. VWC domains from different chordin family proteins were aligned by Multalin. mCHL2: murine Chordin like 2; mCHD: murine Chordin; hCol1IA: human collagen IIA; zCV2: zebra fish Crossveinless-2. Residues are coloured according to conservation (hydrophobic: green; cysteine: yellow; positive charged: red; negative charged: purple; uncharged hydrophilic: blue). *, the determinants of mCHL2-VWC3 and CV2-VWC1. Clip, a short N-terminal segment of zCV2-VWC1. SD1 and SD2, sub-domain 1 and 2 of zCV2-VWC1 (Modification from zhang et al., 2008).

The NMR structure of the Col1IA VWC domain established for the first time a two sub-domains (SD) architecture of the VWC domain (O'Leary et al., 2004). The idea that corresponding sub-domains SD1 and SD2 are present in all VWC domains is further substantiated by the recently solved crystal structure of BMP-2/ CV2-VWC1 complex (Zhang et al., 2008). Furthermore, the crystal structure revealed that the N-terminal extension before the first cysteine termed clip and the SD1 of CV2-VWC1 encode high

affinity binding for BMP-2. The clip of CV2-VWC1 is not conserved in many other VWC domains including VWC1 and VWC3 of mCHL2 (figure 4.4). However, the four mCHL2-VWC3 determinants for BMP-2 binding found in this study are located in a region corresponding to the long-loop between β -strands 1 and 2 of CV2-VWC1 (Figure 4.4). As the residues in this loop of CV2-VWC1 contribute strongly to the hydrophobic interaction with BMP-2, it is tempting to speculate that this loop might be also important for the binding of other VWC domains to BMPs. It should be noted that in contrast to CV2-VWC1, the mCHL2-VWC3 domain binds only to the wrist epitope of BMP-2. Further studies have to establish the architecture of the binding epitopes of mCHL2-VWC3 and whether residues in different parts of the domain can be involved in BMP binding. In addition, as the mCHL2-VWC3 also binds the wrist epitope-binding protein Tsg, it will be interesting to discuss how the mCHL2-VWC3 epitope for Tsg is constructed and whether this epitope is overlapping with or different from that for BMP binding.

Crystallization of CHL2/BMP-2 and CHL2-VWC3/BMP-2 complex

Crystallography is a powerful method to solve the structure of a protein or a protein complex. The crystal structure of the complexes of CHL2/BMP2 and CHL2-VWC3/BMP2 will reveal the protein-protein recognition in atomic details. We have successfully isolated CHL2/BMP-2 and CHL2-VWC3/BMP-2 complexes in reasonable amounts and these complexes are stable in concentration up to 10 mg/ml (Figure 3.40; 3.42). Further experiments have shown that these complexes can be crystallized under many conditions. We have established a sound basis for the possible crystallization of these complexes. The subsequent experiments are under way.

Why do the macroscopically well formed crystals show poor diffraction? There are some possible reasons. One of the main reasons is that the proteins have a high degree of structural flexibility. Therefore protein structural heterogeneity and disorder existing in solution may also exist in the crystalline form, due to freedom afforded by the high solvent content in most protein crystals (DePristo et al., 2004; Smith et al., 1986). Thus,

the screening of ligands, additive, co-factors, temperature, or protein concentrations may reduce or eliminate improper folding of protein and help the target protein to assume a more rigid and homogeneous conformation and thereby improve the diffraction (Hassell et al., 2007). The other reason for the poor diffraction of crystal is structural variations in the protein due to partial deamination, partial oxidation and other post-translational modifications during protein expression or protein purification and even the process of crystallization. Therefore, the optimization of purification methods between proteins expression and crystallization may avoid the possible structural modifications in the protein and improve the diffraction of crystal (Hampton Research. <http://www.hamptonresearch.com>). Furthermore, the high rate of crystal growth may indicate a high level in the number of defects in the crystal lattice. Thus, slowing the rate of crystal growth might help improving the diffraction of the crystal (Yoshizaki et al., 2001). Finally, cryo-method (Juers et al., 2007; Juers and Matthews, 2004) and additive application can affect the diffraction of crystal. We have tested different optimization methods to improve the diffraction pattern of the crystal of mCHL2-VWC3/BMP-2 complex. These methods include pH, precipitant concentration, cryoprotectant and additive screenings. Currently no good condition has been found. Thus, further optimizing steps for crystallization condition or protein constructs are necessary to obtain well diffracting crystals.

5. Summary

The proteins containing Von Willebrandt factor type C (VWC) domains act as extracellular modulators in the BMP/TGF- β signaling pathway. Though the functions of VWC-containing proteins in development and diseases have been studied extensively, the structural basis of BMP/VWC-containing protein interaction is still poorly understood. In this thesis, mouse Chordin-like 2 (mCHL2), a novel Chordin-like protein which is a member of the VWC-containing proteins was selected to study the structural basis of BMP-2/VWC protein interaction. The binding affinities, the binding specificities, the binding epitopes and the binding modes of BMP-2 for mCHL2 and its VWC domains were analyzed. Tsg has been established as a novel binding partner of mCHL2. The isolation and crystallization of the complexes of mCHL2/BMP-2 and mCHL2-VWC3/BMP-2 paved the way for solving the crystal structures of the complexes. According to our results, we can make the following conclusions.

Full-length mCHL2 binds to BMP-2 with high affinities. Two of the three VWCs of mCHL2, VWC1 and VWC3, bind to BMPs, and VWC2 does not. The affinity of mCHL2 for BMP-2 is the result of the cooperative binding of VWC1 and VWC3 domains.

mCHL2 can inhibit the binding of BMP-2 to both type I and type II receptors. With regard to VWC1/VWC3, the mCHL2-VWC1 can only inhibit the BMP-2/type II receptors binding and mCHL2-VWC3 only inhibit the binding of BMP-2 to type I receptors.

Mutational analysis for VWC3 showed that four of the seven mutants VWC3-H237D, VWC3-P238R, VWC3-V240D, and VWC3-G244A exhibited decreased binding affinities for BMP-2 compared to wild type VWC3, indicating that these four amino acids are binding determinants for BMP-2. These residues are located in a region corresponding to the long loop of CV2-VWC1 which has previously been shown to be important for

BMP-2 binding of CV2-VWC1. This probably indicates that similar to CV2-VWC1, the N-terminal part of mCHL2-VWC3 is responsible for BMP-2 binding, even if in contrast to CV2-VWC1, mCHL2-VWC3 binds only to the wrist epitope of BMP-2.

Biacore and chromatographic methods prove that mCHL2 binds to BMP-2 with a stoichiometry of 2:1, which is an important guide for the further isolation of the mCHL2/BMP-2 complex. The stable complexes of mCHL2/BMP2 and mCHL2-VWC3/BMP2 have been successfully isolated for crystallization experiments. Though the crystals obtained can't be analyzed because of their low diffraction, these results suggest that well diffracting crystals can be obtained in the future.

We have established the novel interaction between mCHL2, Tsg and BMP-2 for the first time. Tsg binds to VWC1 and VWC3 of mCHL2 in a cooperative way and plays a role in strengthening the binding affinity. Furthermore, Tsg/mCHL2/BMP-2 ternary complex and Tsg/mCHL2 binary complex have been isolated by gel-filtration chromatography. Therefore mCHL2 can form a ternary complex with Tsg and BMP-2 and this complex makes mCHL2 a better BMP-2 antagonist.

The work presented in this thesis improves understanding the regulatory mechanisms of BMPs/VWC-containing proteins. Further crystallization analysis of mCHL2 or its VWCs and BMP-2 complex is needed to reveal in detail the molecular basis of BMPs/VWC-containing proteins interaction.

6. References

- Aigner, T. (2006). Cartilage in osteoarthritic joints is not automatically osteoarthritic cartilage. *Development* 133, 3497-3498.
- Aigner, T., Stoss, H., Weseloh, G., Zeiler, G., and von der Mark, K. (1992). Activation of collagen type II expression in osteoarthritic and rheumatoid cartilage. *Virchows Arch B Cell Pathol Incl Mol Pathol* 62, 337-345.
- Allendorph, G.P., Vale, W.W., and Choe, S. (2006). Structure of the ternary signaling complex of a TGF-beta superfamily member. *Proc Natl Acad Sci U S A* 103, 7643-7648.
- Attisano, L., and Wrana, J.L. (2002). Signal transduction by the TGF-beta superfamily. *Science* 296, 1646-1647.
- Bachiller, D., Klingensmith, J., Kemp, C., Belo, J.A., Anderson, R.M., May, S.R., McMahon, J.A., McMahon, A.P., Harland, R.M., Rossant, J., *et al.* (2000). The organizer factors Chordin and Noggin are required for mouse forebrain development. *Nature* 403, 658-661.
- Bachiller, D., Klingensmith, J., Shneyder, N., Tran, U., Anderson, R., Rossant, J., and De Robertis, E.M. (2003). The role of chordin/Bmp signals in mammalian pharyngeal development and DiGeorge syndrome. *Development* 130, 3567-3578.
- Binnerts, M.E., Wen, X., Cante-Barrett, K., Bright, J., Chen, H.T., Asundi, V., Sattari, P., Tang, T., Boyle, B., Funk, W., *et al.* (2004). Human Crossveinless-2 is a novel inhibitor of bone morphogenetic proteins. *Biochem Biophys Res Commun* 315, 272-280.
- Blaney Davidson, E.N., van der Kraan, P.M., and van den Berg, W.B. (2007). TGF-beta and osteoarthritis. *Osteoarthritis Cartilage* 15, 597-604.
- Bottinger, E.P. (2007). TGF-beta in renal injury and disease. *Semin Nephrol* 27, 309-320.
- Brunet, L.J., McMahon, J.A., McMahon, A.P., and Harland, R.M. (1998). Noggin, cartilage morphogenesis, and joint formation in the mammalian skeleton. *Science* 280, 1455-1457.
- Buck, M.B., and Knabbe, C. (2006). TGF-beta signaling in breast cancer. *Ann N Y Acad Sci* 1089, 119-126.
- Canalis, E., Economides, A.N., and Gazzerro, E. (2003). Bone morphogenetic proteins, their antagonists, and the skeleton. *Endocr Rev* 24, 218-235.
- Chang, C., Holtzman, D.A., Chau, S., Chickering, T., Woolf, E.A., Holmgren, L.M., Bodorova, J., Gearing, D.P., Holmes, W.E., and Brivanlou, A.H. (2001). Twisted gastrulation can function as a BMP antagonist. *Nature* 410, 483-487.

- Chang, C.F., Lin, S.Z., Chiang, Y.H., Morales, M., Chou, J., Lein, P., Chen, H.L., Hoffer, B.J., and Wang, Y. (2003). Intravenous administration of bone morphogenetic protein-7 after ischemia improves motor function in stroke rats. *Stroke; a journal of cerebral circulation* *34*, 558-564.
- Chen, A.L., Fang, C., Liu, C., Leslie, M.P., Chang, E., and Di Cesare, P.E. (2004). Expression of bone morphogenetic proteins, receptors, and tissue inhibitors in human fetal, adult, and osteoarthritic articular cartilage. *J Orthop Res* *22*, 1188-1192.
- Coffinier, C., Tran, U., Larrain, J., and De Robertis, E.M. (2001). Neuralin-1 is a novel Chordin-related molecule expressed in the mouse neural plate. *Mech Dev* *100*, 119-122.
- Conaway, R.C., Brower, C.S., and Conaway, J.W. (2002). Emerging roles of ubiquitin in transcription regulation. *Science* *296*, 1254-1258.
- Dabek, J., Kulach, A., Monastyrska-Cup, B., and Gasiór, Z. (2006). Transforming growth factor beta and cardiovascular diseases: the other facet of the 'protective cytokine'. *Pharmacol Rep* *58*, 799-805.
- De Robertis, E.M., and Kuroda, H. (2004). Dorsal-ventral patterning and neural induction in *Xenopus* embryos. *Annu Rev Cell Dev Biol* *20*, 285-308.
- DePristo, M.A., de Bakker, P.I., and Blundell, T.L. (2004). Heterogeneity and inaccuracy in protein structures solved by X-ray crystallography. *Structure* *12*, 831-838.
- Derynck, R., Zhang, Y., and Feng, X.H. (1998). Smads: transcriptional activators of TGF-beta responses. *Cell* *95*, 737-740.
- Drissi, H., Zuscik, M., Rosier, R., and O'Keefe, R. (2005). Transcriptional regulation of chondrocyte maturation: potential involvement of transcription factors in OA pathogenesis. *Mol Aspects Med* *26*, 169-179.
- Ebara, S., and Nakayama, K. (2002). Mechanism for the action of bone morphogenetic proteins and regulation of their activity. *Spine* *27*, S10-15.
- Ebisawa, T., Fukuchi, M., Murakami, G., Chiba, T., Tanaka, K., Imamura, T., and Miyazono, K. (2001). Smurf1 interacts with transforming growth factor-beta type I receptor through Smad7 and induces receptor degradation. *J Biol Chem* *276*, 12477-12480.
- Eldar, A., Dorfman, R., Weiss, D., Ashe, H., Shilo, B.Z., and Barkai, N. (2002). Robustness of the BMP morphogen gradient in *Drosophila* embryonic patterning. *Nature* *419*, 304-308.
- Florio, P., Gazzolo, D., Luisi, S., and Petraglia, F. (2007). Activin A in brain injury. *Adv Clin Chem* *43*, 117-130.
- Friedle, H., and Knochel, W. (2002). Cooperative interaction of Xvent-2 and GATA-2 in the activation of the ventral homeobox gene Xvent-1B. *J Biol Chem* *277*, 23872-23881.

Gagliardini, E., and Benigni, A. (2007). Therapeutic potential of TGF-beta inhibition in chronic renal failure. *Expert Opin Biol Ther* 7, 293-304.

Garcia Abreu, J., Coffinier, C., Larrain, J., Oelgeschlager, M., and De Robertis, E.M. (2002). Chordin-like CR domains and the regulation of evolutionarily conserved extracellular signaling systems. *Gene* 287, 39-47.

Gazzerro, E., and Canalis, E. (2006). Bone morphogenetic proteins and their antagonists. *Rev Endocr Metab Disord* 7, 51-65.

Gazzerro, E., Deregowski, V., Stadmeier, L., Gale, N.W., Economides, A.N., and Canalis, E. (2006). Twisted gastrulation, a bone morphogenetic protein agonist/antagonist, is not required for post-natal skeletal function. *Bone* 39, 1252-1260.

Gong, Y., Krakow, D., Marcelino, J., Wilkin, D., Chitayat, D., Babul-Hirji, R., Hudgins, L., Cremers, C.W., Cremers, F.P., Brunner, H.G., *et al.* (1999). Heterozygous mutations in the gene encoding noggin affect human joint morphogenesis. *Nat Genet* 21, 302-304.

Graff, J.M. (1997). Embryonic patterning: to BMP or not to BMP, that is the question. *Cell* 89, 171-174.

Greenwald, J., Groppe, J., Gray, P., Wiater, E., Kwiatkowski, W., Vale, W., and Choe, S. (2003). The BMP7/ActRII extracellular domain complex provides new insights into the cooperative nature of receptor assembly. *Mol Cell* 11, 605-617.

Groppe, J., Greenwald, J., Wiater, E., Rodriguez-Leon, J., Economides, A.N., Kwiatkowski, W., Baban, K., Affolter, M., Vale, W.W., Belmonte, J.C., *et al.* (2003). Structural basis of BMP signaling inhibition by Noggin, a novel twelve-membered cystine knot protein. *J Bone Joint Surg Am* 85-A Suppl 3, 52-58.

Haerry, T.E., Khalsa, O., O'Connor, M.B., and Wharton, K.A. (1998). Synergistic signaling by two BMP ligands through the SAX and TKV receptors controls wing growth and patterning in *Drosophila*. *Development* 125, 3977-3987.

Hahn, T., and Akporiaye, E.T. (2006). Targeting transforming growth factor beta to enhance cancer immunotherapy. *Curr Oncol* 13, 141-143.

Harrington, A.E., Morris-Triggs, S.A., Ruotolo, B.T., Robinson, C.V., Ohnuma, S., and Hyvonen, M. (2006). Structural basis for the inhibition of activin signalling by follistatin. *Embo J* 25, 1035-1045.

Harrison, C.A., Chan, K.L., and Robertson, D.M. (2006). Activin-A binds follistatin and type II receptors through overlapping binding sites: generation of mutants with isolated binding activities. *Endocrinology* 147, 2744-2753.

Hassell, A.M., An, G., Bledsoe, R.K., Bynum, J.M., Carter, H.L., 3rd, Deng, S.J., Gampe, R.T., Grisard, T.E., Madauss, K.P., Nolte, R.T., *et al.* (2007). Crystallization of protein-ligand complexes. *Acta*

crystallographica 63, 72-79.

Hemmati-Brivanlou, A., Kelly, O.G., and Melton, D.A. (1994). Follistatin, an antagonist of activin, is expressed in the Spemann organizer and displays direct neuralizing activity. *Cell* 77, 283-295.

Hogan, B.L. (1996). Bone morphogenetic proteins in development. *Curr Opin Genet Dev* 6, 432-438.

Hollnagel, A., Oehlmann, V., Heymer, J., Ruther, U., and Nordheim, A. (1999). Id genes are direct targets of bone morphogenetic protein induction in embryonic stem cells. *J Biol Chem* 274, 19838-19845.

Hussein, S.M., Duff, E.K., and Sirard, C. (2003). Smad4 and beta-catenin co-activators functionally interact with lymphoid-enhancing factor to regulate graded expression of Msx2. *J Biol Chem* 278, 48805-48814.

Iemura, S., Yamamoto, T.S., Takagi, C., Uchiyama, H., Natsume, T., Shimasaki, S., Sugino, H., and Ueno, N. (1998). Direct binding of follistatin to a complex of bone-morphogenetic protein and its receptor inhibits ventral and epidermal cell fates in early *Xenopus* embryo. *Proc Natl Acad Sci U S A* 95, 9337-9342.

Ikeya, M., Kawada, M., Kiyonari, H., Sasai, N., Nakao, K., Furuta, Y., and Sasai, Y. (2006). Essential pro-Bmp roles of crossveinless 2 in mouse organogenesis. *Development* 133, 4463-4473.

Ito, Y., and Miyazono, K. (2003). RUNX transcription factors as key targets of TGF-beta superfamily signaling. *Curr Opin Genet Dev* 13, 43-47.

Itoh, F., Asao, H., Sugamura, K., Heldin, C.H., ten Dijke, P., and Itoh, S. (2001). Promoting bone morphogenetic protein signaling through negative regulation of inhibitory Smads. *Embo J* 20, 4132-4142.

Juers, D.H., Lovelace, J., Bellamy, H.D., Snell, E.H., Matthews, B.W., and Borgstahl, G.E. (2007). Changes to crystals of *Escherichia coli* beta-galactosidase during room-temperature/low-temperature cycling and their relation to cryo-annealing. *Acta crystallographica* 63, 1139-1153.

Juers, D.H., and Matthews, B.W. (2004). Cryo-cooling in macromolecular crystallography: advantages, disadvantages and optimization. *Quarterly reviews of biophysics* 37, 105-119.

Kalajzic, I., Staal, A., Yang, W.P., Wu, Y., Johnson, S.E., Feyen, J.H., Krueger, W., Maye, P., Yu, F., Zhao, Y., *et al.* (2005). Expression profile of osteoblast lineage at defined stages of differentiation. *J Biol Chem* 280, 24618-24626.

Kavsak, P., Rasmussen, R.K., Causing, C.G., Bonni, S., Zhu, H., Thomsen, G.H., and Wrana, J.L. (2000). Smad7 binds to Smurf2 to form an E3 ubiquitin ligase that targets the TGF beta receptor for degradation. *Mol Cell* 6, 1365-1375.

Keller, S., Nickel, J., Zhang, J.L., Sebald, W., and Mueller, T.D. (2004). Molecular recognition of BMP-2 and BMP receptor IA. *Nat Struct Mol Biol* 11, 481-488.

Kim, J., Johnson, K., Chen, H.J., Carroll, S., and Laughon, A. (1997). *Drosophila* Mad binds to DNA and

directly mediates activation of vestigial by Decapentaplegic. *Nature* 388, 304-308.

Kingsley, D.M. (1994). What do BMPs do in mammals? Clues from the mouse short-ear mutation. *Trends Genet* 10, 16-21.

Kirsch, T., Sebald, W., and Dreyer, M.K. (2000). Crystal structure of the BMP-2-BRIA ectodomain complex. *Nat Struct Biol* 7, 492-496.

Korchynski, O., and ten Dijke, P. (2002). Identification and functional characterization of distinct critically important bone morphogenetic protein-specific response elements in the Id1 promoter. *J Biol Chem* 277, 4883-4891.

Kusanagi, K., Inoue, H., Ishidou, Y., Mishima, H.K., Kawabata, M., and Miyazono, K. (2000). Characterization of a bone morphogenetic protein-responsive Smad-binding element. *Mol Biol Cell* 11, 555-565.

Ladher, R., Mohun, T.J., Smith, J.C., and Snape, A.M. (1996). Xom: a *Xenopus* homeobox gene that mediates the early effects of BMP-4. *Development* 122, 2385-2394.

Lai, C.F., and Cheng, S.L. (2002). Signal transductions induced by bone morphogenetic protein-2 and transforming growth factor-beta in normal human osteoblastic cells. *J Biol Chem* 277, 15514-15522.

Larrain, J., Bachiller, D., Lu, B., Agius, E., Piccolo, S., and De Robertis, E.M. (2000). BMP-binding modules in chordin: a model for signalling regulation in the extracellular space. *Development* 127, 821-830.

Larrain, J., Oelgeschlager, M., Ketpura, N.I., Reversade, B., Zakin, L., and De Robertis, E.M. (2001). Proteolytic cleavage of Chordin as a switch for the dual activities of Twisted gastrulation in BMP signaling. *Development* 128, 4439-4447.

Lee, H.X., Ambrosio, A.L., Reversade, B., and De Robertis, E.M. (2006). Embryonic dorsal-ventral signaling: secreted frizzled-related proteins as inhibitors of tolloid proteinases. *Cell* 124, 147-159.

Lin, J., Patel, S.R., Cheng, X., Cho, E.A., Levitan, I., Ullenbruch, M., Phan, S.H., Park, J.M., and Dressler, G.R. (2005). Kielin/chordin-like protein, a novel enhancer of BMP signaling, attenuates renal fibrotic disease. *Nat Med* 11, 387-393.

Lin, J., Patel, S.R., Wang, M., and Dressler, G.R. (2006). The cysteine-rich domain protein KCP is a suppressor of transforming growth factor beta/activin signaling in renal epithelia. *Mol Cell Biol* 26, 4577-4585.

Lin, X., Liang, M., and Feng, X.H. (2000). Smurf2 is a ubiquitin E3 ligase mediating proteasome-dependent degradation of Smad2 in transforming growth factor-beta signaling. *J Biol Chem* 275, 36818-36822.

Lippiello, L., Hall, D., and Mankin, H.J. (1977). Collagen synthesis in normal and osteoarthritic human cartilage. *J Clin Invest* 59, 593-600.

- Liu, F., Hata, A., Baker, J.C., Doody, J., Carcamo, J., Harland, R.M., and Massague, J. (1996). A human Mad protein acting as a BMP-regulated transcriptional activator. *Nature* *381*, 620-623.
- Liu, F., Ventura, F., Doody, J., and Massague, J. (1995). Human type II receptor for bone morphogenic proteins (BMPs): extension of the two-kinase receptor model to the BMPs. *Mol Cell Biol* *15*, 3479-3486.
- Luo, K. (2003). Negative regulation of BMP signaling by the ski oncoprotein. *J Bone Joint Surg Am* *85-A Suppl 3*, 39-43.
- Macias-Silva, M., Abdollah, S., Hoodless, P.A., Pirone, R., Attisano, L., and Wrana, J.L. (1996). MADR2 is a substrate of the TGFbeta receptor and its phosphorylation is required for nuclear accumulation and signaling. *Cell* *87*, 1215-1224.
- Marcelino, J., Sciortino, C.M., Romero, M.F., Ulatowski, L.M., Ballock, R.T., Economides, A.N., Eimon, P.M., Harland, R.M., and Warman, M.L. (2001). Human disease-causing NOG missense mutations: effects on noggin secretion, dimer formation, and bone morphogenetic protein binding. *Proc Natl Acad Sci U S A* *98*, 11353-11358.
- Massague, J., Blain, S.W., and Lo, R.S. (2000). TGFbeta signaling in growth control, cancer, and heritable disorders. *Cell* *103*, 295-309.
- Matsui, M., Mizuseki, K., Nakatani, J., Nakanishi, S., and Sasai, Y. (2000). Xenopus kielin: A dorsalizing factor containing multiple chordin-type repeats secreted from the embryonic midline. *Proc Natl Acad Sci U S A* *97*, 5291-5296.
- McDonald, N.Q., and Hendrickson, W.A. (1993). A structural superfamily of growth factors containing a cystine knot motif. *Cell* *73*, 421-424.
- McMahon, J.A., Takada, S., Zimmerman, L.B., Fan, C.M., Harland, R.M., and McMahon, A.P. (1998). Noggin-mediated antagonism of BMP signaling is required for growth and patterning of the neural tube and somite. *Genes Dev* *12*, 1438-1452.
- Medici, M., van Meurs, J.B., Rivadeneira, F., Zhao, H., Arp, P.P., Hofman, A., Pols, H.A., and Uitterlinden, A.G. (2006). BMP-2 gene polymorphisms and osteoporosis: the Rotterdam Study. *J Bone Miner Res* *21*, 845-854.
- Miyama, K., Yamada, G., Yamamoto, T.S., Takagi, C., Miyado, K., Sakai, M., Ueno, N., and Shibuya, H. (1999). A BMP-inducible gene, *dlx5*, regulates osteoblast differentiation and mesoderm induction. *Dev Biol* *208*, 123-133.
- Miyazono, K. (2000). Positive and negative regulation of TGF-beta signaling. *J Cell Sci* *113 (Pt 7)*, 1101-1109.
- Miyazono, K., Maeda, S., and Imamura, T. (2004). Coordinate regulation of cell growth and differentiation

by TGF-beta superfamily and Runx proteins. *Oncogene* 23, 4232-4237.

Miyazono, K., Maeda, S., and Imamura, T. (2005). BMP receptor signaling: transcriptional targets, regulation of signals, and signaling cross-talk. *Cytokine Growth Factor Rev* 16, 251-263.

Moustakas, A., and Heldin, C.H. (2005). Non-Smad TGF-beta signals. *J Cell Sci* 118, 3573-3584.

Nakayama, N., Han, C.E., Scully, S., Nishinakamura, R., He, C., Zeni, L., Yamane, H., Chang, D., Yu, D., Yokota, T., *et al.* (2001). A novel chordin-like protein inhibitor for bone morphogenetic proteins expressed preferentially in mesenchymal cell lineages. *Dev Biol* 232, 372-387.

Nakayama, N., Han, C.Y., Cam, L., Lee, J.I., Pretorius, J., Fisher, S., Rosenfeld, R., Scully, S., Nishinakamura, R., Duryea, D., *et al.* (2004). A novel chordin-like BMP inhibitor, CHL2, expressed preferentially in chondrocytes of developing cartilage and osteoarthritic joint cartilage. *Development* 131, 229-240.

Neul, J.L., and Ferguson, E.L. (1998). Spatially restricted activation of the SAX receptor by SCW modulates DPP/TKV signaling in *Drosophila* dorsal-ventral patterning. *Cell* 95, 483-494.

Newfeld, S.J., Wisotzkey, R.G., and Kumar, S. (1999). Molecular evolution of a developmental pathway: phylogenetic analyses of transforming growth factor-beta family ligands, receptors and Smad signal transducers. *Genetics* 152, 783-795.

Nguyen, M., Park, S., Marques, G., and Arora, K. (1998). Interpretation of a BMP activity gradient in *Drosophila* embryos depends on synergistic signaling by two type I receptors, SAX and TKV. *Cell* 95, 495-506.

Nosaka, T., Morita, S., Kitamura, H., Nakajima, H., Shibata, F., Morikawa, Y., Kataoka, Y., Ebihara, Y., Kawashima, T., Itoh, T., *et al.* (2003). Mammalian twisted gastrulation is essential for skeleto-lymphogenesis. *Mol Cell Biol* 23, 2969-2980.

O'Leary, J.M., Hamilton, J.M., Deane, C.M., Valeyev, N.V., Sandell, L.J., and Downing, A.K. (2004). Solution structure and dynamics of a prototypical chordin-like cysteine-rich repeat (von Willebrand Factor type C module) from collagen IIA. *J Biol Chem* 279, 53857-53866.

Oelgeschlager, M., Larrain, J., Geissert, D., and De Robertis, E.M. (2000). The evolutionarily conserved BMP-binding protein Twisted gastrulation promotes BMP signalling. *Nature* 405, 757-763.

Oelgeschlager, M., Reversade, B., Larrain, J., Little, S., Mullins, M.C., and De Robertis, E.M. (2003). The pro-BMP activity of Twisted gastrulation is independent of BMP binding. *Development* 130, 4047-4056.

Onichtchouk, D., Chen, Y.G., Dosch, R., Gawantka, V., Delius, H., Massague, J., and Niehrs, C. (1999). Silencing of TGF-beta signalling by the pseudoreceptor BAMBI. *Nature* 401, 480-485.

Oren, A., Toporik, A., Biton, S., Almogy, N., Eshel, D., Bernstein, J., Savitsky, K., and Rotman, G. (2004).

hCHL2, a novel chordin-related gene, displays differential expression and complex alternative splicing in human tissues and during myoblast and osteoblast maturation. *Gene* 331, 17-31.

Patel, K. (1998). Follistatin. *Int J Biochem Cell Biol* 30, 1087-1093.

Peiffer, D.A., Von Bubnoff, A., Shin, Y., Kitayama, A., Mochii, M., Ueno, N., and Cho, K.W. (2005). A *Xenopus* DNA microarray approach to identify novel direct BMP target genes involved in early embryonic development. *Dev Dyn* 232, 445-456.

Piccolo, S., Agius, E., Lu, B., Goodman, S., Dale, L., and De Robertis, E.M. (1997). Cleavage of Chordin by Xolloid metalloprotease suggests a role for proteolytic processing in the regulation of Spemann organizer activity. *Cell* 91, 407-416.

Piccolo, S., Sasai, Y., Lu, B., and De Robertis, E.M. (1996). Dorsoventral patterning in *Xenopus*: inhibition of ventral signals by direct binding of chordin to BMP-4. *Cell* 86, 589-598.

Rastegar, S., Friedle, H., Frommer, G., and Knochel, W. (1999). Transcriptional regulation of *Xvent* homeobox genes. *Mech Dev* 81, 139-149.

Reddi, A.H. (1998). Role of morphogenetic proteins in skeletal tissue engineering and regeneration. *Nat Biotechnol* 16, 247-252.

Rentzsch, F., Zhang, J., Kramer, C., Sebald, W., and Hammerschmidt, M. (2006). Crossveinless 2 is an essential positive feedback regulator of Bmp signaling during zebrafish gastrulation. *Development* 133, 801-811.

Reynolds, S.D., Zhang, D., Puzas, J.E., O'Keefe, R.J., Rosier, R.N., and Reynolds, P.R. (2000). Cloning of the chick BMP1/Tolloid cDNA and expression in skeletal tissues. *Gene* 248, 233-243.

Rosen, V., and Thies, R.S. (1992). The BMP proteins in bone formation and repair. *Trends Genet* 8, 97-102.

Ross, J.J., Shimmi, O., Vilmos, P., Petryk, A., Kim, H., Gaudenz, K., Hermanson, S., Ekker, S.C., O'Connor, M.B., and Marsh, J.L. (2001). Twisted gastrulation is a conserved extracellular BMP antagonist. *Nature* 410, 479-483.

Sakuta, H., Suzuki, R., Takahashi, H., Kato, A., Shintani, T., Iemura, S., Yamamoto, T.S., Ueno, N., and Noda, M. (2001). Ventroptin: a BMP-4 antagonist expressed in a double-gradient pattern in the retina. *Science* 293, 111-115.

Scheufler, C., Sebald, W., and Hulsmeier, M. (1999). Crystal structure of human bone morphogenetic protein-2 at 2.7 Å resolution. *J Mol Biol* 287, 103-115.

Schmidl, M., Adam, N., Surmann-Schmitt, C., Hattori, T., Stock, M., Dietz, U., de Crombrughe, B., Poschl, E., and von der Mark, K. (2006). Twisted gastrulation modulates bone morphogenetic protein-induced collagen II and X expression in chondrocytes in vitro and in vivo. *J Biol Chem* 281, 31790-31800.

- Schmierer, B., and Hill, C.S. (2007). TGFbeta-SMAD signal transduction: molecular specificity and functional flexibility. *Nat Rev Mol Cell Biol* 8, 970-982.
- Scott, I.C., Blitz, I.L., Pappano, W.N., Maas, S.A., Cho, K.W., and Greenspan, D.S. (2001). Homologues of Twisted gastrulation are extracellular cofactors in antagonism of BMP signalling. *Nature* 410, 475-478.
- Scott, I.C., Steiglit, B.M., Clark, T.G., Pappano, W.N., and Greenspan, D.S. (2000). Spatiotemporal expression patterns of mammalian chordin during postgastrulation embryogenesis and in postnatal brain. *Dev Dyn* 217, 449-456.
- Sebald, W., Nickel, J., Zhang, J.L., and Mueller, T.D. (2004). Molecular recognition in bone morphogenetic protein (BMP)/receptor interaction. *Biol Chem* 385, 697-710.
- Sekimoto, G., Matsuzaki, K., Yoshida, K., Mori, S., Murata, M., Seki, T., Matsui, H., Fujisawa, J., and Okazaki, K. (2007). Reversible Smad-dependent signaling between tumor suppression and oncogenesis. *Cancer Res* 67, 5090-5096.
- Shimmi, O., Umulis, D., Othmer, H., and O'Connor, M.B. (2005). Facilitated transport of a Dpp/Scw heterodimer by Sog/Tsg leads to robust patterning of the Drosophila blastoderm embryo. *Cell* 120, 873-886.
- Smith, J.L., Hendrickson, W.A., Honzatko, R.B., and Sheriff, S. (1986). Structural heterogeneity in protein crystals. *Biochemistry* 25, 5018-5027.
- Smith, W.C., and Harland, R.M. (1992). Expression cloning of noggin, a new dorsalizing factor localized to the Spemann organizer in Xenopus embryos. *Cell* 70, 829-840.
- Sowa, H., Kaji, H., Hendy, G.N., Canaff, L., Komori, T., Sugimoto, T., and Chihara, K. (2004). Menin is required for bone morphogenetic protein 2- and transforming growth factor beta-regulated osteoblastic differentiation through interaction with Smads and Runx2. *J Biol Chem* 279, 40267-40275.
- Suzuki, H., Yagi, K., Kondo, M., Kato, M., Miyazono, K., and Miyazawa, K. (2004). c-Ski inhibits the TGF-beta signaling pathway through stabilization of inactive Smad complexes on Smad-binding elements. *Oncogene* 23, 5068-5076.
- Thompson, T.B., Lerch, T.F., Cook, R.W., Woodruff, T.K., and Jardezy, T.S. (2005). The structure of the follistatin:activin complex reveals antagonism of both type I and type II receptor binding. *Dev Cell* 9, 535-543.
- Thompson, T.B., Woodruff, T.K., and Jardezy, T.S. (2003). Structures of an ActRIIB:activin A complex reveal a novel binding mode for TGF-beta ligand:receptor interactions. *Embo J* 22, 1555-1566.
- Turgeman, G., Zilberman, Y., Zhou, S., Kelly, P., Moutsatsos, I.K., Kharode, Y.P., Borella, L.E., Bex, F.J., Komm, B.S., Bodine, P.V., *et al.* (2002). Systemically administered rhBMP-2 promotes MSC activity and reverses bone and cartilage loss in osteopenic mice. *J Cell Biochem* 86, 461-474.

- Ueki, T., Tanaka, M., Yamashita, K., Mikawa, S., Qiu, Z., Maragakis, N.J., Hevner, R.F., Miura, N., Sugimura, H., and Sato, K. (2003). A novel secretory factor, Neurogenesis-1, provides neurogenic environmental cues for neural stem cells in the adult hippocampus. *J Neurosci* 23, 11732-11740.
- Urist, M.R. (1965). Bone: formation by autoinduction. *Science* 150, 893-899.
- Vaughn, J.L., Goodwin, R.H., Tompkins, G.J., and McCawley, P. (1977). The establishment of two cell lines from the insect *Spodoptera frugiperda* (Lepidoptera; Noctuidae). *In Vitro* 13, 213-217.
- von Bubnoff, A., Peiffer, D.A., Blitz, I.L., Hayata, T., Ogata, S., Zeng, Q., Trunnell, M., and Cho, K.W. (2005). Phylogenetic footprinting and genome scanning identify vertebrate BMP response elements and new target genes. *Dev Biol* 281, 210-226.
- Weber, D., Kotsch, A., Nickel, J., Harth, S., Seher, A., Mueller, U., Sebald, W., and Mueller, T.D. (2007). A silent H-bond can be mutationally activated for high-affinity interaction of BMP-2 and activin type IIB receptor. *BMC Struct Biol* 7, 6.
- Wills, A., Harland, R.M., and Khokha, M.K. (2006). Twisted gastrulation is required for forebrain specification and cooperates with Chordin to inhibit BMP signaling during *X. tropicalis* gastrulation. *Dev Biol* 289, 166-178.
- Wozney, J.M. (1998). The bone morphogenetic protein family: multifunctional cellular regulators in the embryo and adult. *Eur J Oral Sci* 106 Suppl 1, 160-166.
- Wu, X.B., Li, Y., Schneider, A., Yu, W., Rajendren, G., Iqbal, J., Yamamoto, M., Alam, M., Brunet, L.J., Blair, H.C., *et al.* (2003). Impaired osteoblastic differentiation, reduced bone formation, and severe osteoporosis in noggin-overexpressing mice. *J Clin Invest* 112, 924-934.
- Yamashita, H., ten Dijke, P., Huylebroeck, D., Sampath, T.K., Andries, M., Smith, J.C., Heldin, C.H., and Miyazono, K. (1995). Osteogenic protein-1 binds to activin type II receptors and induces certain activin-like effects. *J Cell Biol* 130, 217-226.
- Yoshida, Y., Tanaka, S., Umemori, H., Minowa, O., Usui, M., Ikematsu, N., Hosoda, E., Imamura, T., Kuno, J., Yamashita, T., *et al.* (2000). Negative regulation of BMP/Smad signaling by Tob in osteoblasts. *Cell* 103, 1085-1097.
- Yoshida, Y., von Bubnoff, A., Ikematsu, N., Blitz, I.L., Tsuzuku, J.K., Yoshida, E.H., Umemori, H., Miyazono, K., Yamamoto, T., and Cho, K.W. (2003). Tob proteins enhance inhibitory Smad-receptor interactions to repress BMP signaling. *Mech Dev* 120, 629-637.
- Yoshizaki, I., Sato, T., Igarashi, N., Natsuisaka, M., Tanaka, N., Komatsu, H., and Yoda, S. (2001). Systematic analysis of supersaturation and lysozyme crystal quality. *Acta crystallographica* 57, 1621-1629.
- Zhang, D., Ferguson, C.M., O'Keefe, R.J., Puzas, J.E., Rosier, R.N., and Reynolds, P.R. (2002). A role for

the BMP antagonist chordin in endochondral ossification. *J Bone Miner Res* 17, 293-300.

Zhang, J.L., Huang, Y., Qiu, L.Y., Nickel, J., and Sebald, W. (2007). von Willebrand factor type C domain-containing proteins regulate bone morphogenetic protein signaling through different recognition mechanisms. *J Biol Chem* 282, 20002-20014.

Zhang, J.L., Qiu, L.Y., Kotsch, A., Weidauer, S., Patterson, L., Hammerschmidt, M., Sebald, W., and Mueller, T.D. (2008). Crystal structure analysis reveals how the Chordin family member Crossveinless 2 blocks BMP-2 receptor binding. *Dev Cell* (*To be published*).

Zhang, Y., Chang, C., Gehling, D.J., Hemmati-Brivanlou, A., and Derynck, R. (2001). Regulation of Smad degradation and activity by Smurf2, an E3 ubiquitin ligase. *Proc Natl Acad Sci U S A* 98, 974-979.

Zhang, Y.W., Yasui, N., Ito, K., Huang, G., Fujii, M., Hanai, J., Nogami, H., Ochi, T., Miyazono, K., and Ito, Y. (2000). A RUNX2/PEBP2alpha A/CBFA1 mutation displaying impaired transactivation and Smad interaction in cleidocranial dysplasia. *Proc Natl Acad Sci U S A* 97, 10549-10554.

Zhu, H., Kavsak, P., Abdollah, S., Wrana, J.L., and Thomsen, G.H. (1999). A SMAD ubiquitin ligase targets the BMP pathway and affects embryonic pattern formation. *Nature* 400, 687-693.

Zhu, Y., Usui, H.K., and Sharma, K. (2007). Regulation of transforming growth factor beta in diabetic nephropathy: implications for treatment. *Semin Nephrol* 27, 153-160.

Acknowledgments

The present work was carried out under the supervision of Prof. Dr. Walter Sebald in the period from July 2005 to May 2007 at the department of Physiological Chemistry II at Biocenter of University of Wuerzburg.

I am especially grateful to Prof. Dr. Walter Sebald for giving me the opportunity to perform this work under his supervision, for his constant discussions, and for his invaluable support during reviewing the entire topic. His continuous interest and personal commitment were a motivation and a great help for me at the same time.

I particularly wish to thank Prof. Dr. med. Franz Jakob for being the second referee of this work and for his great support for this work.

I specially would like to thank Dr. Jinli Zhang for introducing me into this project, for his enormous support, excellent cooperation, and coordination of my work, and also for his great help for my everyday life.

I thank Prof. Dr. Thomas Muller and Alexander Kotzsch for their kind help with analysis of protein crystallization.

I would like to say many thanks to Mr. Christian Soeder and Ms. Nicole Hoppe for their great helpfulness and valuable excellent technical assistance.

I would like to say thank you to Dr. Werner Schmitz and Prof. Dr. Ernst Conzelmann for the execution of mass spectrometry analysis and very enjoyable introduction of this technique. I thank Dr. Feichtinger Wolfgang for the execution of DNA Sequencing and patient explanation.

I'm very grateful to the secretary of our department - Mrs. Bettina Lakeit for her zealously and being present and ready to help at anytime.

I thank Dr. Joachim Nickel and Dr. Axel Seher for various useful scientific discussions. My thanks apply also to other members of the lab – Dr. Dionys Weber, Liyan Qiu, Susanne Gebhardt, Stefen Harth, Jannes Ullbrich, Edwin Patino, Kai Heinecke and Birgit Midloch, for their brilliant technical assistance and kind help.

To my parents I would like to thank for the moral support and courage which they gave to me. You are the most important part in my life.

I would like to address my thanks to all the other people, who have not been mentioned here by names, but who helped me during my thesis work and who made my stage in Wuerzburg an wonderful experience.

CURRICULUM VITAE

PERSONAL DATA

Name	Yi Huang
Date of birth	02.02.1978
Nationality	Chinese
Status	Single

EDUCATION

07.2005 - 05.2007 M.D. student at the Department of Physiological Chemistry II, Biocenter, University of Wuerzburg, Germany.

Thesis: The structural and functional analysis of and Chordin-like 2 / BMP-2 interaction.

09.2001 - 07.2004 Master Degree (Medicine), Third Military Medical University, Chongqing, China.

Thesis: Investigation of preparation and pharmacokinetics for hydroxycamptothecin liposome.

09.1996 - 07.2001 Bachelor Degree (Medicine), Third Military Medical University, Chongqing, China.

WORK EXPERIENCE

07.2005 - 05.2007 Dissertation research work under the supervision of Prof., Dr. Walter Sebald at the Department of Physiological Chemistry II, Biocenter, University of Wuerzburg, Germany.

09.2004 - 07.2005 Clinical pharmacologist at the Department of Pharmacy, Southwest Hospital, Chongqing, China